Accepted Manuscript

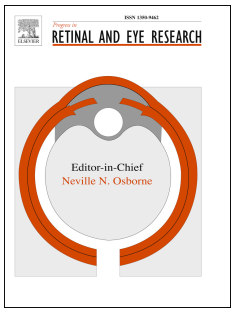

Differentiating drusen: Drusen and drusen-like appearances associated with ageing, age-related macular degeneration, inherited eye disease and other pathological processes

Kamron N. Khan, Omar A. Mahroo, Rehna Khan, Moin D. Mohamed, Martin McKibbin, Alan Bird, Michel Michaelides, Adnan Tufail, Anthony T. Moore

PII: S1350-9462(16)30024-6

DOI: 10.1016/j.preteyeres.2016.04.008

Reference: JPRR 629

To appear in: *Progress in Retinal and Eye Research*

Received Date: 6 December 2015

Revised Date: 24 April 2016

Accepted Date: 27 April 2016

Please cite this article as: Khan, K.N., Mahroo, O.A., Khan, R., Mohamed, M.D., McKibbin, M., Bird, A., Michaelides, M., Tufail, A., Moore, A.T., Differentiating drusen: Drusen and drusen-like appearances associated with ageing, age-related macular degeneration, inherited eye disease and other pathological processes, *Progress in Retinal and Eye Research* (2016), doi: 10.1016/j.preteyeres.2016.04.008.

Differentiating drusen: drusen and drusen-like appearances associated with ageing, age-related macular degeneration, inherited eye disease and other pathological processes

Kamron N Khan[a,b,c]

Omar A Mahroo[a,b,d,e]

Rehna Khan[f]

Moin D Mohamed[g]

Martin McKibbin[c]

Alan Bird[a,b]

Michel Michaelides[a,b]

Adnan Tufail[a,b]

Anthony T Moore[a,b, h]

[a]University College London Institute of Ophthalmology, 11-43 Bath Street, London EC1V 9EL

[b]Medical Retina Service, Moorfields Eye Hospital, 162 City Road, London EC1V 2PD

[c]Section of Ophthalmology and Neuroscience, Leeds Institute of Molecular Medicine, University of Leeds, St James's University Hospital, Leeds LS9 7TF

[d]Department of Ophthalmology, King's College London, St Thomas' Hospital Campus, Westminster Bridge Road, London SE1 7EH

[e]Physiology, Development and Neuroscience, University of Cambridge, Downing Street, Cambridge CB2 3EG

[f]Department of Ophthalmology, Calderdale & Huddersfield NHS Foundation Trust, Acre St, Huddersfield, West Yorkshire HD3 3EA

[g]Department of Ophthalmology, Guys & St Thomas' NHS Foundation Trust, Westminster Bridge Road, London SE1 7EH

[h]Department of Ophthalmology, UCSF School of Medicine, San Francisco CA 94143

Abstract

Drusen are discussed frequently in the context of their association with age-related macular degeneration (AMD). Some types may, however, be regarded as a normal consequence of ageing; others may be observed in young age groups. They also occur in a number of inherited disorders and some systemic conditions. Whilst drusen are classically located external (sclerad) to the retinal pigment epithelium, accumulations of material internal (vitread to) this layer can display a drusen-like appearance, having been variously termed pseudodrusen or subretinal drusenoid deposits. This review first briefly presents an overview of drusen biogenesis and subclinical deposit. The (frequently overlapping) subtypes of clinically detectable deposit, seen usually in the context of ageing or AMD, are then described in more detail, together with appearance on imaging modalities: these include hard and soft drusen, cuticular drusen, reticular pseudodrusen and “ghost drusen”. Eye disorders other than AMD which may exhibit drusen or drusen-like features are subsequently discussed: these include monogenic conditions as well as conditions with undefined inheritance, the latter including some types of early onset drusen such as large colloid drusen. A number of systemic conditions in which drusen-like deposits may be seen are also considered. Throughout this review, high resolution images are presented for most of the conditions discussed, particularly the rarer ones, providing a useful reference library for images of the range of conditions associated with drusen-like appearances. In the final section, some common themes are highlighted, as well as a brief discussion of some future avenues for research.

List of abbreviations

AF	Autofluorescence
AMD	Age-related macular degeneration
AO	Adaptive optics
BlamD	Basal laminar deposit
BlinD	Basal linear deposit
BM	Bruch's Membrane
CD	Cuticular drusen
CSLO	Confocal scanning laser ophthalmoscope
ECM	Extracellular matrix
FFA	Fundus fluorescein angiography
FAF	Fundus autofluorescence
ICGA	Indocyanine green angiography
IRR	Infrared reflectance
L-ORD	Late-onset retinal degeneration
MMP	Matrix metalloproteinase
MPGN	Membranoproliferative glomerulonephritis
NCMD	North Carolina Macular Dystrophy
NIRR	Near infrared reflectance
OCT	Optical coherence tomography
PAS	Periodic acid Schiff
PED	Pigment epithelial detachment
PPi	Pyrophosphate
PXE	Pseudoxanthoma elasticum
RPD	Reticular pseudodrusen
RPE	Retinal pigment epithelium
SDD	Subretinal drusenoid deposit
SFD	Sorsby fundus dystrophy

SLS	Sjogren-Larsson syndrome
SWAF	Short wavelength autofluorescence

Table of Contents

1. Introduction

Drusen (singular: druse) are accumulations of extracellular material immediately beneath (i.e. external, or sclerad, to) the retinal pigment epithelium (RPE). They have been discussed for over 150 years, having been first described by Franciscus Donders who called them "Colloidkugeln" (colloid spheres) (Donders, 1855). He considered them gravestones of the RPE. A year later Heinrich Müller coined the name drusen, after their glistening appearance, from the German word for geode, a rock containing a crystal lined cavity (Muller, 1856). Drusen may be a manifestation of the normal ageing process or represent an important sign associated with retinal disease (Ardeljan and Chan, 2013). Differentiating the two depends upon a careful assessment of the drusen characteristics, although there is a degree of overlap. The biochemical processes associated with ageing, accelerated or modified by genetic and environmental factors, can result in drusen and in progression to disease. Significant advances have been made in our understanding of drusen over the last 10 years especially with the advent of high-resolution *in vivo* retinal imaging.

There are a number of different systems for classifying drusen or drusenoid lesions. These include categorization based on size, location, shape, appearance with multi-modal imaging, microscopic appearance, and molecular composition. The classification systems overlap, but do not map discretely onto one another. Matters are further complicated by the fact that definitions and terms of reference may change: the same name has been used for different phenotypic entities over time. “Location” can refer to whether the lesion is found in the macular region or peripheral retina, and may also refer to the proximal-to-distal layer or sublayer in which the lesion is found (internal to or external to the retinal pigment epithelium (RPE) for example). The former will be referred to as the “x-y location”, and the latter the “z-axis” in this review.

1.1 Structure and scope of the review

In this review we aim to characterise drusen and drusen-like (drusenoid) deposits systematically, highlighting key differentiating features where present. To do this end we will rely primarily on clinically available forms of imaging, but correlate findings with histological data where possible. A key feature of this review is that, in addition to discussing drusen in the traditional context of ageing or age-related macular degeneration (AMD), we will also consider in some detail a range of inherited and/or systemic disorders in which lesions with a drusen-like appearance may occur.

In the first part of the review, we aim to discuss the various phenotypes associated with drusen and drusenoid lesions, starting with a brief review of subclinical features, followed by a comprehensive review of the clinical subtypes, primarily evidenced from studies of age-related macular degeneration (AMD). In the next section, we will go on to discuss the occurrence of drusen and drusen-like lesions in retinal pathological processes other than AMD: these include lesions associated with abnormalities of the visual cycle, other eye-specific disorders, and disorders with systemic manifestations, including renal disease. Many

of the diseases mentioned are monogenic, or have strong genetic associations. Table 1 lists the genes mentioned in the text with OMIM (Online Mendelian Inheritance in Man, an online catalogue of genes and disorders) numbers for reference.

Optic disc drusen (collections of material within retinal ganglion cell axons due to impaired flow) will not be discussed. Crystalline retinopathies (reviewed by Nadim et al., 2002) will not be considered, though in some cases they may resemble calcified drusen. Drusen occurring in the context of localised well-defined choroidal lesions, such as over a choroidal naevus, where they can indicate chronicity, will not be discussed. Also, the inflammatory "white dot syndromes" are beyond the scope of this review.

Table 1. Genes mentioned in this review. (Abbreviations not explained in table: EGF, epidermal growth factor; DFFA, DNA fragmentation factor alpha subunit.)

Name	Meaning of abbreviation	OMIM number	Cytogenetic location	Associated diseases	Drusen/drusenoid appearance phenotype
ABCA4	ATP-binding cassette, subfamily A, member 4	601691	1p22.1	Stargardt disease; macular dystrophy; cone-rod dystrophy	White dots in the central macula (Platano et al.); outer retinal flecks and deposits
ABCC6	ATP-binding cassette, subfamily C, member 6	603234	16p13.11	Pseudoxanthoma elasticum	Subretinal drusenoid deposits, white dots (Platano et al.)
ARMS2	Age-related maculopathy susceptibility 2	611313	10q26.13	Suseceptibility to AMD	Drusen associated with AMD
C2; C3; C9	Complement components 2, 3, 9	613927; 120700; 120940	6p21.33; 19p13.3; 5p13.1	Complement component deficiencies (C2, C3, C9), susceptibility to atypical haemolytic uraemic syndrome (C3), risk of AMD	Drusen associated with AMD
CDHR1	Cadherin-related family, Member 1	609502	10q23.1	Range of retinal phenotypes; cone-rod dystrophy	Hard drusen
CFB	Complement Factor B	138470	6p21.33	Complement factor B deficiency, susceptibility to atypical haemolytic uraemic syndrome, risk of AMD	Drusen associated with AMD
CFH	Complement Factor H	134370	1q31.3	Complement factor H deficiency, membranoproliferative glomerulonephritis type 2, atypical haemolytic uraemic syndrome, risk of AMD	Widespread soft drusen, cuticular drusen, AMD
CFI	Complement Factor I	217030	6p21.33	Complement factor I deficiency, susceptibility to atypical haemolytic uraemic syndrome, risk of AMD	Drusen associated with AMD
CIDEC	Cell-death inducing DFFA-like effector C	612120	3p25.3	Familial partial lipodystrophy type 5	Hard drusen, cuticular drusen
COL4A3	Collagen, Type IV, Alpha-3	120070	2q36.3	Autosomal recessive Alport syndrome; autosomal dominant Alport syndrome; benign familial haematuria	Retinal flecks (hyper-reflective inner limiting membrane); possibly mid-peripheral drusen
COL4A4	Collagen, Type IV, Alpha-4	120131	2q36.3	Autosomal recessive Alport syndrome; benign familial haematuria	
COL4A5	Collagen, Type IV, Alpha-5	303630	Xq22.3	X-linked Alport syndrome	

C1QTNF5	Complement component 1, q subcomponent and tumor necrosis factor-related protein 5	608752	11q23.3	Late-onset retinal degeneration	SDD, hard drusen, soft drusen, 'ghost' drusen
EFEMP1	EGF-containing fibulin-like extracellular matrix protein 1	601548	2p16.1	Doyne honeycomb dystrophy; dominant drusen; Mallatia Leventinese	Hard drusen, cuticular drusen that coalesce
FALDH	Fatty aldehyde dehydrogenase	609523	17p11.2	Sjogren-Larsson syndrome	Superficial retinal crystals
IMPG1	Interphotoreceptor matrix proteoglycan 1	602870	6q14.1	Vitelliform macular dystrophy	Macular hard drusen
IMPG2	Interphotoreceptor matrix proteoglycan 2	607056	3q12.3	Vitelliform macular dystrophy; retinitis pigmentosa	Macular hard drusen
LRAT	Lecithin retinol acyltransferase	604863	4q32.1	Leber congenital amaurosis; early onset severe retinal dystrophy; retinitis pigmentosa	White dots
PLA2G5	Phospholipase A2 Group V	601192	1p36.13-p36.12	Familial benign fleck retina	Numerous white dots sparing the macula
PRDM13	Positive Regulatory (PR) Domain containing 13	Not listed	6q16.2	North Carolina Macular Dystrophy	Grade 1 shows small hard drusen-like lesions
PRPH2	Peripherin 2	179605	6p21.1	Macular dystrophy (vitelliform macular dystrophy; pattern dystrophy); retinitis pigmentosa; Leber congenital amaurosis	Outer retinal dots, flecks or deposit
RBP4	Retinol-binding protein 4	180250	10q23.33	Isolated microphthalmia and/or coloboma; retinal dystrophy, iris coloboma, and comedogenic acne syndrome	RPE migration into retina
RDH5	Retinol dehydrogenase 5	601617	12q13.2	Fundus albipunctatus	Numerous white dots sparing the macula
RDH12	Retinol dehydrogenase 12	608830	14q24.1	Leber congenital amaurosis	Heavy RPE migration and macular fibrosis
RLBP1	Retinaldehyde-binding protein 1	180090	15q26.1	Bothnia dystrophy, fundus albipunctatus, Newfoundland rod-cone dystrophy, retinitis pigmentosa	Numerous white dots sparing the macula, evolve to atrophy
RPE65	Retinal pigment epithelium-specific protein 65-kD	180069	1p31.3-p31.2	Leber congenital amaurosis; early onset severe rod-cone dystrophy	White dots

SPG11	Spastic paraplegia gene 11	610844	15q21.1	Autosomal recessive spastic paraplegia 11; juvenile amyotrophic lateral sclerosis 5	Outer retinal deposit, flecks
TIMP3	Tissue inhibitor of metalloproteinase 3	188826	22q12.3	Sorsby fundus dystrophy	SDD, hard drusen, soft drusen
ZFYVE26	Zinc finger FYVE domain-containing protein 26	612012	14q24.1	Autosomal recessive spastic paraplegia 15	Outer retinal deposit, flecks

1.2 Imaging modalities

Given the importance of multi-modal imaging in characterising drusen and drusenoid deposits, we will provide representative examples of non-invasive retinal imaging appearances of most of the diseases discussed, particularly those which are less frequently encountered, or less well-described in the literature.

There is a range of retinal and choroidal imaging technology currently available, some incorporating automated segmentation, volume quantification and even drusen analysis (Kanagasingam et al., 2014). Relative strengths of commercially available systems from different manufacturers will not be discussed. The systems used to generate the images featured in this review are as follows. Colour fundus images in most cases were acquired with the Topcon colour fundus camera (Topcon TRC 50IA, Topcon Corporation, Tokyo, Japan) unless wide-field imaging is specified, in which case images were acquired using the Optos wide-field system (Optos plc, Dunfermline, Scotland, UK), which provides a pseudocolour image generated from the two monochromatic laser wavelengths used. Short wavelength autofluorescence (Appiah et al.), infrared reflectance (IRR) and spectral domain optical coherence tomography (Procter et al.) images were acquired using the Spectralis multi-modal confocal scanning laser ophthalmoscope imaging system (Heidelberg Engineering, Heidelberg, Germany). Some images acquired using the "Multicolor" setting of this instrument (combining red, green and blue wavelength reflectance imaging) are shown. Also, in a few cases, wide-field autofluorescence images acquired with the Optos system are used. Finally, in Figure 21 the OCT scans and colour fundus photograph in the upper panels were acquired using the Topcon 3D-OCT 2000 imaging system (Topcon Corporation, Tokyo, Japan).

2. Biogenesis of drusen and types of subclinical deposit

2.1 Overview of drusen biogenesis

Bruch's membrane is a lamellar extracellular matrix (ECM), consisting of an elastic layer sandwiched between two collagenous membranes, themselves bordered by basement membranes from the RPE (internally) and choriocapillaris (externally). Lipoproteins begin to accumulate within the elastic layer during early adulthood and slowly fill the interfibrillar spaces of both the elastic layer and the inner collagenous layer. The hydraulic conductivity of Bruch's membrane has been shown to drop with age, and this is more pronounced at the macula (Moore et al., 1995). Consequent disruption of transport between RPE and choroid is likely to be of relevance. The site of greatest resistance has been shown to be the inner collagenous layer (Starita et al., 1997). The reduction in transport capability with age appears to be, partly at least, dependent on the lipid content (Starita et al., 1996).

The "lipid wall" has been proposed as a necessary, but not sufficient, step in drusen biogenesis (Curcio et al., 2011). Oxidation of the trapped lipoproteins results in the

generation of toxic intermediates, with consequent activation of the inflammatory cascade, either via direct complement activation or indirectly by inducing tissue injury and triggering apoptosis (Beattie, 2009; Dasari et al., 2010; Kaemmerer et al., 2007). Dendritic cells are subsequently recruited (Hageman et al., 2001). Depending upon the genetic background, this inflammatory response may be abnormally propagated for years, with the addition of peripheral substrates to the initial inflammatory core.

The molecular processes involved in drusen biogenesis are a major focus of research, and several studies have implicated altered heavy metal homeostasis. Maculas affected by AMD have increased levels of iron (Hahn et al., 2003). Iron accumulation has been specifically demonstrated within Bruch's membrane and in RPE and choroidal melanosomes in eyes affected with AMD (Biesemeier et al., 2015). Zinc is likely to play an important role: levels are high in in sub-RPE deposits (Lengyel et al., 2007), and in excess of that required to facilitate oligomerisation of complement factor H and C3b (Nan et al., 2013; the role of complement in drusen formation is discussed below in section 2.3). It is likely that protein self-association may precede or promote subsequent lipid accumulation.

Thompson and colleagues have recently investigated human BM using fluorescence microscopy and X-ray diffraction, identifying small (<20 μm in diameter), hollow hydroxyapatite spherules (Thompson et al., 2015). Secondary ion mass spectrometry imaging confirmed the presence of calcium phosphate in the spherules and identified cholesterol enrichment in their core. They proceeded to show that all types of sub-RPE deposits in the retina contain numerous hydroxyapatite spherules, and are coated with proteins characteristic of sub-RPE deposits, such as complement factor H, vitronectin, and amyloid beta. Hydroxyapatite spherules were also found outside the sub-RPE deposits, ready to bind proteins at the RPE/choroid interface. Based on these discoveries, the authors propose a novel mechanism for the growth, and possibly formation of sub-RPE deposits; this begins with the deposition of hydroxyapatite shells around naturally occurring, cholesterol-containing extracellular lipid droplets at the RPE/choroid interface, proteins and lipids then attach to these shells, resulting in growth of sub-RPE deposits (Thompson et al., 2015).

In addition, the role of alterations in cholesterol homeostasis in drusen development is becoming a subject of increasing research with likely important implications for AMD pathogenesis (Pikuleva and Curcio, 2014).

2.2 Types of subclinical deposit

Long before we are able to visualise drusen, major subclinical changes have already taken place. Thus clinically apparent drusen may be thought of as "the tip of the iceberg". The following sections briefly summarise subclinical deposits with respect to location (z-axis). Figure 1 depicts the development of these changes schematically.

Figure 1. Development of subclinical deposits and soft drusen. In this cartoon the healthy configuration is shown on the left. With ageing (middle diagram), basal laminar deposits accumulate (internal to the RPE basement membrane) and vacuoles appear within RPE cells; early basal linear deposits (external to the RPE basement membrane) may also develop. The right-hand side shows more extensive BlinD coalescing to form soft drusen.

(PR OS, photoreceptor outer segment; RPE, retinal pigment epithelium; BL, basal lamina; CL, collagenous layer; EL, elastic layer; CC, choriocapillaris; BlamD, basal laminar deposit; BlinD, basal linear deposit).

2.2.1 Subclinical deposit internal to the RPE basement membrane

Histologically, these early preclinical stages are defined by the presence of widespread thickening of BM, originally termed basal linear deposit (BlinD) by Sarks et al. (Loffler and Lee, 1986; Sarks, 1973). As the overlying RPE remains intact, this thickening is ophthalmoscopically invisible. Histologically, with a trichrome stain, the deposit appears similar to collagen, whilst with a periodic acid Schiff (PAS) stain it shares similarity with glycoproteins. Using electron microscopy**,** the material is visible as small deposits on the RPE basement membrane (basal lamina), between the basal lamina and the cytoplasmic membrane. This deposit, previously referred to as BlinD, was then renamed basal laminar deposit (BlamD), due to its accumulation along the basal lamina of the RPE (van der Schaft et al., 1991). It consists mainly of fibrous long-spacing collagen (FLSC), structures that are also seen on ageing basement membrane in the cornea (Descemet membrane) and iridocorneal angle (trabecular basement membrane) (van der Schaft et al., 1991). As this material accumulates, the RPE cells are slowly elevated from their basement membrane until subclinical (microscopic) detachments develop.

BlamD does not appear to be specific to or "diagnostic" for AMD and is part of ageing. It may be thought of a generic epithelial cell stress response, as the ageing RPE secretes excessive amount of basement membrane in an attempt to remain adherent. There is however a strong relationship between macular BlamD and the subsequent development of exudative AMD and visual loss (Feeney-Burns and Ellersieck, 1985; Loffler and Lee, 1986; Spraul and Grossniklaus, 1997). BlamD-like deposition is observed in monogenic macular disorders with a clinical appearance similar to AMD namely Sorsby fundus dystrophy, Late Onset Retinal Degeneration (Folwell et al.) and Dominant Drusen (Milam et al., 2000). Most recently Loeffler and Lee have suggested that the term basement membrane deposit (BMD) be used instead of BlamD (Loeffler and Lee, 1998). As BlinD had become an orphan term, it was subsequently reintroduced by Green and Enger to describe the diffuse deposit that accumulates external to the RPE basement membrane (Green and Enger, 1993).

2.2.2 Subclinical deposit external to the RPE basement membrane

BlinD consists primarily of a diffuse collection of membranous debris located between the RPE basement membrane and the inner collagenous layer of BM. BlinD was initially described using light microscopy as lipid-like vesicles with varying diameters, as the membranous collections themselves were not visible (Sarks et al., 1980). The material has subsequently been shown to be comprised primarily of lipoprotein particles containing neutral lipids, including esterified cholesterol (Curcio et al., 2005; Sarks et al., 2007; Sarks et al., 1980). Imaged by electron microscopy, these fragments appear to be released from the basal surfaces of the RPE in blebs, analogous to the shedding of outer segment discs by the

photoreceptors (Sarks et al., 1988). This material is deposited in layers, a little scattered within BlamD, whilst the majority is between the RPE basement membrane and the inner collagenous layer of BM, forming BlinD. Focal accumulation of membranous debris result in basal mounds, and the degree of membranous debris appears to influence the course of disease (Sarks et al., 2007). Basal mounds do not appear until BlamD have thickened sufficiently, indicating that membranous debris and early BlinD continue to develop together. As the mounds enlarge and fuse together, the RPE cells show progressive dysfunction and eventually die. The accumulation of this material is thus dependent upon a ready source of material, photoreceptor outer segment, and processing machinery - the RPE. In the absence of either of these, membranous debris will not accumulate. Membranous debris formation may also be thought of as an additional stress response; non-apoptotic cell blebbing has been observed in RPE cells cultured *in vitro* when exposed to stressors (Malorni et al., 1991; Marin-Castano et al., 2005).

2.2.3 Subclinical deposit within the RPE

In addition to being found external to the RPE basement membrane, membranous debris also accumulate inside the RPE cells within vacuoles, and at the apical surface (Sarks et al., 1988).

2.2.4 Subclinical deposit internal to the RPE apical membrane (between the RPE and photoreceptors)

A photoreceptor-derived source for subretinal deposit was first proposed by Sarks, as the membranous debris disappear when the photoreceptors undergo atrophy (Sarks et al., 1988). Others have contested this, suggesting that the filipin fluorescence of the sub-retinal debris is much higher than that seen in photoreceptor outer segments, and that the deposit lacks immunoreactivity for key photoreceptor proteins (GFAP, opsin) (Curcio et al., 2005). It is possible however that significant outer segment processing takes place, accounting for the difference in composition. Indeed *in vitro* work has confirmed that the removal of phospholipid elevates the cholesterol concentration from that found in native outer segments to the level expected in subretinal deposit (Kruth, 1985; Skarlatos et al., 1993). Alternatively apical extrusion of material with a slightly different composition may represent a separate consequence of RPE stress.

2.2.5 Summary of subclinical responses

Subclinical changes therefore set the scene for the future phenotype. Progressive BlamD accumulation indicates one cellular response to stress, which eventually may manifest as RPE hyperplasia and atrophy, and occurs in the absence of soft drusen. Membranous debris accumulation represents a second way in which the RPE responds to stress, and the direction (apical versus basal) and magnitude of this reaction determines the clinical signs. If the debris accumulates internal to the RPE as a result of apical movement, subretinal

deposit rather than conventional drusen form. RPE dysfunction may additionally compromise photoreceptor outer segment phagocytosis, adding to the accumulating deposit. If the debris extends into BM from the basal RPE surface via a separate mechanism, soft drusen form. Historically this has been considered the hallmark of AMD and may represent one consequence of the para-inflammatory process (Xu et al., 2009).The patterns of RPE response to stress are therefore likely to determine the clinical signs that later develop – RPE atrophy and hyperplasia, soft drusen formation and subretinal drusenoid deposit.

2.3 Complement and drusen

Proteins of the complement system have long been identified as key druse components (Baudouin et al., 1992; van der Schaft et al., 1993) and the complement cascade is thought to be activated by the products of visual cycle (Anderson et al., 2010). Retinoids accumulating inside the RPE are inaccessible to proteins of the complement cascade, however once externalised they are free to interact with the various forms of C3, and these locally deposited activation products (C3a, C3b, C3dg) then serve as ligands for leukocyte receptors (Anderson et al., 2010). Drusen also contain the regulatory protein CFH. Histological studies have been followed by genetic endeavours, aiming to identify risk factors for AMD. In 2005 four groups independently reported a significant association between AMD and a common variant (rs1061170) in CFH (Edwards et al., 2005; Hageman et al., 2005; Haines et al., 2005; Klein et al., 2005). This variant (Y402H) is associated with functional consequences, as it limits the binding of CFH to various complement-activating targets, reducing its inhibitory activity and thus prolonging the activity of C3 convertase (Herbert et al., 2007; Laine et al., 2007). Other rare variants in *CFH* have also been reported (R1210C, R53C and D90G) (Raychaudhuri et al., 2011; Yu et al., 2014). R1210C is extremely rare, with a minor allele frequency of 0.0173% (ExAC database accessed 16.11.15), but has an even stronger association with AMD than Y402H, perhaps acting as a functionally null allele (Raychaudhuri et al., 2011). R1210C is also associated with atypical hemolytic uremic syndrome (OMIM 134371). The drusen phenotype associated with the R1210C risk allele has recently been described (Ferrara and Seddon, 2015). The authors identified widespread soft drusen, both at the macular and outside the arcades, an unusual combination as such drusen are rarely observed in the peripheral retina. It is plausible that a spectrum of polymorphisms in *CFH, CFB, CFI C2, C3 and C9* all contribute to drusen biogenesis, with additional stimuli arriving from exogenous factors such as smoking. Identifying alleles of low penetrance, acting in a complex (oligogenic) manner will be difficult. Studies designed to enrich for more highly penetrant alleles, by recruiting extreme phenotypes e.g. “young-onset AMD”, will help.

3. Clinically detectable deposits (seen in ageing and AMD)

Historically the assessment of drusen has relied on either clinical examination or the evaluation of colour fundus photographs and this technique has produced the widely used Wisconsin Age-Related Maculopathy Grading System, the International Classification system and the AREDS (Age-related Eye Disease Study) classification system (Bird et al., 1995; Davis et al., 2005; Klein et al., 1991). These systems yield the terms, “hard drusen”, “intermediate drusen”, and “soft drusen” (the latter often used synonymously with “large drusen”). This is predominantly, and somewhat arbitrarily, based on size: hard drusen are smaller than 63 µm (this diameter corresponding to half the width of a large vein at the optic disc margin); intermediate drusen are 63-125 µm; soft (‘large’) drusen are larger than 125 µm. A classification based purely on size however will miss the fact that small soft drusen exist, and consequently will report them as hard drusen. Similarly, cuticular drusen, which are also small in size, may be simply classed as hard drusen if graded from photographs alone.

In a more recent clinical classification scale (Ferris et al., 2013), individuals over 55 years of age with small (<63 µm) drusen were considered to have normal ageing, with the term “drupelets” also suggested for these lesions. Those with medium drusen (63-125 µm) and no pigmentary abnormalities were classified as early AMD. Those with larger drusen, or with pigmentary abnormalities associated with medium drusen, had intermediate AMD (see Figure 2). Individuals had late AMD if they had neovascular AMD or geographic atrophy.

The risk of developing late AMD increases with increasing drusen size and also with the presence of pigmentary abnormalities. If lesions are present in both eyes, the risk increases further. Ferris et al. (2013) summarised previous AREDS data to provide the five-year rate of developing advanced AMD for different lesion types (see their Table 1). In the absence of pigment abnormalities in either eye, the rate of developing advanced AMD was 0.4% in subjects with no drusen or small drusen only. The rates were 0.5% and 2.1% for subjects with intermediate drusen in one eye or both eyes respectively; these rates increased respectively to 3.9% and 13% for large drusen. If pigmentary abnormalities were also present in both eyes, the rates risks increased significantly: for subjects with intermediate drusen in one or both eyes, the rates were 12.9% and 20% respectively; for large drusen, the rates were 25.6% and 47.3% respectively. In addition, the presence of reticular pseudodrusen (Section 3.5) appears to be have prognostic significance: Zhou et al. (2016) recently showed, from analysis of fellow eyes in the Comparison of Age-Related Macular Degeneration Treatment Trials, that pseudodrusen were associated independently with a higher risk of advanced AMD; in particular, dot pseudodrusen were associated with neovascular AMD whilst confluent pseudodrusen were associated with geographic atrophy.

The incidence and prevalence of different drusen subtypes is known to vary between populations. When participants of the Blue Mountains Eye Study and the Singapore Epidemiology of Eye Disease Study were compared (Joachim et al., 2014), age-standardised prevalence of distinct soft drusen was significantly higher in Singaporeans compared to Australians whilst indistinct soft drusen and reticular drusen were more prevalent in Australians. In addition, Australians were more likely to have soft drusen in the central macula. Fisher et al. (2016) recently described incidence of AMD in different ethnicities residing in the United States from the Multi-Ethnic Study of Atherosclerosis cohort (3811

participants aged 46 to 86). The overall 8-year age- and sex-standardized incidence was 4.1% for early AMD and 2.3% for late AMD. Incidence of early and late AMD respectively in different ethnicities was as follows: 5.3% and 4.1% in whites; 4.5% and 2.2% in Chinese; 3.3% and 0.8% in Hispanics; black participants had the lowest incidences (1.6% and 0.4%). For the combined group as a whole, previously described AMD risk factors, namely age, ethnicity, current smoking, hyperopia, and AMD-susceptibility genotypes Complement Factor H (CFH) RS1061170 and Age Related Maculopathy Susceptibility 2 (ARMS2) RS3793917 were independently associated with incident early AMD. Interestingly, Chinese subjects had a greater incidence of drusen greater than 125 micrometres in diameter than whites (10.9 vs 8.4%) and greater incidence of soft distinct drusen (18.4% vs 11.9%); white subjects on the other hand had greater incidence of soft indistinct drusen than Chinese subjects (5.8% vs 3.8%), whilst both ethnicities had equal incidence (3.3%) for drusen area greater of 500 square micrometres or greater (Fisher et al, 2016).

In the following section we shall discuss, in some detail, the varied phenotypes associated with drusen and drusenoid deposits. Historically, specific drusen subtypes have been associated with only one or two pathological processes; however, as more detailed descriptions of the rarer retinal phenotypes are reported we are beginning to appreciate that these deposits may represent a final common pathway for divergent pathological processes. As AMD is the most commonly encountered disease associated with drusen most of the clinical studies referenced will relate to AMD; however, that is not to say the phenotype being described is only seen in that condition.

Hard and soft drusen will be considered first as they are the most commonly encountered. Cuticular drusen, a specific sub-type of small drusen, will then follow. Following the discussion of these conventional drusen phenotypes will be a short description of refractile or calcified drusen (Section 3.4), as calcification may be a feature of all drusen.

Focal deposits, accumulating between the outer retina and RPE (subretinal drusenoid deposit (SDD), also termed reticular pseudodrusen (RPD)), often observed alongside other forms of conventional drusen will then be discussed. In each case, appearance on colour photography will be discussed, followed by histological features, aiming to provide context to the clinical signs. Characteristic features seen on other forms of imaging, both non-invasive (spectral domain OCT and SWAF) and invasive (fluorescein and indocyanine green angiography) will be presented, as well as, in the case of RPD, the addition of a section describing appearance and insights revealed from multimodal reflectance imaging. Although not truly drusen (which are deposits located immediately external to the RPE), they share many features with them.

Table 2 summarises the imaging features of the drusen subtypes. Most of the drusen are features of ageing or age-related maculopathy, although cuticular drusen may be seen in younger subjects. In the final part of this section, we discuss other structures identified on OCT that have been termed outer retinal corrugations, hyperreflective pyramidal structures and “ghost drusen” (Section 3.6).

Table 2. Features of different drusen sub-types on retinal imaging. Near infra red reflectance imaging (not included) is particularly useful for identifying reticular pseudodrusen (see text).

	Small Drusen		Large Drusen	Subretinal deposit
	Hard drusen	**Cuticular drusen**	**Soft drusen**	**Reticular pseudodrusen**
Colour fundus photography (CFP)	Small (<63 µm) discrete yellow-white deposits with distinct edges. Found in macula and peripheral retina.	Numerous (>50) small (25-75 µm) dot-like deposits in macula and peripheral retina (may be more numerous in periphery, and first visible here). Early stages not readily detectable on CFP.	Larger (usually >125 µm) less discrete deposits found only in the posterior pole (more frequent in central macula, superior and temporal quadrants). Yellow appearance; central part may be whiter.	Variable diameter (c. 100 µm); may be dot-like or reticular. Found preferentially in the perifovea (often more predominant superiorly). Whiter and more irregular than conventional drusen. Near infrared CSLO reflectance imaging is more sensitive than CFP.
Short wavelength auto-fluorescence	Foci of reduced AF sometimes surrounded by increased AF	Hypoautofluorescent dots. May appear larger than on CFP (although CFP may be more sensitive).	Moderate hyperautofluorescence. Larger drusen may show heterogenous AF signal.	Reticular pattern, hypoautofluorescent. A minority may be atypically hyperautofluorescent.
OCT	Small sub-RPE deposits, hyperreflective. Sometimes less discernible than on colour fundus photography.	Sub-RPE. Prolate shape, moderate hyperreflectivity. Saw-tooth configuration. Larger drusen erode into the RPE monolayer; apex only thinly covered by RPE.	Larger sub-RPE deposits, hyperreflective.	Deposits between the RPE and inner segment ellipsoid lines (stages 1 and 2), later breaking through the ellipsoid line (stage 3) and subsequently fading (Stage 4). Light stripes may be visible in the underlying choroid.
Fundus fluorescein angiography	Possible mild hyperfluorescence	"Starry sky" appearance: densely distributed hyperfluorescent dots. Earlier lesions not visible (but seen on AF).	Variable, usually some late hyperfluorescence.	Hypofluorescence or no change
Indocyanine green angiography	Hyperfluorescent	Early hyperfluorescence	Hypofluorescent	Hypofluorescence in mid to late-phase.

Although not a primary focus of this review, mention will be made in some of the following subsections of neovascular complications. Neovascularisation (associated frequently, but not exclusively, with AMD) has been classified as type 1 (below the RPE), type 2 (above the RPE, in the subretinal space) and type 3 (also termed retinal angiomatous proliferation), with SD-OCT being the imaging modality most suited to establishing this distinction *in vivo* Type 1 membranes appear most likely to be associated with drusen or the subclinical deposits mentioned in the Section 2; a recent histopathological study confirmed the presence of basal laminar deposits in type 1 neovascularisation (Curcio et al., 2015). Other types may develop in absence of drusen or may be associated with the presence of subretinal drusenoid deposit (Freund et al., 2010).

3.1 Hard drusen

3.1.1 Colour fundus photography of hard drusen

Hard drusen are defined as discrete yellow-white deposits sited underneath the RPE. They are small, with a diameter of less than 63µm, have sharply defined edges and uniform colour density from their centre to edge (Age-Related Eye Disease Study Research, 2001; Bird et al., 1995). Figure 2 shows imaging from an AMD patient with hard and soft drusen. Small, hard drusen are common with a prevalence of 93.6% in subjects aged 43 to 86 years in the Beaver Dam Eye study. Hard drusen are the only drusenoid deposits that are considered a normal consequence of age (Rudolf et al., 2008a), though AMD frequently begins with hard drusen.

Widefield photography is particularly useful for identifying the distribution of drusen throughout the retina. Hard drusen are widespread, and are found throughout the peripheral (outside the vascular arcades) as well as central retina. Hard drusen may also be more visible than other drusen despite their small size, as they are often refractile.

3.1.2 Histology of hard drusen

In a recent analysis of druse subtypes, Rudolf and colleagues categorised drusen based on histological appearance (Rudolf et al., 2008a). Deposits that were round, with sharply demarcated borders filled with homogeneous hyalinised material were called hard drusen. They have an eosinophillic, amorphous appearance and are PAS positive, shared by other drusen types, but are significantly more compact structures than soft drusen. In comparison with other druse types, hard drusen, both at the macula and in the periphery were associated with a loss of overlying RPE cells. Centrally located hard drusen were also found to be larger, associated with a thicker BlamD and had a more heterogenous substructure with more amyloid assemblies (concentric ring like structures of β-amyloid) than peripheral hard drusen. In addition, macular hard drusen tend to calcify more readily than peripheral drusen. Hard drusen do share similarities with soft drusen, as both selectively accumulate proteins, some of which may be plasma derived (amyloid P component, prothrombin) whist others are more likely to be locally secreted (vitronectin, complement proteins C3, C5, and C9, and apolipoproteins B and E) (Anderson et al., 1999; Osusky et al., 1997; Ozaki et al., 1999).

3.1.3 OCT of hard drusen

Whilst OCT has been effectively used to help classify drusen there has been relatively little published on the characteristics of hard drusen, as researchers have preferred to concentrate on subtypes with a stronger disease association. Khanifar and colleagues described 17 morphological druse patterns on OCT imaging, broadly separating deposits based on shape, reflectivity and internal consistency (Khanifar et al., 2008). An important finding when they attempted to correlate photographic findings (hard, soft, calcific or

reticular drusen) with OCT findings was that no one druse type had a specific OCT signature. Interestingly, the authors were unable to identify any hard drusen in their photographs, unusual for eyes with AMD. For small, flat hard drusen, however, colour fundus photography might be more sensitive than OCT, as yellow on red colour discrimination over a druse diameter may be more readily discernible than a separation of highly reflective lines on OCT representing BM and the RPE.

3.1.4 Fundus autofluorescence of hard drusen

In 2000 Delori and colleagues reported a novel pattern of druse autofluorescence consisting of decreased AF in the centre of the druse surrounded, in most cases by an annulus of increased AF (Delori et al., 2000). The dark central focus of the AF pattern is not black, but is as much as 30% lower than the surrounding background (Delori et al., 2000). The reduction in AF was however not thought to be due to RPE melanin as monochromatic imaging showed no evidence of melanin absorption (Delori et al., 2000). Several explanations were then proposed, primarily relating to the number of lipofuscin granules in the overlying RPE. The authors reported that hard and soft drusen (between 60 and 175 µm in size) are characterised by foci of reduced autofluorescence that may or may not be surrounded by an annulus of increased autofluorescence. Irregular areas of low AF can be observed in large drusen, consistent with the idea that they develop as a result of fusion of smaller hard or soft drusen (Delori et al., 2000).

3.1.5 Fluorescein angiography of hard drusen

Hard drusen may show mild hyperfluorescence on fundus fluorescein angiography (FFA). Hyperfluorescence may also be seen on indocyanine green angiography (ICGA). Fluorescein binding correlates more with the biochemical composition of drusen rather than size: deposits with a high content of phospholipids bind more fluorescein, and tend to have high proportions of fibronectin; deposits with higher proportions of neutral lipids show less fluorescein binding (Pauleikhoff, Zuels et al., 1992).

3.2 Soft drusen

3.2.1 Colour fundus photography of soft drusen

In terms of x-y location, soft drusen are only found at the posterior pole of the fundus, more frequently in the central macula, and in the superior and temporal quadrants of the macula (Wang, Chappell et al., 1996; Knudtson, Klein et al., 2004). They appear less well demarcated than hard drusen (Figure 2), as mound-like elevations, usually ≥ 125µm in diameter but on occasion smaller. The central portion of the druse may appear whiter than its yellow edge (Spaide and Curcio 2010). Soft distinct drusen have a uniform density whereas soft indistinct drusen have a graded density from their centre to periphery with blurred edges.

Figure 2. Retinal imaging from the left eye of an 84-year old man with AMD. *A*, colour photograph shows multiple drusen of varying size (small, medium and large) as well as pigmentary change. *B*, Short-wavelength AF image shows variable hyper- and hypo-autofluorescence. *C*, Horizontal OCT scan with corresponding infrared reflectance image showing OCT appearance of large and small drusen.

3.2.2 Histology of soft drusen

Soft drusen are low mounds that can be connected by basal linear deposit. They are only found at the posterior pole. RPE coverage (number of overlying cells) does not seem to be reduced over soft drusen, although their morphology and pigmentation may be affected (Rudolf et al., 2008). Both soft drusen and BlinD are filled with 'membranous debris', appearing as coiled membranes and vesicular outlines (Rudolf et al., 2008a; Sarks et al., 1988). Membranous debris has also been referred to as 'lipoprotein derived debris' aiming to reflect the high esterified cholesterol content in these lesions, whilst retaining the possibility that shed cellular membranes do appear in drusen (Wang et al., 2009a). This debris appears to comprise solid particles rich in neutral lipid (Curcio et al., 2005). Soft drusen contain significant pools of esterified cholesterol and as a result it has been suggested that soft drusen record a higher cholesterol content and lower lipoprotein content than hard drusen (Malek et al., 2003). Consequently both soft drusen and BlinD are easily disrupted, and do not survive chemical processing well. It has been hypothesized that the presence of separation between the RPE basement membrane and the inner collagenous layer of BM by such material may facilitate the spread of choroidal neovascularisation within this cleavage plane, possibly helping explain the association between soft drusen and advanced AMD.

3.2.3 OCT of soft drusen

Soft drusen are seen as mound-shaped, moderately hyperreflective elevations of the RPE on OCT of varying size. The thickness does not seem to correlate with the colour on fundus photography (Spaide & Curcio, 2010). Overall druse size however seems to be very similar between the two modalities (Jain et al., 2010). At the extremes of size, small drusen appear easier to detect using colour fundus photography whilst larger drusen may be more accurately sized with OCT due to better visualisation of their boundaries (Jain et al., 2010). As soft drusen and BlinD represent two forms of the same AMD lesion, they display a dynamic relationship that may be visualised with detailed retinal imaging. Despite appreciating such changes, their evolutionary course is not predictable, as sequential OCT imaging studies have identified a range of endpoints (minimal change, drusen regression, increase in number of drusen, outer retinal atrophy, neovascularisation) from similar starting points (Yehoshua et al., 2011).

3.2.4 Fundus autofluorescence of soft drusen

As first reported by Delori and colleagues, on autofluorescence imaging the edges of some soft drusen appear slightly hyper-autofluorescent as compared with the central portion (Delori 1999). This is more easily visualised using a fundus camera based system than CSLO. This might be related to the different excitatory wavelengths of the two systems (approximately 530-580 nm for camera based system; 488 nm for CSLO).

3.2.5 Fluorescein angiography of soft drusen

Soft drusen can show varying levels of fluorescence, although usually they show some evidence of late hyperfluorescence. Hypofluorescence may be seen on ICGA. Fluorescein binding relates to the balance between neutral and polar lipids as mentioned earlier.

3.3 Cuticular drusen

These are multiple small drusen that may cluster, and were first described with reference to their characteristic "starry sky" appearance on fluorescein angiography (Section 3.3.5). They are most strongly associated with AMD, but also dense deposit disease (type 2 membranoproliferative glomerulonephritis/C3 glomerulonephritis/C3 nephropathy) (McAvoy and Silvestri, 2005) and causative variants in the gene CFH (Complement Factor H) (Boon et al., 2008). They are a type of small, hard, early onset drusen, and have also been termed basal laminar drusen, though it has been suggested that the latter term is a misnomer (Russell et al., 2000). Figure 3 shows imaging from a patient with cuticular drusen.

Figure 3. Images from the right eye of a 47 year-old man with cuticular drusen. *A,* Colour fundus photograph showing drusen and pigmentary change. *B,* Fundus fluorescein angiogram (at 27 seconds after dye injection) showing the characteristic "starry sky" appearance. *C,* Short-wavelength AF showing a mixture of hypo and hyper-autofluorescence. *D,* Horizontal enhanced depth OCT scan with corresponding infrared reflectance image.

3.3.1 Colour fundus photography of cuticular drusen

Cuticular drusen are numerous (>50), small (25-75um), round, dot-like drusen that densely populate the retina (Gass, 1977). They occur both in the macula and peripheral retina. In the periphery they may be even more numerous, and occur in regions with senile reticular pigmentary change (Boon et al., 2013; Gass, 1977; van de Ven et al., 2012). The periphery is also the site where cuticular drusen are often first visible (Boon et al., 2013). Individually they may be mistaken for hard drusen, and it is their occurrence in such large numbers that facilitates identification on colour fundus photography. Over time, as drusen accumulate, individual drusen may eventually coalesce, and they can also be mistaken for soft drusen at this stage. Clinical detection is otherwise difficult since the lesions are not associated with abnormal pigmentation, at least not until late on, and so are of low contrast against the RPE.

Their low elevation similarly does not allow lesions to be distinguished stereoscopically. As a result colour fundus photography is not sufficiently sensitive at identifying cuticular drusen, particularly in their early stages. Larger lesions may be detected with red-free photography or infrared reflectance imaging with a CSLO, as both modalities enhance contrast with the RPE.

3.3.2 Histology of cuticular drusen

Histological analysis followed the initial clinical description of cuticular drusen. Using both light and electron microscopy, diffuse and nodular thickening of the inner portion of BM was identified. The thickening was associated with accumulation of vesicular and curvilinear membranous profiles and basement membrane-like material, apparently derived from the RPE (Kenyon et al., 1985). Gass proposed that these drusen were actually focal nodular thickenings of the RPE basal lamina; a hypothesis that was later challenged by Russell and colleagues (Gass et al., 1985; Russell et al., 2000). They argued that cuticular drusen were cellular aggregations (carbohydrates, lipid and protein) located between the basal lamina of the RPE and the inner collagenous layer of BM (Russell et al., 2000). The identified genetic associations are in keeping with a role of parainflammation (variants in *CFH*, *CFI*) (Boon et al., 2008; Grassi et al., 2007; Seddon et al., 2009; van de Ven et al., 2012) and ECM dysregulation (Albig and Schiemann, 2005; Mullins, 2007; Nguyen et al., 2004; Stone et al., 2004), which supports the view that alterations in BM anatomy or function contribute to the formation of cuticular drusen.

3.3.3 OCT of cuticular drusen

In cross-section cuticular drusen have a prolate shape, with moderate hyperreflectivity. As the basal diameter for many cuticular drusen is about the same as their height they assume a saw tooth configuration in SD-OCT examination (Spaide and Curcio, 2010). Larger cuticular drusen seem to erode into the RPE monolayer and so the apex of each cuticular druse has only a thin covering of pigment epithelium. These RPE changes may reverse as drusen regress (van de Ven et al., 2012). Cuticular drusen have been associated with AMD and pseudovitelliform macular detachment, with one study suggesting that neovascularization is present in up to one third of eyes (Boon et al., 2013; Cohen et al., 1994; Gass et al., 1985). Others have described subretinal fluid in the absence of CNVM, attributed to loss of RPE function and have therefore cautioned against the injudicious use of anti-VEGF therapy (Cohen et al., 1994; Pilli et al., 2011). It appears therefore that in the advanced stages, the presence of significant coalesced cuticular drusen also implies widespread loss of RPE function.

3.3.4 Fundus autofluorescence of cuticular drusen

Recently Meyerle and colleagues have compared the appearance of cuticular drusen using different imaging modalities (Meyerle et al., 2007). Small “early” cuticular drusen that have

not eroded through the RPE tend not to be visible by FFA but are identifiable by AF, as discrete hypoautofluorescent dots (Meyerle et al., 2007). Larger lesions tend to have a similar appearance (but fluoresce after dye injection). Occasionally, as individual drusen merge forming larger deposits, they may exhibit greater autofluorescence levels. When drusen are compared using colour photography and AF, they appear larger in the AF images, suggesting that only the centre of the druse is identified with white light (Meyerle et al., 2007).

3.3.5 Fundus fluorescein angiography of cuticular drusen

These drusen were first recognised by their "starry sky" appearance on FFA, a reference to the multitude of densely packed hyperfluorescent deposits (Gass, 1977). Cuticular drusen fluoresce brightly from their apices, probably as a result of focal erosion of the overlying RPE and consequent window defect into the choriocapillaris. Less mature drusen do not possess this property. As expected, their fluorescence (of choroidal origin) begins earlier in the angiogram than is seen with other drusen. The alternative hypothesis, that the bright fluorescence results from a uniquely hydrophilic core, is perhaps less likely, as ultrastructurally cuticular drusen appear similar to other types of drusen (Russell et al., 2000). On ICGA, early hyperfluorescence is seen.

3.4 Calcified drusen

The finding (described in Section 2.1) of hypdroxyapatite spherules in all types of subretinal deposits (Thompson et al., 2015) suggests that all drusen are calcified, just to differing extents. The more calcified deposits appear phenotypically different, however, from those with lower calcium content. Suzuki and associates have investigated this performing multimodal imaging on 10 eyes (Suzuki et al., 2015). They report that calcified drusen are hypoautofluorescent, although this varied with the deposit location, with central calcific drusen casting a larger hypofluorescent shadow than the peripherally placed drusen. They also identified hyperautofluorescent "conventional" drusen located peripheral to calcified drusen. Imaging these lesions with SD-OCT demonstrated that the calcified drusen have a heterogeneous internal hyperreflectivity, with dots and curvilinear structures. Alongside these clinical signs the authors were additionally able to describe histological changes in 19 calcified drusen from 6 donor eyes. All contained mineral deposits consistent with calcium. The overlying RPE was disrupted in all but two cases and most were associated with morphological changes in the photoreceptor outer segment. In addition, some drusen also contained Müller cell processes, RPE cells, or macrophages (Suzuki et al., 2015).

Calcification is likely to be vital for drusen formation, with levels of calcium changing throughout their lifecycle. As drusen eventually regress, with increasing chronicity, their calcium content may increase. All drusen are thought to contain some calcium, perhaps essential for formation, and as such calcific drusen are not a unique type of drusen; rather, calcification may correlate with druse age.

3.5 Reticular pseudodrusen (RPD)

In 1990 Mimoun et al. coined the phrase “pseudodrusen visible en lumière bleue” (pseudodrusen visible with blue reflectance fundus photography) to describe retinal lesions with a variable diameter of about 100 microns that did not appear hyperfluorescent on fluorescein angiography (Mimoun et al., 1990). They were considered a variant of conventional drusen and thought to arise from below the RPE. Accordingly, a year later, these deposits were then included in the Wisconsin age-related maculopathy grading system as “ill-defined networks of broad, interlacing ribbons” and Klein referred to them as reticular drusen (Klein et al., 1991). No comment was made regarding their significance however. With the advent of newer imaging techniques, the original conclusions were questioned and the nomenclature of this drusen type changed. Smith et al. introduced the term “reticular macular disease” and Zweifel et al. favoured the term “subretinal drusenoid deposits” (SDD) (Smith et al., 2009; Zweifel et al., 2010). Others debate whether reticular pseudodrusen are indeed the same entity as subretinal drusenoid deposit, citing disparity between the two when different imaging modalities are used (Grewal et al., 2014; Sohrab et al., 2011). Whilst co-registration error is a plausible explanation, studies designed to account for this still suggest that RPD and SDD may not be topographically identical (Heiferman et al., 2015). Here we will review the characteristic features of these lesions as we currently understand them. We choose to use the historical term RPD when referring to signs of ageing/AMD, and SDD in reference to non-AMD pathology, as the latter simply refers to the anatomical location in which a variety of deposit may accumulate, in association with a range of diseases. It remains to be definitively determined if RPD are a subtype of SDD or in fact the same lesion.

3.5.1 Colour fundus photography of reticular pseudodrusen

RPD were first identified with blue light photography (Mimoun et al., 1990). On colour images, RPD may appear as either dot-like or reticular deposits, more blue, or at least whiter, than conventional soft drusen. Unlike soft drusen, which have a predilection for the foveal region, RPD are most often first noted in the upper part of the macula sparing the fovea. As they spread outwards the gaps in the network narrow and ultimately the deposits become unrecognisable, producing a featureless yellow or yellow-grey background. RPD also fade around neovascular membranes and hence they have been considered a transient phenomenon; extramacular RPD however are often more stable in appearance.

Generally the *en face* appearance of individual RPD is more irregular, sinusoidal or ring shaped compared to the typical round shape of conventional drusen. Despite this they tend to have a uniform pattern across a large retinal area, in contrast to other drusen that are more randomly distributed. RPD tend not to be associated with co-existing pigmentary change. Whilst conventional drusen can abut the optic nerve, RPD appear not to do so, and extend only as far as the RPE edge. The fact the central fovea and peripapillary retina, both cone rich regions, are spared may be significant for theories of RPD biogenesis. RPD also

appear larger in colour images when compared to near infrared reflectance (NIRR) images. Suzuki et al. have recently shown that the ribbon subtype of RPD are more easily identifiable on colour photography compared with infrared reflectance (Suzuki et al., 2014). The high specificity of blue wavelength and red-free light for reflective deposits above the RPE may be in part due to the high absorbance of blue light by RPE melanosome, increasing the contrast between reticular lesions and the darker background. Despite good specificity, monochromatic blue and red-free light offer low sensitivity as they are highly affected by media opacity. The appearance of RPD on confocal scanning laser ophthalmoloscopy (Macauley et al.) will be described subsequently.

3.5.2 Histology of reticular pseudodrusen

Location (Z axis)

Prior to their clinical recognition subretinal deposit had been identified histologically. Sarks et al used low magnification transmission electron microscopy (TEM), to show well organized, spherical, and homogeneous aggregations of membranous debris (Sarks et al., 1988). These deposits were only present where photoreceptors co-existed. Following on from the original clinical description, Arnold et al. were the first to correlate clinical findings with histological changes (Arnold et al., 1995). They analysed images from 100 patients with reticular pseudodrusen retrospectively, and performed a histological examination in a single eye with early stage disease. They were able to confirm that pseudodrusen did not correspond to the accumulation of basal laminar or basal linear deposit, nor with conventional drusen, and speculated that the reticular pattern correlates with the lobular choroid anatomy, identifying selective loss of the middle choroidal small vessels. They concluded by proposing that RPD originate as a primary choroidal disease, manifest as vascular attenuation and reticular fibrosis, and proposed the term “reticular pseudodrusen” (RPD) (Arnold et al., 1995). The RPD themselves however were not identifiable within the sections (as the retina was missing) and the authors had to infer their location from clinical observations, potentially weakening their correlative conclusions. Sixteen years later, the same group were able to perform a more complete histological retinal examination, again of a single eye with RPD, however this time they were able to identify subretinal deposition of membranous deposit. They concluded that the RPD phenotype resulted from material collecting internal to the RPE (Sarks et al., 2011).

Location (X-Y)

RPD are found preferentially at a perifoveal location. Within the perifovea, the superior retina appears to be more severely affected (Curcio et al., 2013). BlinD in contrast is thickest at the fovea, where cones are maximally dense (Curcio et al., 2013). These anatomical differences suggest that RPD and BlinD may reflect differences in rod and cone physiology. Where RPD and BlinD do show topographical overlap, they tend not to appear on opposite aspects of the same RPE cells (Curcio et al., 2013). In recent imaging studies, RPD have been

shown to follow the choroidal vasculature, supporting a role for the choroid in their aetiology as previously postulated (Grewal et al., 2014).

Composition

Postmortem studies have identified that RPD share superficial ultrastructural and compositional similarities with soft drusen. These include the presence of membranous vesicles, membrane-bounded particles with neutral lipid interiors, unesterified cholesterol (UC), apolipoprotein E (apoE), complement factor H, and vitronectin (Rudolf et al., 2008b). The same material has also been identified enclosed within RPE intracellular vacuoles and so it has been suggested that these vacuoles eventually release their contents, forming conventional drusen at the basolateral RPE surface or RPD if released from the apical surface (Curcio et al., 2013; Curcio and Millican, 1999; Curcio et al., 2005; Sarks et al., 1988; Sarks et al., 2007). It is quite conceivable that a metabolically stressed RPE cell may lose its polarity, resulting in material deposition on its internal rather than external surface. The fact that BlinD and RPD tend not to occur on either side of the same cell is in keeping with this hypothesis. RPD however do differ from drusen in some constituents, and have low levels of apoB, apoA-I, and esterified cholesterol, thought to represent components of an RPE-produced lipoprotein (Li et al., 2006). RPD were also thought to lack immunoreactivity for photoreceptor, Müller cell, and RPE marker proteins (Rudolf et al., 2008b). However Sarks et al. have identified components of disorganized and undigested photoreceptor outer segment in the same specimens as RPD (Sarks et al., 2011). The compositional differences in RPD and BlinD may in fact reflect physiological differences between photoreceptors; rod outer segment disc membranes have very low concentrations of unesterified cholesterol in comparison to cone disc membranes (invaginations of the plasma membrane). To compensate rod outer segment membranes increase their content of the fatty acid docosahexaenoate (DHA). RPE cells that serve cone photoreceptors therefore have to process more unesterified cholesterol, whilst rod RPE cells process more DHA (Curcio et al., 2013).

3.5.3 OCT of reticular pseudodrusen

The advent of spectral domain OCT offered the opportunity to perform a more detailed *in vivo* study of the retinal layer affected by RPD. In 2010 three separate groups published their findings with Zweifel and colleagues being the first (Zweifel et al., 2010). They used a point-to-point correlation between AF images and SD-OCT and for the first time in a living eye were able to correlate RPD with abnormal material lying internal to the RPE. They coined the term “subretinal drusenoid deposits”. A second group in Germany correlated their OCT findings with near infrared reflectance images, arriving at the same conclusion (Schmitz-Valckenberg et al., 2010). The final report by Spaide and Curcio confirmed these findings and added histological evidence (Spaide and Curcio, 2010).

Querques and colleagues were then able to use SD-OCT to propose a four stage classification for RPD, depending on the retinal layer affected by deposit (Querques et al., 2012a). Stage 1 pseudodrusen were defined as granular material between the RPE and the inner segment/outer segment (IS/OS); stage 2 as mounds of material sufficient to alter the

contour of the IS/OS; stage 3 as thicker material adopting a conical appearance and breaking through the IS/OS; and stage 4 as fading of the material due to resorption and migration within the inner retinal layers. In the same work they were able to quantify the changes in stage over time, identifying that RPD progress though these stages. More recently, Suzuki et al. have described a complimentary approach, using multimodal imaging techniques to define three unique types of pseudodrusen according to their reflectance properties (Suzuki et al., 2014). Two of these (dot and ribbon) occur in the posterior retina with a third type (mid-peripheral) being found outside the arcades, although this type was seen in only 8/140 eyes with RPD. The main SD-OCT feature differentiating these lesions is their B scan profile, peaked for dot lesions, broader mounds for ribbons and more rounded for the mid-peripheral type (Suzuki et al., 2014). Overall a sensitivity of 94.6% has been reported for the use of SD-OCT for identifying all types of RPD, alongside a specificity of 98.4%, indicating the utility of this examination for detecting these deposits (Ueda-Arakawa et al., 2013).

An interesting phenomenon observed in SD-OCT imaging of RPD are light "stripes" visible in the choroid under a subset of pseudodrusen. These result from enhanced infrared light penetrating in certain regions. Loss of structures that absorb these wavelengths are thought to cause this appearance, and so this is likely to represent the impact of RPD on the RPE. As not all RPD are associated with light stripes this sign may signify progression to a stage of RPD that causes local RPE degeneration. This phenomenon appears to be independent of the size of RPD and is seen without manifest alteration to the RPE/BM line on SD-OCT (Meadway et al., 2014).

Figure 4 shows the OCT (and infrared reflectance) appearance of RPD together with an age-matched control subject for comparison.

Figure 4. Appearance of reticular pseudodrusen (RPD) on OCT and infrared reflectance. *A*, Infrared reflectance and horizontal OCT scan through the fovea of an 81 year-old subject with a healthy macula. *B*, Corresponding images from an 87 year-old patient with both conventional sub-RPE drusen and RPD (clearly visible on the infrared reflectance image). *C* and *D*, images from the superior macula in both subjects. "Light stripes" in the choroid are also evident in the patient with RPD.

OCT has also been useful in recording the associated choroidal changes of reduced choroidal thickness, macular choroidal volume and narrowing of the choroidal vessels. The exact relationship of these changes to RPD development is yet to be resolved (Ueda-Arakawa et al., 2014).

3.5.4 Fundus autofluorescence of reticular pseudodrusen

With the advance of AF imaging, reticular patterns of change were described, first by Lois et al. (Lois et al., 2002). In their report, however, they did not attribute these changes to RPD, but did comment that there was poor concordance with visible drusen. RPD visible on fundus photographs were then later correlated with the reticular pattern seen on FAF imaging (Smith et al., 2006). Using this technique, RPD are characterised by

hypofluorescence, in an interconnected network, matching the “reticular pattern of FAF” previously described by Lois et al (Lois et al., 2002). This contrasts with the moderately increased AF exhibited by foveal soft drusen and the variable degree of AF possessed by other typical drusen (Lois et al., 2002). A subretinal location is likely to block reflectivity from the RPE accounting for the characteristic dark appearance on AF imaging. The hypoautofluorescent nature of these lesions additionally suggests that they are not directly derived from photoreceptor outer segments as these would be highly autofluorescent due to abundant bisretinoid. Recently, Lee and Ham have identified a minority of RPD that display hyperautofluorescence, which suggests that these deposits additionally contain retinoid components either from the photoreceptor, or lipofuscin from the RPE (Lee and Ham, 2014). They conclude by suggesting that RPD may fall into at least two types, classical hypoautofluorescent RPD and a hyperautofluorescent variant (Lee and Ham, 2014).

3.5.5 Fundus fluorescein angiography of reticular pseudodrusen

In the original description of RPD, Mimoun et al. reported lesions that were hypofluorescent using FFA (Mimoun et al., 1990). Subsequently only subtle variation from this has been described, ranging from no demonstrable change to minimal hypofluorescence (Prenner et al., 2003). Others have suggested that there are visible choriocapillaris filling defects in the early phase of the angiogram (Smith et al., 2009). As RPD are found above the RPE this is likely to influence their angiographic phenotype. Whilst the lack of RPE filtering may be most important when imaging with other modalities, RPD occupy a site inside the blood-retina barrier, limiting their exposure to fluorescein, perhaps in part explaining their hypofluorescence. RPD are also hypofluorescent in the mid- to late-phase ICGA (Arnold et al., 1997). Smith et al. found a sensitivity of 100% for ICGA, whereas Ueda-Arakawa et al. suggested a lower figure of 73% (Smith et al., 2009; Ueda-Arakawa et al., 2013). These differences may reflect contrasting study design, as the former was a retrospective review that included ICGA data for 9 eyes whereas the latter prospectively examined 220 eyes.

3.5.6 Multimodal confocal scanning laser ophthalmoscope imaging of reticular pseudodrusen

Confocal scanning laser ophthalmoscopy (Macauley et al.) uses a focused laser beam, illuminating a small retinal area, which is then scanned across the retina to produce a full image. The reflected light is then captured through a small aperture (a confocal pinhole) which suppresses light reflected or scattered from outside of the focal plane, which would otherwise result in a blurred image. This results in a sharp, high contrast image of the object layer located at the focal plane. Comparing camera-based imaging systems with CSLO has shown that the camera produces lower quality images due to its inability to separate reflected and scattered light (Elsner AE, 1990). CSLO may be used with a range of excitation sources (infrared, near-infrared, blue, green) and also in conjunction with barrier filters, in order to acquire AF as well as reflectance images. Illuminating with longer wavelength light results in greater fundus reflectance and for near infrared (NIR) light, it is approximately 1

log unit higher than visible light, aiding imaging of deeper structures (Elsner AE, 1990). Fig. 4D shows infrared reflectance imaging in RPD.

Infrared (815nm) reflectance (IRR)

Two groups, 4 years apart, have compared different techniques for diagnosing reticular lesions, and in both cases identified IRR as one of the most sensitive methods for detecting RPD (95% and 94.6%, respectively) (Smith et al., 2009; Ueda-Arakawa et al., 2013). Querques et al were also able to identify RPD better on IRR CSLO than blue light and camera based reflectance methods (Querques et al., 2012a). Additionally IRR is able to identify central macular lesions better than blue wavelength light, and this is thought to relate to the presence of luteal pigment that preferentially absorbs the shorter wavelength light (Smith et al., 2009). Suzuki et al. also found it easier to identify dot type RPD (that also tended to be more central) using IRR compared to colour fundus photography (Suzuki et al., 2014).

Near infrared (790nm) reflectance (NIRR)

Using near infrared CSLO RPD are characterised as groups of hyporeflectant lesions against a mild hyperreflectant background (Querques et al., 2012a). Less commonly, they may also be seen faintly at the fovea on AF and in near infrared light. A distinct, and frequently evident feature of RPD lesions is the so-called "target lesion", as some lesions, there is a hyporeflective annulus and an isoreflective centre (Querques et al., 2012a). The authors attribute the target aspect to an interruption of the ellipsoid zone (EZ), which correlates to RPD stage 3 (Querques et al., 2012a). Adding a barrier filter to block pure reflectance allows NIR- FAF detection, although this is the least sensitive imaging modality due to the decreased contrast between the lesions and the background.

Multicolour Reflectance (Blue, Green, Infrared)

Recently, Alten et al. have used multispectral CSLO (infrared, green and blue) to detect RPD reporting detection rates comparable to the use of NIRR and short wavelength autofluorescence (Alten et al., 2014). However if the RPD contained a "target aspect" multicolour reflectance appeared to be the more sensitive modality, detecting RPD in an additional 23% of eyes where NIRR and short wavelength autofluorescence failed to identify the lesions (Alten et al., 2014).

As RPD identification using a single-image modality is challenging, to enable an accurate diagnosis, we suggest that RPD detection should be performed with two or more image modalities (particularly OCT and infra red reflectance).

3.6 Outer retinal corrugations, hyperreflective pyramidal structures and "ghost drusen"

In 2008 Fleckenstein and colleagues reported their SD-OCT findings in 81 eyes of 56 patients with geographic atrophy secondary to AMD (Fleckenstein et al., 2008). They divided the retina into atrophic, junctional and peri-lesional zones and reported “crownlike structures with debris” occurring within the atrophic site (Fleckenstein et al., 2008). These lesions were associated with increased AF. Subsequently Ooto et al reported their SD-OCT findings in a similar cohort, and describe a curvilinear, hyperreflective, density above the line representing BM and within atrophic retina on OCT (Ooto et al., 2014). Below this line was a relatively hyporeflective space. These findings were present both in eyes with advanced geographic atrophy and neovascular disease. The authors follow the clinical description with a detailed analysis of their histological findings, which revealed a rippled layer of basal laminar deposit, in an area of RPE atrophy, at the same level as the curvilinear line seen in the OCT images. They conclude by suggesting that BlamD may correspond to the “outer retinal corrugations” visible on OCT.

Shortly after, in the same year, Bonnet et al described their own findings in patients with GA (Bonnet et al., 2014). These authors preferred to introduce the term “hyperreflective pyramidal structures” (HPS) to describe the same OCT feature that Ooto and colleagues had called outer retinal corrugations (Bonnet 2014). HPS appeared on IR image as a hyporeflective lesion surrounded by a hyperreflective halo (Bonnet et al., 2014). Using short wavelength autofluorescence, HPS were most commonly hypoautofluorescent, in 57 of 96 cases (59%). Multicolor reflectance imaging identifies these structures as having a “peculiar green reflectivity” (Bonnet et al., 2014). Imaging with SD-OCT, HPS present a heterogeneous hyper-reflective internal boundary with a hyporeflective core. The same authors hypothesised that HPS may represent the end stage of soft drusen, with spontaneous drusen regression leaving only the “scaffold” which is visible on OCT. Due to the hollow appearance and pseudopyramidal structure the authors compare their likeness to a cartoon ghost, and as they are found in areas of “dead” RPE introduce the term “ghost drusen”.

The lesions reported by Fleckenstein and Bonnet may actually represent different stages of the same process, the former retaining some autofluorescence associated with the debris contained within the internal hyperreflective boundary. If the lesions are internally hyporeflective, as in the studies of Ooto and Bonnet, then these structures are hypoautofluorescent. As they occur in regions of GA, where no RPE is expected, it has been suggested that the hyperrelective material is not derived from lipofuscin or retinoid components. Recent work however has questioned if regions of GA really represent cell deserts, as patchy preservation of both the RPE and neurosensory retina has been observed (Zanzottera et al., 2015).

In addition to their presence in advanced AMD, we have identified the same lesions in patients with advanced Late-Onset Retinal Degeneration (L-ORD), and also in Sorsby Fundus Dystrophy (Figure 5). HPS appear to assume different conformations: “soft edged” individual pyramids in the mid-peripheral macula, peaked “invasive” pyramids at the fovea and coalescing pyramids in the far periphery. The highly reflective boundary of these structures may represent translocating mitochondria, as they move into the innermost retinal remnant of the photoreceptor, together with Muller cell gliosis. We have not observed HPS co-

existing with outer retinal tubulations (ORT). As both lesions are found in regions of advanced outer retinal atrophy, HPS may represent an earlier form of ORT that still remain "attached" at their base. However, it remains possible that they represent alternative endpoints.

Figure 5. Hyperreflective pyramidal structures ("ghost drusen"). *A*, Short wavelength AF image from the right eye of a 68 year-old male patient with genetically confirmed late-onset retinal degeneration (L-ORD), showing marked RPE loss at the posterior pole. *B*, Infrared reflectance (left) and corresponding horizontal OCT line scan (right) through an area of geographic atrophy. C and D, Corresponding images from a patient with Sorsby Fundus Dystrophy (SFD). Hyperreflective pyramidal structures are visible on the OCT images.

4. Eye disorders with drusen or drusen-like deposit (excluding AMD)

In this section, we will describe eye conditions, other than age-related macular degeneration, in which drusen or drusen-like lesions may occur. Macular dystrophies can mimic a number of AMD features (recently reviewed by Saksens et al., 2014), but here the focus is particularly on those conditions yielding drusen-like lesions as part of their phenotype. In the first part (Section 4.1), we will discuss inherited conditions, beginning with inherited defects in the retinoid cycle, which can result in white dots. Some of these lesions can be localised to the subretinal space on OCT, and we will therefore refer to them collectively as subretinal drusenoid deposit SDD. In general, these conditions may also be associated with reduced autofluorescence signal (with the exception of ABCA4 retinopathy which exhibits a much higher signal). Subsequently, we discuss a range of other disorders associated with drusenoid lesions. These conditions are largely monogenic. In the next section (Section 4.2), we go on to discuss conditions whose inheritance has not yet been established that may result in whitish deposits.

4.1 Inherited retinal conditions

4.1.1 Genetic abnormalities of the retinoid cycle resulting in white dots

Vertebrate phototransduction is initiated by a photochemical reaction. Here, 11-cis-retinal bound to its opsin undergoes isomerisation to all-trans-retinal producing conformational changes in the opsin (for a comprehensive review, see (Lamb, 2013). Restoration of a photosensitive visual pigment requires the regeneration of 11-cis-retinal from all-trans-retinal via the retinoid cycle. In this section, instead of listing each genetic disorder separately, we will discuss important steps in this process, and highlight where dysfunction can be associated with drusenoid, yellow-white deposits. Figure 6 depicts schematically steps in the retinoid cycle. Table 3 list the relevant genetic disorders that can lead to white dots.

An acquired cause of reduced retinoid cycle activity, Vitamin A deficiency, can also result in white dots, and will be discussed in Section 5.

Figure 6. Schematic representation of the retinoid cycle. Asterisks indicate particular proteins in which mutations in the coding genes can give rise to white dots. ABCA4 is shown here facilitating removal of all-trans-retinal from the outer segment disc lumen.

Reduction of all-trans retinal to all-trans retinol takes place in photoreceptor outer segments; all other reactions, including isomerisation, occur within RPE. The all-trans retinylidene Schiff base hydrolyses and all-trans-retinal dissociates from the binding pocket of opsin. Removal of all-trans retinal from the discs, into the photoreceptor cytoplasm, may be facilitated by an ATP-binding cassette transporter (ABCR) (Beharry et al., 2004). Mutations of this protein, in particular subunit A4 (ABCA4), are known to cause an array of retinal diseases including macular, cone and cone-rod dystrophies (Allikmets et al., 1997). Typically, yellow-white deposit accumulates at the outer retina/RPE interface, classically described as pisciform flecks. These can be easily differentiated from drusen by their appearance on fundus photography and intense hyperautofluorescence on FAF imaging. The deposits are usually first identified in the first to third decades, and so are not mistaken for age-related drusen. Lastly their anatomical location within the retina can be variable, as the lesions evolve, and the deposits may even migrate into the outer nuclear layer (Voigt et al., 2010). Occasionally, if examined in the earliest stages of disease, white dots, rather than flecks, may be observed in the central macula, prior to the atrophic changes (Figure 7).

Figure 7. Fundus appearance of a patient with genetically proven biallelic mutations in *ABCA4* (Stargardt macular dystrophy), aged 16 (left images), 21 (middle images) and 25 years (right images). *A-C*, colour fundus photographs, with the macular region magnified in the middle panels (Amel et al.), and corresponding short wavelength autofluorescence images in the lower panels (*G-I*). The characteristic hyperautofluorescent flecks are evident in the later images, but white dots are also apparent, particularly in the earliest image.

In the next step of the retinoid cycle, all-trans-retinal is reduced to all-trans-retinol by NADPH-dependent all-trans retinol dehydrogenase, a membrane-associated enzyme encoded by the gene *RDH12* (Haeseleer et al., 1998). All-trans retinol then exits the photoreceptor and translocates to the RPE bound to interphotoreceptor retinoid binding protein (IRBP), and enters the RPE (Ala-Laurila et al., 2006; Bunt-Milam and Saari, 1983; Okajima et al., 1994; Wu et al., 2007).

Once inside, all-trans retinol is transferred to the cellular retinoid binding protein (CRBP) and

delivered to the first visual cycle enzyme in the RPE, lecithin retinol acyl transferase (LRAT) (Saari, 1982; Saari and Bredberg, 1989). LRAT links all-trans retinol to phosphatidyl choline in the RPE membrane, and in the process transfers an acyl group, generating all-trans retinyl esters. All-trans retinol from the systemic circulation also enters the visual cycle through the basal surface of RPE cells and is esterified here by LRAT. Homozygous frameshift mutations in *LRAT* associated with Leber Congenital Amaurosis (early-onset rod-cone dystrophy) can result in white dots (Littink et al., 2012).

Retinyl esters generated by LRAT are the primary storage form of vitamin A in the eye. Impairment of vitamin A supply, either as a result of dietary deficiency, lack of a transporter protein (RBP4) or even perhaps limited diffusion across a thickened BM (such as in Sorsby macular dystrophy and pseudoxanthoma elasticum – see Section 5) can also result in white dots.

The next step of the visual cycle involves two simultaneous processes, both performed by the enzyme RPE65: a trans/cis alkene bond isomerisation and an ester bond cleavage, generating 11-cis retinol (Deigner et al., 1989; Jin et al., 2005; Mata et al., 2004; Redmond et al., 1998). RPE65 is essential for the regeneration of 11-cis retinoid, and there is no isomerohydrolase activity in its absence (Redmond et al., 2005). RPE65 deficiency can also be associated with white dots (Weleber et al., 2011) in the form of SDD.

11-cis retinol then binds cellular retinaldyhyde binding protein (CRALBP) (Saari et al., 2001). Mutations in the gene *RLBP1* that encodes the protein CRALBP cause Bothnia dystrophy and Newfoundland rod-cone dystrophy, highly recognisable retinal phenotypes due the numerous white dots spread throughout the fundus (Burstedt and Golovleva, 2010; Eichers et al., 2002). Early in disease patients with Bothnia Dystrophy have changes similar to those with *RDH5* retinopathy, however the former progress to significant chorioretinal atrophy (Figure 8) that may then be mistaken for Gyrate Atrophy. Colour fundus photography appears to show two types of deposit: peripheral white dots of varying sizes which are easily visible, and also barely visible macular changes (Fig. 8). These central lesions are visible on IR reflectance imaging (Fig. 8*E,F*), as they distort the outer retinal structure, particularly the ellipsoid zone, and are reminiscent of dot subretinal drusenoid deposit. In keeping with this, the lesions can evolve appearing to erode through the ellipsoid zone and towards the external limiting membrane.

Figure 8. Retinal imaging in a 6 year old patient (*A-F*) and a 75 year old patient (*G,H*) with Bothnia Dystrophy. *A-D*, colour fundus images from the younger patient (*A* and *B* show widefield images; *C* and *D* show the posterior pole). *E*, Infrared reflectance image of right macula with OCT scan through the fovea. *F*, OCT and infrared reflectance image for the left eye. The OCT shows what appear to be subretinal drusenoid deposits. *G,H,* Wide-field fundus images from the older patient showing widespread chorioretinal atrophy.

CRALBP delivers 11-cis retinol to 11-cis retinol dehydrogenase (11-cis RDH) for the final enzymatic step within the RPE. 11-cis RDH oxidizes 11-cis retinol to 11-cis retinal using NAD as a cofactor (Driessen et al., 1995; Simon et al., 1995). Mutations in *RDH5*, the gene encoding 11-cis RDH cause fundus albipunctatus (FA) another recognisable phenotype

(Figure 9). Similar to mutation of *RLBP1*, pathogenic variants in *RDH5* appear to result in subretinal deposit deposition. Similar lesions appear on the OCT images presented by Pichi et al. (Pichi et al., 2013). In contrast to AMD related SDD, the subretinal deposits in FA start as a ring around the macula, leaving the central area unaffected, and spread towards the equator. The dots are white, or greyish white; distinct and individual, and mostly uniform in size. On FFA, most of these dots are not seen or they block fluorescence. The fundus shows low overall levels of autofluoresence, but when the gain is increased, some central deposits show higher than background levels of autofluorescence, suggesting that they contain some bisretinoid product, even if the absolute levels are low (Sergouniotis et al., 2011b).

Figure 9. Images from a patient with fundus albipunctatus (*RDH5*-associated retinopathy). *A* and *B*, colour fundus images from right eye aged 7 (*A*) and 10 (*B*) years. The later image shows a few additional deposits. *C* and *D*, Infrared reflectance and OCT images from the right eye (aged 10): the deposits appear to be subretinal, but with some discontinuity in the ellipsoid layer seen also. *E*, Short wavelength autofluorescence image from the right eye (aged 11): a low overall autofluorescence is seen, but the deposits have higher levels of autofluorescence than the background and are visible when the gain is increased.

11-cis retinal, again transported by IRBP, crosses the sub-retinal space and re-enters the photoreceptors (Ala-Laurila et al., 2006; Crouch et al., 1992; Wu et al., 2007). Once inside the outer segment it is transported back into the disc membrane, and the newly generated 11-cis retinal can re-bind opsin - a functional visual pigment has been regenerated.

Table 3. Visual cycle genes in which bi-allelic mutations may lead to white dots as part of the retinal phenotype. Function of the encoded protein is listed together with the disease entities, and phenotypic features. The white dots sometimes seen early in *ABCA4*-associated retinopathy are seen at the macula, and are phenotypically different from those seen in the other conditions, in which the dots tend to spare the perifoveal area. *RDH5*-associated retinopathy is usually non-progressive. The full names of the genes are given in table 1.

Gene	Function	Disease entities	Retinal phenotypic features
ABCA4	Binds both all-trans retinal and N-retinylidene-phosphatidylethanolamine; Facilitates transport of all-trans retinal from outer segment discs and also may play a role in removal of excess accumulation	Stargardt disease, fundus flavimaculatus, cone and cone-rod dystrophies	Hyperautofluorescent retinal flecks; bull's eye maculopathy; areas of atrophy; white dots may be seen in early disease.

	of bisretinoid products		
LRAT	Generates all-trans retinyl esters from all-trans retinol	Leber congenital amaurosis, early onset severe rod-cone dystrophy	White dots may be seen; progressive outer retinal atrophy
RPE65	Generates 11-cis retinol from all-trans retinyl esters	Leber congenital amaurosis; early onset severe rod-cone dystrophy	White dots may be seen; progressive outer retinal atrophy
RLBP1	Encodes CRALBP which binds 11-cis retinol and delivers it to RDH	Bothnia dystrophy; Newfoundland Rod-Cone Dystrophy; fundus albipunctatus	Numerous white dots (similar to *RDH5*, but later progresses to extensive chorioretinal atrophy)
RDH5	Oxidises 11-cis retinol to 11-cis retinal within the RPE.	Fundus albipunctatus	Numerous white dots (generally non-progressive)

Cone photoreceptors are believed to also access an alternative visual cycle via Muller cells that can bypass the RPE (Mata et al., 2002). Here, all-trans retinol generated in photoreceptors is transported to Müller cells and isomerized to 11-cis retinol by an unidentified isomerase. 11-cis retinol from Müller cells then enters the inner segments of cone photoreceptors and is oxidised to 11-cis retinal for visual pigment formation (Bunt-Milam and Saari, 1983; Saari et al., 1985). A functional relationship between IRBP, Müller cells, and cone inner segments in a cone-specific pathway is yet to be proven however, but this hypothesis does perhaps explain the relative foveal sparing of *RDH5*, *RLBP1* and *RPE65* related retinopathies, at least early on in the disease course.

4.1.2 Familial benign fleck retinopathy (*PLA2G5*)

An identical appearance to the retinopathies associated with mutation of *RDH5* and *RLBP1* can also be observed with bi-allelic mutation of *PLA2G5.* Although there is phenotypic overlap the latter patients do not suffer from any loss of function (Sergouniotis et al., 2011a). Figure 10 shows the fundus appearance. In contrast to defects in the retinoid cycle, there is no low overall autofluorescence, but the dots are hyperautofluorescent. The OCT images resemble subretinal drusenoid deposits, though some disturbance of the RPE may be evident.

Figure 10. Retinal images of a 39 year-old female with bi-allelic mutation in *PLA2G5*. *A,B,C* Images from the right eye. *D,E,F,* Images from left eye. *A* and *D* are colour fundus photographs showing numerous white dots. *B* and *E* are short wavelength AF images showing that the lesions are hyperautofluorescent. *C* and *F* show infrared reflectance and OCT images.

4.1.3 Dominant drusen (*EFEMP1*)

Patients with dominantly inherited drusen (DD) were originally described as Doyne honeycomb retinal dystrophy in the UK and as Malattia Leventinese in Switzerland (Doyne, 1899; Vogt, 1925). It was later realised that both conditions were the same, as a single missense mutation (p.Arg345Trp) in *EFEMP1* is responsible (Stone et al., 1999). Mutation of Fibulin-3, the protein encoded by *EFEMP1*, has been shown to result in focal thickening of BM, evident at the macula and sparing the peripheral basement membrane (Marmorstein 2002, Sohn 2015). Characteristic signs are early-onset drusen at the posterior pole (Figure 11) and in the peripapillary area, with a radial distribution in some cases; although drusen abutting the optic nerve head has been shown to be most suggestive of DD (Michaelides et al., 2006). With age the drusen become confluent and BM becomes increasingly separated from the RPE. Dysfunction is usually confined to the macula, and consequently the ffERG is usually normal (Michaelides et al., 2006). Three groups have looked in detail at the clinical phenotype associated with mutation of *EFEMP1* (Michaelides et al., 2006; Querques et al., 2013; Zweifel et al., 2012). In the first two studies, a radial pattern was not always seen (Michaelides et al., 2006; Zweifel et al., 2012). Most drusen exhibited very early hyperfluorescence, identical to that seen with cuticular drusen. SD-OCT imaging suggested the presence of two different phenotypes – a saw-tooth like elevation of the RPE, consistent with cuticular drusen, which may become confluent with time, and deposit lying anterior to the RPE, typical of SDD. The NI-R and AF signatures were however not characteristic of RPD. The third report by Querques and colleagues concurred with the identification of cuticular drusen but suggested the larger drusen shared more similarities with conventional drusen rather than SDD (Querques et al., 2013). These conclusions have been extended by the recent work demonstrating that although the drusen of DD share many similarities with those seen in AMD, morphological differences do exist (Sohn et al., 2015). DD is characterised by a major disruption to the ECM, consequently these drusen, unlike those of AMD, contain elevated levels collagen type IV but reduced levels of TIMP3 (Sohn et al., 2015). DD also display an unusual onion skin–like lamination separating the eosinophilic and sudanophilic layers, which is thought to relate to ECM molecules aggregating with fixed periodicity. These drusen also display high immunoreactivity to antibodies directed against the membrane attack complex (C5b-9) component of complement, a feature shared with hard but not soft drusen (Sohn et al., 2015).

As seen with substantial coalescing cuticular drusen, subretinal fluid may accumulate in DD, even in the absence of identifiable neovascular disease. Such cases may be observed, as the fluid tends not to increase significantly, nor does haemorrhagic transformation tend to occur in our experience. Additionally, when treated with intravitreal anti-VEGF therapy, the subretinal fluid often persists. Macular atrophy is seen as a late event.

Figure 11. Examples of phenotypes seen in *EFEMP1* disease ("dominant drusen"). The panels show (from left to right) colour fundus photographs, short wavelength autofluorescence, infrared reflectance and horizontal OCT scans, all from the right eye. Upper panels (*A*-*C*) are from a 21 year old patient with early disease. The middle and lower panels are from a sister and brother showing how expression can be variable in the same family. The middle panels (Amel et al.) are from a 62 year old female with severe disease.

The lower panels (*G-I*) are from her brother (aged 59) who has mild disease. The commonly described appearance of radially distributed drusen is not evident in these cases, but drusen abutting the optic nerve head are visible (middle and lower panels).

4.1.4 Sorsby fundus dystrophy (*TIMP3*)

Sorsby fundus dystrophy (SFD) is a rare autosomal dominantly inherited retinal dystrophy producing symptoms after the third decade of life (Sorsby, 1949). The most common presentation is due to central visual loss but in almost all cases this is preceded by a period of disturbance of dark adaptation and nyctalopia (Steinmetz et al., 1992). SFD is now known to result from mutation of a single gene - the tissue inhibitor of metalloprotease 3 (*TIMP3*) with causative genetic variants being found almost exclusively in exon 5 or the preceding exon-intron boundary (Weber et al., 1994). The mutated TIMP3 protein is thought to form dimers, almost always the result of a gain or loss of a cysteine residue. These dimers are more resistant to normal catabolic cellular metabolism and so accumulate in BM. Histologically these changes result in widespread thickening of BM (Capon et al., 1989). In some cases this may be visible on imaging with SD-OCT. A major feature of early SFD is the presence of yellow drusenoid deposit, that later progress to atrophy. A major contributor to the yellow deposits are SDD (reticular pseudodrusen) (Gliem et al., 2015b), as shown in Fig. 12. Perhaps as a consequence of premature BM thickening, the SDD of SFD occur at an earlier age of onset compared to those seen in AMD. In more severe or advanced disease, as in AMD, marked atrophy may ensue with hyperreflective pyramidal structures seen on OCT (Fig. 5).

Figure 12. Retinal imaging from two patients with early or mild SFD. *A*, Colour fundus photograph from the right eye of a 41 year-old female patient. *B*, Colour fundus photograph from the right eye of a 49 year-old female patient. *C* and *D*, "Multicolor" and short-wavelength AF imaging with CSLO of the patient in *A*. *E* and *F*, corresponding images from patient in *B*. *G* and *H*, Infrared reflectance and OCT imaging from both patients. The lesions are more possibly more easily defined on the CSLO images (Gauter-Fleckenstein et al.) than on the colour fundus photographs (*A,B*), and OCT imaging shows the majority to be SDD. An SFD patient with more advanced disease is shown in Figure 5.

4.1.5 Late-onset retinal degeneration (*C1QTNF5*)

Late-onset retinal degeneration (L-ORD) is an autosomal dominantly inherited disorder, characterized by loss of rod function starting in the fifth to sixth decade. Central visual loss then ensues as a result of severe chorioretinal atrophy or neovascularization. All cases to date harbour the p.Arg163Ser mutation in *C1QTNF5* (Hayward et al., 2003). Histopathology of a donor eye revealed a thick layer of extracellular deposits between the RPE and BM underlying marked areas of photoreceptor loss (Kuntz et al., 1996; Milam et al., 2000). The deposit is estimated to be approximately 50 µm, containing a mixture of substances rich in lipids, collagen mucopolysaccharide, elastin, Muller cell processes and rhodopsin-positive neurons extending from the central retina to the ora serrata (Kuntz et al., 1996; Milam et al.,

2000; Shu et al., 2006). Similar to SFD, early L-ORD is characterized by nyctalopia and the presence of SDD (Figure 13). Later in disease, ghost drusen dominate (HPS) as shown previously in Figure 5.

Figure 13. Images from a 60 year-old female with late-onset retinal degeneration. *A,* colour fundus photograph from the right eye. *B,* Infrared reflectance and horizontal foveal OCT scan. *C,* Short wavelength autofluorescence imaging. *D,* Slit lamp photograph of anterior segment showing anteriorly placed zonular insertions, which are seen in this condition. Images from a patient with more advanced disease are shown in Fig. 5.

4.1.6 *IMPG1* and *IMPG2* carriers

IMPG1 (interphotoreceptor matrix proteoglycan 1) encodes SPACR, a 150kDa sialoprotein associated with rod and cone photoreceptors. It is a major component of the interphotoreceptor matrix, the site where rods and cones interact with the RPE (Felbor et al., 1998; Kuehn and Hageman, 1999). SPACR is highly homologous to SPACRCAN (sialoprotein associated with photoreceptor cone and rod proteoglycans), a 200 kDa protein encoded by *IMPG2* (interphotoreceptor matrix proteoglycan 2) and also found in the interphotoreceptor matrix (Acharya et al., 2000). Mutations in *IMPG1* have been associated with both dominant and recessive forms of atypical vitelliform macular dystrophy (VMD) (Manes et al., 2013). In one family carriers of heterozygous mutations that result in recessive VMD showed an early onset drusen phenotype (family NA186) (Manes et al., 2013). Heterozygous *IMPG2* mutations have also been reported to cause atypical vitelliform macular dystrophy whilst bi-allelic mutations cause RP, often with early macular involvement (Bandah-Rozenfeld et al., 2010). We have also recently seen the early onset drusen phenotype in a carrier of an *IMPG2* mutation Figure 14); it is possible that this may be a feature of the carrier status for specific *IMPG1/2* variants.

Figure 14. Fundus images from patients with *IMPG2* mutations. *A*, Wide-field colour fundus photograph of the right eye of a 19 year-old male with retinitis pigmentosa found to have bi-allelic mutations in IMPG2. *B-D*, images from the right eye of the patient's mother (aged 39). *B*, Colour fundus photograph showing subtle drusen-like lesions around the fovea and superotemporally. *C*, Short-wavelength autofluorescence image showing hyper-autofluorescence of the lesions. *D*, Infrared reflectance image with horizontal foveal OCT scan.

4.1.7 *PRPH2*–associated retinopathy

Mutations in *PRPH2* (Peripherin 2) are associated with a range of fundus phenotypes including those limited to the macula (adult vitelliform, butterfly pattern dystrophy, central areolar choroidal dystrophy), as well as those with more widespread changes associated with rod-cone, cone or cone-rod dystrophies. The latter may take the form of a classical retinitis pigmentosa phenotype, or appear similar to the flecked retina associated with mutation of *ABCA4*. Whilst these yellow outer retinal deposits are subretinal rather than

subRPE in location, using colour fundus imaging alone may lead to these deposits being mistaken for drusen. This may be especially the case for families where there is non-penetrance, or at least variable expression of the fundus changes, as a history of dominant disease, or premature sight loss may not be elicited. This is particularly prevalent with the p.R172W mutation. For a comprehensive review of the phenotypic spectrum of PRPH2-associated retinopathy see (Boon, 2014).

4.1.8 *CDHR1* retinopathy

CDHR1 (cadherin 1) encodes the photoreceptor cadherin, a structural, transmembrane protein localized to the base of rod and cone outer segments that appears to be involved in maintaining their structure (Rattner et al., 2001). A range of fundus phenotypes have been reported with bi-allelic mutation of *CDHR1* including irregular pigmentary changes, bulls-eye maculopathy, macular sheen, RPE migration into the retina, and outer retinal atrophy (Ba-Abbad et al., 2013; Cohen et al., 2012; Duncan et al., 2012). We have recently examined a 43 year old lady with early onset drusenoid deposit, where molecular genetic testing has identified recessive mutations in *CDHR1*. Figure 15 shows the retinal imaging findings in this patient.

Figure 15. Images from the right eye of a patient with bi-allelic mutations in *CDHR1*. *A*, Colour fundus photograph shows a bulls-eye maculopathy appearance, with fine yellow dots at the periphery of the lesion. *B,* Short wavelength autofluorescence shows speckled hyperautofluorescent foci throughout the lesion. *C*, Infrared reflectance with a horizontal OCT scan showing, in addition to outer retinal/RPE atrophy, fine hyperreflective foci at the level of the photoreceptor outer segments.

4.1.9 North Carolina Macular Dystrophy and NCMD-Like Disorders

North Carolina Macular Dystrophy (NCMD, MCDR1) is an autosomal dominant congenital maculopathy first described as hereditary macular degeneration and aminoaciduria by Lefler, Wadworth, and Sidbury (Lefler, 1971). The origins have been traced to two Irish brothers who settled in North Carolina in the 1830s and the original North Carolina pedigree now consists of over 5,000 individuals (Small 1992). It has also been found in other unrelated individuals around the globe. Linkage studies have mapped MCDR1 to a locus on chromosome 6q16 which has latterly been refined to a 1.8 mb region (Yang et al., 2008). Just this year, Small and colleagues applied whole genome sequencing techniques to identify variants which segregate with the disease (Small et al., 2015). Bioinformatic filtering followed by segregation and gene expression studies have now implicated *PRDM13* as the gene underlying the MCDR1 locus, a transcription factor now understood to be critical for macular development.

The disease is characterized by symmetric, small, yellow, well defined drusen-like deposits confined to the foveal region with minimal impact on visual acuity (Grade 1); confluent yellow flecks with intermediate visual impairment (Grade 2); or a macular coloboma

surrounded by chorioretinal atrophy and pigmentation associated with moderate to severe visual impairment (Grade 3) (Small, 1989). These changes are either congenital, or appear in early infancy. Lesions are typically non-progressive however occasionally choroidal neovascularization occurs, resulting in anatomical remodeling and late vision loss (Small, 1991). Peripheral changes have also been described with linear drusen accumulating (Pauleikhoff 1997; Reichel, 1998, Pichi, 2013). Functional testing usually establishes that disease is confined to the central macula however. Grade 1 lesions may not be easily identifiable by SD-OCT. They are usually hyperautofluorescent on FAF imaging and easily visible with this modality, suggesting that they may contain significant amounts of bisretinoid or another fluorophore (given that, with such early onset lesions, it may be unlikely that significant bisretinoid will have accumulated).

NCMD-like phenotypes mapping to genetic loci other than MCDR1 have also been described (MCDR3, MCDR4 and Sorsby Syndrome), for a recent review see (Michaelides et al., 2012). Affected individuals with both MCDR3 and MCDR4 can present with fine drusen-like deposits. MCDR3 may potentially be differentiated from NCMD by progressive drusen accumulation (Michaelides et al., 2003), whilst all affected family members of the sole MCDR4 pedigree also reported progressive sensorineural hearing loss (Francis et al., 2003).

Figure 16. Images from a mother and son affected by North Carolina Macular Dystrophy. Upper panels show colour fundus photographs; lower panels show short wavelength AF images. *A,C,* Images from 16 year-old male with grade 1 NCMD. *B,D,* Images from 42 year-old female with grade 3 disease.

4.2 Eye disorders with undefined inheritance

4.2.1 Gass' grouped albinotic spots; Flecked Retina of Kandori

Kandori described 4 cases from Japan with an unusual retinal appearance but good visual function (Kandori, 1959; Kandori et al., 1966; Kandori et al., 1972). The characteristic changes were large, irregular but sharply defined yellow patches in mid-peripheral retina and sparing the macula. These findings were not associated with electrophysiological abnormality. A similar case has been also reported by Fried et al. with additional signs of ectodermal dysplasia (Fried, 1972). No molecular genetic investigations have been performed in any of the reported families.

Gass suggested that these lesions are identical to those seen in another condition, that he has termed congenital, grouped albinotic spots of the RPE (Gass, 1977). These lesions may be similarly numerous, although most commonly are much smaller in size than the cases of flecked retina reported above. A single case of familial disease exists, with the mother and three siblings from a Brazilian family of Italian heritage all affected (Arana et al., 2010). Gass proposed that this phenotype results from deposition of white material within the RPE, although no histological analysis has been performed. Window defects are observed over the white lesions during FFA. Kandori's original and subsequent descriptions included cases

also with night blindness and more widespread lesions, so it is possible that some of these may now be classified as fundus albipunctatus or the benign fleck retinopathy associated with *PLA2G5*.

Figure 17 shows some examples of grouped albinotic spots. The lesions are not visible on OCT. They are seen as high intensity lesions on short wavelength AF imaging, suggesting that they do not simply represent depigmented RPE cells, but additional hyperautofluorescent material. The radial pattern is consistent with RPE migration during development. Interestingly, the third case shown in the lower panels of Figure 17 (albinotic spots confined to the superior or superonasal mid-periphery) does not exhibit hyper-autofluorescence. The AF image in this case (Fig. 17*H*) was obtained with the wide-field Optos system, as opposed to the CSLO-acquired AF images in (panels *B* and *E*). The difference might reflect a real difference in the properties of the deposits in the different cases or might be due to the different methods of image acquisition. The fundus appearance of the patient shown in the upper panels of Fig. 17 was stable over the course of 3 years, suggesting that these spots do not change over time.

Figure 17. Images from patients with albinotic spots. *A-C*, 9 year-old girl; *D-F*, 25 year-old female; *G,H*, 11 year-old male). Images are colour fundus photographs (*A,D,E*), short wavelength autofluorescence (*B,D,G*) and infrared reflectance with horizontal OCT scans (*C,F*).

4.2.2 Large colloid drusen

Large Colloid Drusen (LCD) are large (200-300 µm), bilateral, and yellowish lesions located in the macula and/or peripheral retina (Figure 18), and have been described relatively recently as a new type of early-onset drusen (Guigui et al., 2011). They lie external to RPE, in common with conventional drusen. With short wavelength (488nm) autofluorescence they show variable, mild hyperautofluorescence, most commonly surrounded by a halo of hypoautofluorescence. In the late phase of ICGA, their core is hypofluorescent surrounded by a hyperfluorescent ring; Guigui and colleagues have referred to this as the “doughnut effect”. When investigated with FFA the doughnut occurs in the early phase, with late central hyperfluorescence. The bright surrounding halo is also present even without dye imaging using near infrared reflectance (Guigui et al., 2011). SD-OCT imaging suggests that the smallest LCD have no effect on the ellipsoid zone, and this is confirmed when the photoreceptor mosaic is imaged using adaptive optics SLO (AO-SLO) (Querques et al., 2012b). Larger LCD erode into the photoreceptors (Querques et al., 2012b). Generally speaking however LCD are associated with minimal functional deficits (Guigui et al., 2011).

Very recently there has been a single case report of LCD co-occurring with posterior polymorphous corneal dystrophy (PPCD), a presumed collagenopathy limited to Descemet’s membrane (DM) (Del Turco et al., 2015). As both DM and BM are collagen rich matrices this may suggest a common pathogenetic mechanism. Other associations are yet to be established.

Table 4. Features of large colloid drusen on retinal imaging.

Colour fundus photography (CFP)	Large (200-300 µm) yellowish lesions, most common in the temporal macula initially but can be more widespread.
Short wavelength auto-fluorescence	Variable, mild hyperautofluorescence, surrounded by a halo of reduced AF.
OCT	Sub-RPE deposits. Larger lesions may erode into the photoreceptors. The core tends to exhibit lower reflectivity than other drusen and in some cases can appear optically empty.
Fundus fluorescein angiography	Early central hypofluorescence with late hyperfluorescence.
Indocyanine green angiography	In the late phase, a hypofluorescent central core surrounded by a hyperfluorescent ring (the "doughnut" effect).

Figure 18. Retinal imaging of a 19 year-old female with large colloid drusen. *A* and *B*, Colour fundus photographs from right and left eye respectively. *C* and *D*, Short wavelength AF images. *E* and *F*, Infrared reflectance and horizontal OCT scans from right and left eye respectively.

4.2.3 Early onset drusen otherwise unclassified

A large number of patients exist with early onset drusen that do not easily fit into any of the above diagnostic categories, differing either by phenotype or genotype. In almost all cases there is no manifest systemic disease and the patients' history does not suggest an acquired cause. The symmetry and premature onset however hint at a genetic aetiology (Figure 19 shows an example), although to date this hypothesis remains largely untested. These patients should not be considered a uniform cohort, rather they are most likely to represent a collection of unique groups, each with their own combination of risk factors that happen to share a final common pathway. Within this group certain patterns may be recognised, depending upon the site affected (macula only or more widespread), natural history (static or progressive) and degree of dysfunction. It is likely that future genetic, proteomic and metabolomics studies will be useful in sub-classifying these patients.

Fig 19. Retinal images from a 41 year-old female with bilateral drusen. This patient underwent testing for mutations in the known genes underlying retinal or macular dystrophies with a negative result. The symmetry suggests a genetic aetiology. *A*, Colour fundus photographs (from a wide-field imaging system). *B*, Horizontal enhanced depth OCT image through the fovea of the right eye with corresponding infrared reflectance image. *C*, Short wavelength AF images. *D*, OCT and infrared images from the left eye.

5. Disorders with systemic features

In this section we discuss disorders with systemic features, beginning with renal disease (Section 5.1) and then a number of other systemic conditions that may be associated with drusenoid lesions.

5.1 Renal disease

There are a number of diseases that may affect the eye and kidney. This is not confined to common diseases affecting the microvasculature in both organs, such as diabetes and hypertension, but also a number of more rare inherited diseases. Previous authors (including Savige et al., 2011) have pointed out the existence of shared developmental pathways for the eye and kidney, the importance of ciliary function in both podocytes and the photoreceptors, and similarities between the choriocapillaris and the fenestrated capillaries of the glomerulus. Drusen or drusen-like deposits may be seen in a few renal diseases. We will discuss membranoproliferative glomerulonephritis, which, like AMD, has an association with complement factor H variants. We will also discuss Alport syndrome, caused by abnormalities in Type IV collagen, in which white-yellow retinal lesions may be apparent.

5.1.1 Type II membranoproliferative glomerulonephritis, dense deposit disease and C3 glomerulopathy.

The initial classifications of membranoprofliferative glomerulonephritis (MPGN) were based on morphological characteristics, either with electron microscopy (defining dense deposit disease) or light microscopy (identifying mesangioprofliferative, membranoproliferative, and cresentic patterns). Recently this has been updated, with immunofluorescence techniques now being preferred to differentiate between disease processes. Accordingly, “C3 glomerulopathy” (C3G) has been introduced to describe nephropathy associated with isolated deposits of C3, a hallmark of dysregulation in the alternative pathway of complement (Fakhouri et al., 2010). Included within this group are “C3 glomerulonephritis” (C3GN) (including some forms of MPGN 1 and 3) and dense deposit disease (MPGN2) (Servais et al., 2007). Other types of MPGN (the remaining forms of type 1 and type 3) result from mixed deposits of immunoglobulin and complement and are therefore not considered part of C3G.

C3G is an inflammatory disease affecting the glomerulus of the kidney, in particular the capillary tuft, glomerular basement membrane and glomerular epithelium. As this site shares significant homology with the choriocapillaris, BM and RPE interface, these ocular structures may also be expected to show signs of damage in C3G. Whilst MPGN is associated with a range of other disorders, both autoimmune (SLE), chronic inflammatory conditions (hepatitis B and C) and immunoglobulinaemias to name a few, C3G is specifically associated with those relating to dysregulation in the alternative complement pathway. Many of the references below relate to historical descriptions reporting retinal phenotypes observed in patients with renal disease and so we refer to the nephropathy as the authors have. For clarity MPGN2, synonymous with DDD, is part of C3G. Similarly subgroups of MPGN type 1 and 3 that are characterised by C3 deposition are included as C3G, in the sub-group C3GN,

for review see (D'Agati and Bomback, 2012).

In 1989, Duvall-Young and colleagues working in the Renal Unit at Manchester Royal Infirmary described the presence of drusen-like retinal deposits in patients with biopsy proven MPGN2 (Duvall-Young et al., 1989). Subsequently Mullins and associates, were able to examine eyes obtained from two human donors with MPGN2 (Mullins et al., 2001). Histologically these deposits exhibit sudanophilia, bind filipin, react with antibodies directed against vitronectin, complement C5 and C5b-9 complexes, TIMP-3 and amyloid P component, all hallmarks of AMD associated drusen. They concluded that the ultrastructural characteristics of these deposits were also identical with those of AMD associated Drusen (Mullins et al., 2001). Cuticular drusen were then identified as the major druse subtype, and are present in nearly 80% of dense deposit disease patients (McAvoy and Silvestri, 2005). Their widespread presence, at a young age, and in association with renal dysfunction may be considered pathognomonic of MPGN.

Individuals with MPGN2 develop drusen from their second decade. Their distribution is variable and as in AMD in the early stages, is not associated with ocular morbidity (Colville et al., 2003; Duvall-Young et al., 1989). With time retinal dysfunction may develop, detectable even when the patient is asymptomatic (Colville et al., 2003; D'Souza Y et al., 2009; O'Brien et al., 1993). Further progression can be associated with choroidal neovascularisation and serous macular detachment, although how frequently this occurs and whether it is complicated by the necessary pharmacotherapy is not known (Colville et al., 2003). In contrast D'Souza and colleagues, reporting on the 10 year follow up of the original cohort described by Duvall-Young et al., did not find any evidence for a progressive retinopathy in the four surviving patients (no atrophy or CNVM) (D'Souza et al., 2008). Although limited by the small sample size, this group accurately characterised the clinical characteristics of the drusen in MPGN2. They found numerous (>20) deposits, with a variety of small (hard) and large (soft) drusen, even outside the arcades and small drusen that fluoresced greatly on angiography (cuticular drusen). Although we may not be able to use clinical signs to differentiate drusen associated with MPGN2 from those seen in AMD, they occur a significantly younger age (20s versus 60s) and are associated with renal dysfunction. Similar drusen have also been reported in MPGN1 (n=1) and MPGN3 (n=2) (Dalvin et al., 2015; Han and Sievers, 2009), perhaps unsurprising as we now recognise that isolated complement dysregulation is a defining feature for a subgroup of MPGN1 and 3.

Figure 20. Retinal images from a 21 year-old female with histologically confirmed MPGN type 2. *A*, Colour fundus photographs. *B*, Horizontal OCT image through the fovea of the right eye with corresponding infrared reflectance image. *C*, Short wavelength AF images. *D*, OCT and infrared images from the left eye. The drusen-like lesions are visible on colour, AF and infrared imaging, but not easily discernible on OCT.

5.1.2 Alport syndrome

Alport syndrome is an important cause of inherited kidney disease and of early onset renal failure. It results from mutations in genes coding for type IV collagen α3α4α5, which is found

in a number of basement membranes including the lens capsule, the internal limiting membrane and BM, the glomerular basement membrane and the cochlea. Over 80% of Alport syndrome is X-linked, resulting from mutations in *COL4A5*. Autosomal inheritance syndrome results from mutations in *COL4A3* or *COL4A4*, and the majority of this is autosomal recessive Alport syndrome. Extra-renal manifestations include deafness and ocular abnormalities. The latter include anterior lenticonus (which is pathognomonic, but present in a minority) and retinal abnormalities, which may aid diagnosis (Savige and Colville, 2009). Dots and flecks may be seen in the macula, with the flecks sometimes outlining a macular "lozenge". The macular flecks appear to be related to hyper-reflectivity of the ILM on OCT imaging, and the macular "lozenge" appears to be related to temporal macular thinning (Savige et al., 2010). Mid-peripheral retinal flecks are also commonly observed, and at least in some patients, these have the appearance of mid-peripheral drusen.

Figure 21 shows the fundus appearance of patients with X-linked and autosomal recessive Alport syndrome. The temporal macular thinning is evident (and extends nasal to the foveola also), and appears to be characteristic. We have seen a similar appearance only in some patients with sickle cell retinopathy, but the appearance in those patients is not usually so symmetrical. The macular white-yellow lesions appear to relate to hyperreflectivity of the ILM rather than drusen or drusenoid deposits. However, the mid-peripheral lesions might be drusenoid though are too peripheral to easily capture with OCT.

Figure 21. Retinal imaging from patients with X-linked Alport syndrome (*A*-*C*) and autosomal recessive Alport syndrome (Amel et al.). *A*, Horizontal OCT line scan through the fovea of a male patient with X-linked Alport syndrome, showing inner retinal thinning largely temporal to the foveola and hyper-reflectivity of the ILM. *B*, Colour fundus photograph from the left eye showing the dot/fleck maculopathy and the macular "lozenge" appearance. *C*, OCT from the left eye (corresponding to the green arrow in *B*) showing that the white yellow lesions appear to correspond to the hyper-reflective ILM rather than any drusenoid deposits. *D*, Montage of colour fundus photographs from a male patient with autosomal recessive Alport syndrome showing minimal macular dots, but mid-peripheral changes that could be drusenoid. *E*, *F*, infrared reflectance and OCT images from the right and left eye of the patient depicted in *D*. Temporal macular thinning is again seen together with a hyper-reflective ILM.

5.2 Other diseases with systemic manifestations

5.2.1 Vitamin A deficiency

Dietary deficiency, malabsorption syndromes and self-inflicted vitamin A deficiency have all been described in association with retinal changes (Fell, 1969; Fuchs, 1928, 1959; Uyemura, 1928). Yellow-white dots in the outer retina or RPE are seen, and SDD are evident on OCT.

The yellow dots have been reported to reduce in number with treatment. The SDD changes over time have been less well documented. As might be expected from a condition in which retinoid delivery is reduced, the appearance is similar to that seen in disorders of retinoid cycle (Section 4.1.1), and symptoms include nyctalopia. Full-field electroretinography is abnormal, with reduced rod-driven responses, though cone system function may be relatively preserved.

Other ocular signs include conjunctival xerosis and Bitot's spots and corneal xerosis (Venkatswamy, 1967). Systemic signs include angular stomatitis and dry, thickened skin. Figure 22 shows images from a patient with Vitamin A deficiency due to advanced liver disease (Vitamin A replacement in this situation is complicated due to hepatoxiocity). White dots are apparent on colour fundus photography, and CSLO imaging shows multiple small discrete entities, shown to be SDD on OCT.

Figure 22. Retinal imaging from a patient with vitamin A deficiency due to liver disease. *A*, Colour fundus photograph showing white dots. *B*, "Multicolour" CSLO imaging showing small discrete deposits. *C*, Short-wavelength AF imaging showing hypo-autofluorescent spots. *D*, Infrared reflectance imaging and OCT scan showing that the lesions are consistent with subretinal drusenoid deposits. *E-F*, Corresponding images from the left eye of the same patient.

5.2.2 Pseudoxanthoma elasticum

Pseudoxanthoma elasticum (PXE) is a systemic inherited disorder of calcium metabolism resulting from mutation of *ABCC6* (Bergen et al., 2000; Le Saux et al., 2000; Ringpfeil et al., 2000). ABCC6 is a transporter protein present in hepatocytes, when mutated there is a reduced ability to carry its substrate pyrophosphate (PPi), resulting in low serum PPi. This facilitates ectopic calcification, which preferentially occurs in elastic lamina of the eye and systemic arterial vasculature. Retinal features include angioid streaks and a "peau d'orange" appearance of areas of retina (a mottled or stippled pattern of yellowish lesions, which may be due to focal calcification of BM). This term was introduced by Smith and coworkers (Smith et al., 1964), and may be the same as entities previously described by Bischler (Bischler, 1955) and Shimuzu (Shimuzu, 1961).

SDD have also recently been reported to occur as a consequence of BM calcification in PXE (Gliem et al., 2015a). In addition, we have recently observed retinal changes resembling white dots in an 11 year old girl with PXE (Figure 23), similar to changes reported previously in children with PXE (Aydin et al., 2007). These white dots share phenotypic features similar to those observed in retinoid cycling disorders, and might suggest that a thickened BM may not fully support transfer of vitamin A at physiological levels. However, this would be expected to affect dark adaptation, and a previous study of dark adaptation and scotopic perimetry over the peau d'orange area in six PXE subjects found normal thresholds and kinetics (Holz et al., 1994).

Figure 23. Retinal images from a girl with PXE. *A*, Colour fundus photograph of the right eye aged 11 showing optic disc drusen as well as multiple white-yellow lesions. *B*, Short wavelength AF imaging taken aged 12, showing autofluorescence of disc drusen, but no obvious change in AF over the lesions. *C*, Infrared reflectance image and OCT: there is some mottling seen on the infrared reflectance image, but the OCT does not show discrete lesions, although BM may be thickened or hyper-reflective. *D-F*, corresponding images from the left eye.

5.2.3 Sjogren-Larsson syndrome (SLS)

This is a rare autosomal recessive neurocutaneous syndrome characterised by intellectual disability, spastic diplegia or tetraplegia and congenital icthyosis. Affected individuals may also show retinal involvement, particularly the appearance of bilateral, glistening white dots, usually present in the first few years of life. The retinal deposits appear to increase with age but have no correlation with the severity of systemic involvement. SLS results from a deficiency of fatty aldehyde dehydrogenase (FALDH), an enzyme necessary for the oxidation of fatty alcohol to fatty acid (Rogers et al., 1997). Consequently aldehyde modified lipids or fatty alcohols accumulate, which are likely to disrupt the function of membranes in the eye, brain and skin. The deposits are fine, often hard to photograph, hyperautofluorescent and not associated with electrophysiological abnormality (Jagell et al., 1980; Mirshahi and Piri, 2009).

5.2.4 Kjellin syndrome

Kjellin described a cohort of patients with spastic paraplegia, mental retardation, amyotrophia and central retinal degeneration (Kjellin, 1959). Many years later, the retinal phenotype was described further in a family survey (Frisch et al., 2002). Colour photography revealed widespread retinal flecks throughout the posterior pole and extending beyond the arcades, with a similar appearance to that in ABCA4 retinopathy. CSLO AF imaging revealed that the flecks have a central hyperautofluorescent region surrounded by a hypoautofluorescent boundary, thus subtly different to the flecks seen with mutation of *ABCA4*. FFA shows absence of a dark choroid, blockage of choroidal fluorescence over the lesions with a hyperfluorecent halo in the later stages of angiography. Similar to *ABCA4* retinopathy, electrophysiological changes may not be easily predicted from the anatomical changes, as those with widespread flecks may have normal results, or show reduction in full field ERG a wave amplitude with increased latency. Despite many similarities, Kjellin syndrome is not confused with Stargardt disease as neurological signs and symptoms predate the retinal changes (Puech et al., 2011). Recently two genes, *ZFYVE26* and *SPG11*, have been identified where bi-allelic mutation results in Kjellin syndrome (Hanein et al., 2008; Orlen et al., 2009).

5.2.5 Partial Lipodystrophy

Lipodystrophies are a large group of disorders involving varying degrees of fat loss. Nolis has recently reviewed the more common genetic and acquired types (Nolis, 2014). Familial partial lipodystrophy (FPLD) is a rare disorder involving selective and progressive alteration in adipose tissue from various areas of the body. Commonly this involves loss of fat from the arms, legs, head and trunk regions but may also include subcutaneous fat accumulation in other areas of the body, especially the neck, face and intra-abdominal regions. In most cases these changes begin during puberty. Six different subtypes of FPLD have been identified each with a different genetic aetiology (FPLD1-6). Four forms of FPLD are inherited as autosomal dominant traits; one form (FPLD5) is inherited as an autosomal recessive trait (resulting from mutations in the *CIDEC* gene). The mode of inheritance of FPLD1 is unknown.

FPLD can be associated with a variety of metabolic abnormalities (glucose intolerance, hypertriglycerideaemia) and the extent of adipose tissue loss usually relates to the severity of the associated metabolic complications. Systemic lupus erythematosus and dermatomyositis may also co-exist as autoimmune conditions.

FPLD is frequently associated with MPGN2, and often associated with the antibody C3 nephritic factor (Mathieson et al., 1993). This binds to and stabilises C3 convertase, leading to the activation of the alternative complement factor pathway and excessive consumption of C3 (Misra et al., 2004; Savage et al., 2009). Increased activity of C3 convertase activity has also been proposed as a risk for developing AMD (Helgason et al., 2013; Seddon et al., 2013; Zhan et al., 2013). High-risk alleles in *CFH* similarly act in this pathway.

Retinal changes similar to those described in MPGN2 and ARMD have been described, even in the absence of renal disease. Multiple widespread drusen have been identified which later either evolve to atrophy or neovascularization (Jansen et al., 2013; Patel and Page, 2006; Trabucchi et al., 1998). At least early on, these changes are not associated with abnormality in the full field electroretinogram, but a reduced electro-oculogram is noted when tested (Trabucchi et al., 1998).

5.2.6 Ring chromosome 17

Five cases of ring chromosome 17 have been reported with ocular involvement, all with features of short stature, mental retardation, epilepsy and café au lait spot in addition to a flecked retina appearance (Charles et al., 1991; Gass and Taney, 1994; Kumari et al., 2009; Ono et al., 1974; Shashi et al., 2003). Despite these retinal changes, no visual loss has been recorded in any of the cases (all under 34 years old). Ring chromosome formation may occur by direct telomere-telomere fusion, presumed to be associated with palindromic terminal DNA sequences. Alternatively chromosomal material may be lost. The retinopathy may result as a non-specific consequence of ring chromosome formation, with a generalized effect on cell cycle, or relate to gene dysregulation within the deleted (telomeric) regions. Figure 24 shows the retinal appearance of an affected patient, showing multiple yellow lesions in the macula that may be drusen or drusenoid deposits.

Figure 24. Findings from a patient with ring choromosome 17. A, Karyotyping showing the abnormal chromosome. B, Colour fundus photograph from the left eye showing small yellow lesions at the macula. Image courtesy of Graeme Black.

5.2.7 Partial Trisomy 10q

Partial trisomy of the long arm of chromosome 10 is an extremely rare genetic disorder first recognised in 1965 (de Grouchy and Canet, 1965). Subsequent reports have highlighted the syndromic features of disease, describing severe mental, growth, neurological, cardiac and skeletal disease. Facial features include microcephaly, a prominent forehead, low set ears and micrognathia, ocular findings predominantly involve the surface and adnexal tissue. Retinal abnormalities are less common. The first three reports describing the fundus findings did not identify any drusen-like changes (Laurent C, 1973; Prosperi et al., 1977; Yunis and Sanchez, 1974), however in two subsequent cases, widespread multiple fine drusen were observed (Neely et al., 1988; Tabandeh et al., 2000), and in one case there was associated RPE atrophy (Tabandeh et al., 2000). The same year Lam et al described a similar case but with widespread RPE abnormalities (Lam et al., 2000).

The duplicated region almost always includes 10qter, with the most frequent proximal breakpoint at 10q24. Variation in the clinical features most likely relates to the exact length and location of the duplicated portion of chromosome 10q, and that widespread genetic dysregulation contributes to the range of tissues affected rather than a dysfunction in a common pathway. Currently, as detailed fundus examinations have not been performed in all cases, the genetic link with drusen remains elusive.

6. Conclusions and future directions

The wide spectrum of retinopathies with drusen or drusen-like phenotypes highlight the wide range of associated aetiologies. Some patterns however do seem to emerge; soft drusen are rarely found outside the macula (except when associated with the CFH mutation R1210C); SDD seem to occur in visual cycle disorders and as a consequence of BM thickening (PXE, L-ORD, SFD) and spare the fovea. Drusen are likely to represent phenotypic convergence for a number of diverse biological processes. Their outcomes, however, vary, and it would be valuable to improve our ability to predict the associated long-term effects of each druse subtype. Recognising the various forms, and classifying them, is a start.

As our ability to characterise drusen continues to evolve, further insights into their biogenesis are obtained. Future autofluorescent imaging modules will provide quantitative as well as qualitative information, both in terms of the amplitude of autofluorescence as well as the duration of fluorescence lifetime (Ach et al., 2014). Advances in adaptive optics imaging now offer the opportunity to reduce the light backscattered from photoreceptors,

revealing the *in vivo* human RPE mosaic (shown in Figure 25), and the opportunity for visualisation of the earliest stages of disease. Another relatively under-investigated structure is the choroid, especially as this site is known to show high levels of complement activity prior to druse formation. As non-invasive techniques for choroidal imaging (enhanced depth imaging, swept source OCT, OCT angiography) are now available and changes within this vascular bed may now be routinely visualised and quantified. Along with an improved characterisation of fine anatomical details, the importance of functional testing is increasingly being appreciated. Psychophysical tests and dynamic electrophysiology offer assessment of the kinetics of the visual cycle *in vivo,* and detailed microperimetry, including scotopic and adaptive optics based techniques, adds spatial information to this (Tuten et al., 2012). Together, these approaches will provide outcome measures for future clinical treatments.

The disorders associated with drusen may seem diverse but two mechanistic themes seem to recur – dysregulation of the complement cascade and disruption in the visual cycle. Consequently, there has been considerable interest in identifying ways to modify these pathways. Lampalizumab is a monoclonal antibody fragment designed to inhibit human complement factor D, a rate-limiting enzyme in the alternative pathway. Other targets include modulating activity of the plasma protein C3, important in activation, amplification and effector generation in the complement response. In parallel strategies, groups are targeting bisretinoid production by attempting to modify the visual cycle. Emixustat hydrochloride (ACU-4429), specifically designed to inhibit the visual cycle isomerase (RPE65) is the first in this category to be tested in a phase II clinical trial (Dugel et al., 2015). Other visual cycle modulators are expected to follow, as well as attempts to prevent bisretinoid production without affecting the visual cycle.

We may also need to rethink our strategy for discovering the mechanisms underlying conventional druse formation. Genome wide association studies have provided much needed insight identifying a few common variants with high pathogenicity but most associated polymorphisms are of low effect. Performing the same studies recruiting patients with onset of drusen in earlier adult life may help identify rare variants of greater effect, involved in the same or novel biological pathways. As the cost of nucleotide sequencing continues to fall, these studies may be better performed using whole genome sequencing. As it is possible that intronic, or regulatory regions of DNA may be involved, candidate genes or regulatory sequences will need further functional analysis. This is now possible, using patient-specific RPE cells, generated using an induced pluripotency stem cell model. These cells can be aged in a controlled manner, with genetic, epigenetic and environmental factors investigated for the effects on cellular phenotypes. With time, rather than culturing monolayers of single cells, three-dimensional structures, comprising the RPE and neurosensory retina will become possible, providing a more accurate reproducing *in vivo* physiology.

Although our understanding of drusen has changed relatively little since their recognition over 150 years ago, the future now holds significant promise. Neovascular AMD is now considered a treatable disease, and our expectations are shifting towards managing the

earliest stages, with more attention now focussed on drusen. Strategies to prevent drusen formation could be one goal. However, as drusen could also be considered a marker for underlying pathogenic processes, prevention of drusen in themselves may not be sufficient. Diffuse, rather than focal, thickening of Bruch's membrane may be more important, and strategies aimed at improving transport across this structure may be beneficial. This might include upregulation of those matrix metalloproteinases (MMP) shown, over a decade ago, to improve hydraulic conductivity, such as MMP-9 (Ahir et al., 2002).

As more is understood regarding the molecular events, and their genetic and environmental modifiers, optimal strategies of disease prevention may emerge. Detailed clinical investigations, providing insight into *in vivo* biology may now be complemented by *in vitro* disease modelling, providing powerful tools to help solve currently unanswered questions.

Figure 25. Adaptive optics scanning laser ophthalmoscope imaging of the human RPE mosaic *in vivo*.

Acknowledgements

The authors acknowledge the following funding sources: National Institute for Health Research (NIHR) Biomedical Research Centre at Moorfields Eye Hospital National Health Service Foundation Trust and UCL Institute of Ophthalmology (UK; KNK, OAM, AT, AB, ATM, MM), Research to Prevent Blindness USA (ATM); Fight for Sight (UK; OAM, MM), the Foundation Fighting Blindness (FFB, USA; ATM, MM), Retinitis Pigmentosa Fighting Blindness (UK; ATM, MM). MM is a recipient of a Career Development award from FFB. KNK is supported by an NIHR Rare Disease Fellowship. This research has been supported by the National Institute for Health Research Rare Diseases Translational Research Collaboration (NIHR RD-TRC). The views expressed are those of the authors and not necessarily those of the NHS, the NIHR or the Department of Health

The authors acknowledge Professor Graeme Black, Matthew Robertson, Professor Andrew Webster and Melissa Kasilian for assistance with patients and images.

References

Ach, T., Huisingh, C., McGwin, G., Jr., Messinger, J.D., Zhang, T., Bentley, M.J., Gutierrez, D.B., Ablonczy, Z., Smith, R.T., Sloan, K.R., Curcio, C.A., 2014. Quantitative autofluorescence and cell density maps of the human retinal pigment epithelium. Invest Ophthalmol Vis Sci 55, 4832-4841.

Acharya, S., Foletta, V.C., Lee, J.W., Rayborn, M.E., Rodriguez, I.R., Young, W.S., 3rd, Hollyfield, J.G., 2000. SPACRCAN, a novel human interphotoreceptor matrix hyaluronan-binding proteoglycan synthesized by photoreceptors and pinealocytes. The Journal of biological chemistry 275, 6945-6955.

Age-Related Eye Disease Study Research, G., 2001. The age-related eye disease study (AREDS) system for classifying cataracts from photographs: AREDS report no. 4. American journal of ophthalmology 131, 167-175.

Ahir, A., Guo, L., Hussain, A.A., Marshall, J., 2002. Expression of metalloproteinases from human retinal pigment epithelial cells and their effects on the hydraulic conductivity of Bruch's membrane. Invest Ophthalmol Vis Sci 43, 458-465.

Ala-Laurila, P., Kolesnikov, A.V., Crouch, R.K., Tsina, E., Shukolyukov, S.A., Govardovskii, V.I., Koutalos, Y., Wiggert, B., Estevez, M.E., Cornwall, M.C., 2006. Visual cycle: Dependence of retinol production and removal on photoproduct decay and cell morphology. The Journal of general physiology 128, 153-169.

Albig, A.R., Schiemann, W.P., 2005. Identification and characterization of regulator of G protein signaling 4 (RGS4) as a novel inhibitor of tubulogenesis: RGS4 inhibits mitogen-

activated protein kinases and vascular endothelial growth factor signaling. Molecular biology of the cell 16, 609-625.

Allikmets, R., Singh, N., Sun, H., Shroyer, N.F., Hutchinson, A., Chidambaram, A., Gerrard, B., Baird, L., Stauffer, D., Peiffer, A., Rattner, A., Smallwood, P., Li, Y., Anderson, K.L., Lewis, R.A., Nathans, J., Leppert, M., Dean, M., Lupski, J.R., 1997. A photoreceptor cell-specific ATP-binding transporter gene (ABCR) is mutated in recessive Stargardt macular dystrophy. Nature genetics 15, 236-246.

Alten, F., Clemens, C.R., Heiduschka, P., Eter, N., 2014. Characterisation of reticular pseudodrusen and their central target aspect in multi-spectral, confocal scanning laser ophthalmoscopy. Graefe's archive for clinical and experimental ophthalmology = Albrecht von Graefes Archiv fur klinische und experimentelle Ophthalmologie 252, 715-721.

Amel, T., Samia, T., Imed, E., Hassen, M., Med-Faouzi, G., 2000. [Pregnancy in adolescence: maternal-fetal prognosis]. La Tunisie medicale 78, 658-661.

Anderson, D.H., Hageman, G.S., Mullins, R.F., Neitz, M., Neitz, J., Ozaki, S., Preissner, K.T., Johnson, L.V., 1999. Vitronectin gene expression in the adult human retina. Investigative ophthalmology & visual science 40, 3305-3315.

Anderson, D.H., Radeke, M.J., Gallo, N.B., Chapin, E.A., Johnson, P.T., Curletti, C.R., Hancox, L.S., Hu, J., Ebright, J.N., Malek, G., Hauser, M.A., Rickman, C.B., Bok, D., Hageman, G.S., Johnson, L.V., 2010. The pivotal role of the complement system in aging and age-related macular degeneration: hypothesis re-visited. Progress in retinal and eye research 29, 95-112.

Appiah, K.K., Blat, Y., Robertson, B.J., Pearce, B.C., Pedicord, D.L., Gentles, R.G., Yu, X.C., Mseeh, F., Nguyen, N., Swaffield, J.C., Harden, D.G., Westphal, R.S., Banks, M.N., O'Connell, J.C., 2014. Identification of small molecules that selectively inhibit diacylglycerol lipase-alpha activity. Journal of biomolecular screening 19, 595-605.

Arana, L.A., Sato, M., Arana, J., 2010. Familial congenital grouped albinotic retinal pigment epithelial spots. Archives of ophthalmology 128, 1362-1364.

Ardeljan, D., Chan, C.C., 2013. Aging is not a disease: distinguishing age-related macular degeneration from aging. Prog Retin Eye Res 37, 68-89.

Arnold, J.J., Quaranta, M., Soubrane, G., Sarks, S.H., Coscas, G., 1997. Indocyanine green angiography of drusen. American journal of ophthalmology 124, 344-356.

Arnold, J.J., Sarks, S.H., Killingsworth, M.C., Sarks, J.P., 1995. Reticular pseudodrusen. A risk factor in age-related maculopathy. Retina 15, 183-191.

Aydin, E., Demir, H.D., Batioglu, F., Sezer, E., 2007. Atypical fundus lesions in juvenile pseudoxanthoma elasticum. Ophthalmic research 39, 344-347.

Ba-Abbad, R., Sergouniotis, P.I., Plagnol, V., Robson, A.G., Michaelides, M., Holder, G.E., Webster, A.R., 2013. Clinical characteristics of early retinal disease due to CDHR1 mutation. Molecular vision 19, 2250-2259.

Bandah-Rozenfeld, D., Collin, R.W., Banin, E., van den Born, L.I., Coene, K.L., Siemiatkowska, A.M., Zelinger, L., Khan, M.I., Lefeber, D.J., Erdinest, I., Testa, F., Simonelli, F., Voesenek, K., Blokland, E.A., Strom, T.M., Klaver, C.C., Qamar, R., Banfi, S., Cremers, F.P., Sharon, D., den Hollander, A.I., 2010. Mutations in IMPG2, encoding interphotoreceptor matrix proteoglycan 2, cause autosomal-recessive retinitis pigmentosa. American journal of human genetics 87, 199-208.

Baudouin, C., Peyman, G.A., Fredj-Reygrobellet, D., Gordon, W.C., Lapalus, P., Gastaud, P., Bazan, N.G., 1992. Immunohistological study of subretinal membranes in age-related macular degeneration. Japanese journal of ophthalmology 36, 443-451.

Beattie, S., 2009. Lipids. Rn 72, 16-18, 20-11.

Beharry, S., Zhong, M., Molday, R.S., 2004. N-retinylidene-phosphatidylethanolamine is the preferred retinoid substrate for the photoreceptor-specific ABC transporter ABCA4 (ABCR). The Journal of biological chemistry 279, 53972-53979.

Bergen, A.A., Plomp, A.S., Schuurman, E.J., Terry, S., Breuning, M., Dauwerse, H., Swart, J., Kool, M., van Soest, S., Baas, F., ten Brink, J.B., de Jong, P.T., 2000. Mutations in ABCC6 cause pseudoxanthoma elasticum. Nature genetics 25, 228-231.

Biesemeier, A., Yoeruek, E., Eibl, O., Schraermeyer, U., 2015. Iron accumulation in Bruch's membrane and melanosomes of donor eyes with age-related macular degeneration. Exp Eye Res 137, 39-49.

Bird, A.C., Bressler, N.M., Bressler, S.B., Chisholm, I.H., Coscas, G., Davis, M.D., de Jong, P.T., Klaver, C.C., Klein, B.E., Klein, R., et al., 1995. An international classification and grading system for age-related maculopathy and age-related macular degeneration. The International ARM Epidemiological Study Group. Survey of ophthalmology 39, 367-374.

Bischler, V., 1955. [The importance of changes in the fundus oculi in the diagnosis of disease of vascular origin]. Praxis 44, 1110-1112.

Bonnet, C., Querques, G., Zerbib, J., Oubraham, H., Garavito, R.B., Puche, N., Souied, E.H., 2014. Hyperreflective pyramidal structures on optical coherence tomography in geographic atrophy areas. Retina 34, 1524-1530.

Boon, C., 2014. Retinal Dystrophies Associated with the PRPH2 gene. Chapter: Inherited Chorioretinal Dystrophies, pp 213-233.

Boon, C.J., Klevering, B.J., Hoyng, C.B., Zonneveld-Vrieling, M.N., Nabuurs, S.B., Blokland, E., Cremers, F.P., den Hollander, A.I., 2008. Basal laminar drusen caused by compound heterozygous variants in the CFH gene. Am J Hum Genet 82, 516-523.

Boon, C.J., van de Ven, J.P., Hoyng, C.B., den Hollander, A.I., Klevering, B.J., 2013. Cuticular drusen: stars in the sky. Prog Retin Eye Res 37, 90-113.

Bunt-Milam, A.H., Saari, J.C., 1983. Immunocytochemical localization of two retinoid-binding proteins in vertebrate retina. The Journal of cell biology 97, 703-712.

Burstedt, M.S., Golovleva, I., 2010. Central retinal findings in Bothnia dystrophy caused by RLBP1 sequence variation. Archives of ophthalmology 128, 989-995.

Capon, M.R., Marshall, J., Krafft, J.I., Alexander, R.A., Hiscott, P.S., Bird, A.C., 1989. Sorsby's fundus dystrophy. A light and electron microscopic study. Ophthalmology 96, 1769-1777.

Charles, S.J., Moore, A.T., Davison, B.C., Dyson, H.M., Willatt, L., 1991. Flecked retina associated with ring 17 chromosome. The British journal of ophthalmology 75, 125-127.

Cohen, B., Chervinsky, E., Jabaly-Habib, H., Shalev, S.A., Briscoe, D., Ben-Yosef, T., 2012. A novel splice site mutation of CDHR1 in a consanguineous Israeli Christian Arab family segregating autosomal recessive cone-rod dystrophy. Molecular vision 18, 2915-2921.

Cohen, S.Y., Meunier, I., Soubrane, G., Glacet-Bernard, A., Coscas, G.J., 1994. Visual function and course of basal laminar drusen combined with vitelliform macular detachment. The British journal of ophthalmology 78, 437-440.

Colville, D., Guymer, R., Sinclair, R.A., Savige, J., 2003. Visual impairment caused by retinal abnormalities in mesangiocapillary (membranoproliferative) glomerulonephritis type II ("dense deposit disease"). American journal of kidney diseases : the official journal of the National Kidney Foundation 42, E2-5.

Crouch, R.K., Hazard, E.S., Lind, T., Wiggert, B., Chader, G., Corson, D.W., 1992. Interphotoreceptor retinoid-binding protein and alpha-tocopherol preserve the isomeric and oxidation state of retinol. Photochemistry and photobiology 56, 251-255.

Curcio, C.A., Balaratnasingam, C., Messinger, J.D., Yannuzzi, L.A., Freund, K.B., 2015. Correlation of Type 1 Neovascularization Associated With Acquired Vitelliform Lesion in the Setting of Age-Related Macular Degeneration. Am J Ophthalmol 160, 1024-1033 e1023.

Curcio, C.A., Johnson, M., Rudolf, M., Huang, J.D., 2011. The oil spill in ageing Bruch membrane. The British journal of ophthalmology 95, 1638-1645.

Curcio, C.A., Messinger, J.D., Sloan, K.R., McGwin, G., Medeiros, N.E., Spaide, R.F., 2013. Subretinal drusenoid deposits in non-neovascular age-related macular degeneration: morphology, prevalence, topography, and biogenesis model. Retina 33, 265-276.

Curcio, C.A., Millican, C.L., 1999. Basal linear deposit and large drusen are specific for early age-related maculopathy. Archives of ophthalmology 117, 329-339.

Curcio, C.A., Presley, J.B., Malek, G., Medeiros, N.E., Avery, D.V., Kruth, H.S., 2005. Esterified and unesterified cholesterol in drusen and basal deposits of eyes with age-related maculopathy. Experimental eye research 81, 731-741.

D'Agati, V.D., Bomback, A.S., 2012. C3 glomerulopathy: what's in a name? Kidney international 82, 379-381.

D'Souza Y, B., Jones, C.J., Short, C.D., Roberts, I.S., Bonshek, R.E., 2009. Oligosaccharide composition is similar in drusen and dense deposits in membranoproliferative glomerulonephritis type II. Kidney international 75, 824-827.

D'Souza, Y., Short, C.D., McLeod, D., Bonshek, R.E., 2008. Long-term follow-up of drusen-like lesions in patients with type II mesangiocapillary glomerulonephritis. The British journal of ophthalmology 92, 950-953.

Dalvin, L.A., Fervenza, F.C., Sethi, S., Pulido, J.S., 2015. Shedding Light on Fundus Drusen Associated with Membranoproliferative Glomerulonephritis: Breaking Stereotypes of Types I, Ii, and Iii. Retinal cases & brief reports.

Dasari, B., Prasanthi, J.R., Marwarha, G., Singh, B.B., Ghribi, O., 2010. The oxysterol 27-hydroxycholesterol increases beta-amyloid and oxidative stress in retinal pigment epithelial cells. BMC ophthalmology 10, 22.

Davis, M.D., Gangnon, R.E., Lee, L.Y., Hubbard, L.D., Klein, B.E., Klein, R., Ferris, F.L., Bressler, S.B., Milton, R.C., Age-Related Eye Disease Study, G., 2005. The Age-Related Eye Disease Study severity scale for age-related macular degeneration: AREDS Report No. 17. Archives of ophthalmology 123, 1484-1498.

de Grouchy, J., Canet, J., 1965. [6-12 13-15 translocation and partial 6-12 trisomy (probably 10)]. Annales de genetique 8, 16-20.

Deigner, P.S., Law, W.C., Canada, F.J., Rando, R.R., 1989. Membranes as the energy source in the endergonic transformation of vitamin A to 11-cis-retinol. Science 244, 968-971.

Del Turco, C., Pierro, L., Querques, G., Gagliardi, M., Corvi, F., Manitto, M.P., Bandello, F.M., 2015. Posterior polymorphous corneal dystrophy concomitant to large colloid drusen. European journal of ophthalmology 25, 177-179.

Delori, F.C., Fleckner, M.R., Goger, D.G., Weiter, J.J., Dorey, C.K., 2000. Autofluorescence distribution associated with drusen in age-related macular degeneration. Investigative ophthalmology & visual science 41, 496-504.

Donders, F., 1855. Beitrage zur pathologischen Anatomie des Auges. Graefe's archive for clinical and experimental ophthalmology = Albrecht von Graefes Archiv fur klinische und experimentelle Ophthalmologie 1, 106-118.

Doyne, R.W., 1899. A peculiar condition of choroiditis occurring in several members of the same family. Trans. Ophthal. Soc. U.K. 19, 71.

Driessen, C.A., Janssen, B.P., Winkens, H.J., van Vugt, A.H., de Leeuw, T.L., Janssen, J.J., 1995. Cloning and expression of a cDNA encoding bovine retinal pigment epithelial 11-cis retinol dehydrogenase. Investigative ophthalmology & visual science 36, 1988-1996.

Dugel, P.U., Novack, R.L., Csaky, K.G., Richmond, P.P., Birch, D.G., Kubota, R., 2015. Phase ii, randomized, placebo-controlled, 90-day study of emixustat hydrochloride in geographic atrophy associated with dry age-related macular degeneration. Retina 35, 1173-1183.

Duncan, J.L., Roorda, A., Navani, M., Vishweswaraiah, S., Syed, R., Soudry, S., Ratnam, K., Gudiseva, H.V., Lee, P., Gaasterland, T., Ayyagari, R., 2012. Identification of a novel mutation in the CDHR1 gene in a family with recessive retinal degeneration. Archives of ophthalmology 130, 1301-1308.

Duvall-Young, J., MacDonald, M.K., McKechnie, N.M., 1989. Fundus changes in (type II) mesangiocapillary glomerulonephritis simulating drusen: a histopathological report. The British journal of ophthalmology 73, 297-302.

Edwards, A.O., Ritter, R., 3rd, Abel, K.J., Manning, A., Panhuysen, C., Farrer, L.A., 2005. Complement factor H polymorphism and age-related macular degeneration. Science 308, 421-424.

Eichers, E.R., Green, J.S., Stockton, D.W., Jackman, C.S., Whelan, J., McNamara, J.A., Johnson, G.J., Lupski, J.R., Katsanis, N., 2002. Newfoundland rod-cone dystrophy, an early-onset retinal dystrophy, is caused by splice-junction mutations in RLBP1. American journal of human genetics 70, 955-964.

Elsner AE, B.S., Delori FC, Webb RH, 1990. Quantitative Reflectometry with SLO. Quintessenz-Verlag 109-121.

Fakhouri, F., Fremeaux-Bacchi, V., Noel, L.H., Cook, H.T., Pickering, M.C., 2010. C3 glomerulopathy: a new classification. Nature reviews. Nephrology 6, 494-499.

Feeney-Burns, L., Ellersieck, M.R., 1985. Age-related changes in the ultrastructure of Bruch's membrane. American journal of ophthalmology 100, 686-697.

Felbor, U., Gehrig, A., Sauer, C.G., Marquardt, A., Kohler, M., Schmid, M., Weber, B.H., 1998. Genomic organization and chromosomal localization of the interphotoreceptor matrix proteoglycan-1 (IMPG1) gene: a candidate for 6q-linked retinopathies. Cytogenetics and cell genetics 81, 12-17.

Fell, H.B., 1969. Vitamin A and enzymes, membranes, differentiation and reproduction. Introduction. The American journal of clinical nutrition 22, 975-977.

Ferrara, D., Seddon, J.M., 2015. Phenotypic Characterization of Complement Factor H R1210C Rare Genetic Variant in Age-Related Macular Degeneration. JAMA ophthalmology 133, 785-791.

Ferris, F.L., 3rd, Wilkinson, C.P., Bird, A., Chakravarthy, U., Chew, E., Csaky, K., Sadda, S.R., Beckman Initiative for Macular Research Classification, C., 2013. Clinical classification of age-related macular degeneration. Ophthalmology 120, 844-851.

Fisher, D.E., Klein, B.E., Wong, T.Y., Rotter, J.I., Li, X., Shrager, S., Burke, G.L., Klein, R., Cotch, M.F., 2016. Incidence of Age-Related Macular Degeneration in a Multi-Ethnic United States Population: The Multi-Ethnic Study of Atherosclerosis. Ophthalmology.

Fleckenstein, M., Charbel Issa, P., Helb, H.M., Schmitz-Valckenberg, S., Finger, R.P., Scholl, H.P., Loeffler, K.U., Holz, F.G., 2008. High-resolution spectral domain-OCT imaging in geographic atrophy associated with age-related macular degeneration. Investigative ophthalmology & visual science 49, 4137-4144.

Folwell, A.J., Macdiarmid, S.A., Crowder, H.J., Lord, A.D., Arnold, E.P., 1997. Desmopressin for nocturnal enuresis: urinary osmolality and response. British journal of urology 80, 480-484.

Francis, P.J., Johnson, S., Edmunds, B., Kelsell, R.E., Sheridan, E., Garrett, C., Holder, G.E., Hunt, D.M., Moore, A.T., 2003. Genetic linkage analysis of a novel syndrome comprising North Carolina-like macular dystrophy and progressive sensorineural hearing loss. The British journal of ophthalmology 87, 893-898.

Freund, K.B., Zweifel, S.A., Engelbert, M., 2010. Do we need a new classification for choroidal neovascularization in age-related macular degeneration? Retina 30, 1333-1349.

Fried, M., 1972. Report of a case resembling the Fleck Retina of Kandori with Ectodermal Peculiarities and Macular Degeneration. ALbrecht v Graefes Arch klin exp Ophthal 211, 307-311.

Frisch, I.B., Haag, P., Steffen, H., Weber, B.H., Holz, F.G., 2002. Kjellin's syndrome: fundus autofluorescence, angiographic, and electrophysiologic findings. Ophthalmology 109, 1484-1491.

Fuchs, A., 1928. On Pseudoglaucoma. The British journal of ophthalmology 12, 65-73.

Fuchs, A., 1959. White spots of the fundus combined with night blindness and xerosis (Uyemura's syndrome). American journal of ophthalmology 48, 101-103.

Gass, J., 1977. Stereoscopic atlas of macular disease: diagnosis and treatment (2nd Edition) St. Louis: Mosby.

Gass, J.D., Jallow, S., Davis, B., 1985. Adult vitelliform macular detachment occurring in patients with basal laminar drusen. American journal of ophthalmology 99, 445-459.

Gass, J.D., Taney, B.S., 1994. Flecked retina associated with cafe au lait spots, microcephaly, epilepsy, short stature, and ring 17 chromosome. Archives of ophthalmology 112, 738-739.

Gauter-Fleckenstein, B., Fleckenstein, K., Owzar, K., Jiang, C., Batinic-Haberle, I., Vujaskovic, Z., 2008. Comparison of two Mn porphyrin-based mimics of superoxide dismutase in pulmonary radioprotection. Free radical biology & medicine 44, 982-989.

Gliem, M., Hendig, D., Finger, R.P., Holz, F.G., Charbel Issa, P., 2015a. Reticular pseudodrusen associated with a diseased bruch membrane in pseudoxanthoma elasticum. JAMA ophthalmology 133, 581-588.

Gliem, M., Muller, P.L., Mangold, E., Holz, F.G., Bolz, H.J., Stohr, H., Weber, B.H., Charbel Issa, P., 2015b. Sorsby Fundus Dystrophy: Novel Mutations, Novel Phenotypic Characteristics, and Treatment Outcomes. Investigative ophthalmology & visual science 56, 2664-2676.

Grassi, M.A., Folk, J.C., Scheetz, T.E., Taylor, C.M., Sheffield, V.C., Stone, E.M., 2007. Complement factor H polymorphism p.Tyr402His and cuticular Drusen. Archives of ophthalmology 125, 93-97.

Green, W.R., Enger, C., 1993. Age-related macular degeneration histopathologic studies. The 1992 Lorenz E. Zimmerman Lecture. Ophthalmology 100, 1519-1535.

Grewal, D.S., Chou, J., Rollins, S.D., Fawzi, A.A., 2014. A pilot quantitative study of topographic correlation between reticular pseudodrusen and the choroidal vasculature using en face optical coherence tomography. PLoS One 9, e92841.

Guigui, B., Leveziel, N., Martinet, V., Massamba, N., Sterkers, M., Coscas, G., Souied, E.H., 2011. Angiography features of early onset drusen. The British journal of ophthalmology 95, 238-244.

Haeseleer, F., Huang, J., Lebioda, L., Saari, J.C., Palczewski, K., 1998. Molecular characterization of a novel short-chain dehydrogenase/reductase that reduces all-trans-retinal. The Journal of biological chemistry 273, 21790-21799.

Hageman, G.S., Anderson, D.H., Johnson, L.V., Hancox, L.S., Taiber, A.J., Hardisty, L.I., Hageman, J.L., Stockman, H.A., Borchardt, J.D., Gehrs, K.M., Smith, R.J., Silvestri, G., Russell, S.R., Klaver, C.C., Barbazetto, I., Chang, S., Yannuzzi, L.A., Barile, G.R., Merriam, J.C., Smith, R.T., Olsh, A.K., Bergeron, J., Zernant, J., Merriam, J.E., Gold, B., Dean, M., Allikmets, R., 2005. A common haplotype in the complement regulatory gene factor H (HF1/CFH) predisposes individuals to age-related macular degeneration. Proceedings of the National Academy of Sciences of the United States of America 102, 7227-7232.

Hageman, G.S., Luthert, P.J., Victor Chong, N.H., Johnson, L.V., Anderson, D.H., Mullins, R.F., 2001. An integrated hypothesis that considers drusen as biomarkers of immune-mediated processes at the RPE-Bruch's membrane interface in aging and age-related macular degeneration. Progress in retinal and eye research 20, 705-732.

Hahn, P., Milam, A.H., Dunaief, J.L., 2003. Maculas affected by age-related macular degeneration contain increased chelatable iron in the retinal pigment epithelium and Bruch's membrane. Arch Ophthalmol 121, 1099-1105.

Haines, J.L., Hauser, M.A., Schmidt, S., Scott, W.K., Olson, L.M., Gallins, P., Spencer, K.L., Kwan, S.Y., Noureddine, M., Gilbert, J.R., Schnetz-Boutaud, N., Agarwal, A., Postel, E.A., Pericak-Vance, M.A., 2005. Complement factor H variant increases the risk of age-related macular degeneration. Science 308, 419-421.

Han, D.P., Sievers, S., 2009. Extensive drusen in type I membranoproliferative glomerulonephritis. Archives of ophthalmology 127, 577-579.

Hanein, S., Martin, E., Boukhris, A., Byrne, P., Goizet, C., Hamri, A., Benomar, A., Lossos, A., Denora, P., Fernandez, J., Elleuch, N., Forlani, S., Durr, A., Feki, I., Hutchinson, M., Santorelli, F.M., Mhiri, C., Brice, A., Stevanin, G., 2008. Identification of the SPG15 gene, encoding spastizin, as a frequent cause of complicated autosomal-recessive spastic paraplegia, including Kjellin syndrome. American journal of human genetics 82, 992-1002.

Hayward, C., Shu, X., Cideciyan, A.V., Lennon, A., Barran, P., Zareparsi, S., Sawyer, L., Hendry, G., Dhillon, B., Milam, A.H., Luthert, P.J., Swaroop, A., Hastie, N.D., Jacobson, S.G., Wright, A.F., 2003. Mutation in a short-chain collagen gene, CTRP5, results in extracellular deposit formation in late-onset retinal degeneration: a genetic model for age-related macular degeneration. Human molecular genetics 12, 2657-2667.

Heiferman, M.J., Fernandes, J.K., Munk, M., Mirza, R.G., Jampol, L.M., Fawzi, A.A., 2015. Reticular Pseudodrusen on Infrared Imaging Are Topographically Distinct from Subretinal Drusenoid Deposits on En Face Optical Coherence Tomography. Retina.

Helgason, H., Sulem, P., Duvvari, M.R., Luo, H., Thorleifsson, G., Stefansson, H., Jonsdottir, I., Masson, G., Gudbjartsson, D.F., Walters, G.B., Magnusson, O.T., Kong, A., Rafnar, T., Kiemeney, L.A., Schoenmaker-Koller, F.E., Zhao, L., Boon, C.J., Song, Y., Fauser, S., Pei, M., Ristau, T., Patel, S., Liakopoulos, S., van de Ven, J.P., Hoyng, C.B., Ferreyra, H., Duan, Y., Bernstein, P.S., Geirsdottir, A., Helgadottir, G., Stefansson, E., den Hollander, A.I., Zhang, K., Jonasson, F., Sigurdsson, H., Thorsteinsdottir, U., Stefansson, K., 2013. A rare nonsynonymous sequence variant in C3 is associated with high risk of age-related macular degeneration. Nat Genet 45, 1371-1374.

Herbert, A.P., Deakin, J.A., Schmidt, C.Q., Blaum, B.S., Egan, C., Ferreira, V.P., Pangburn, M.K., Lyon, M., Uhrin, D., Barlow, P.N., 2007. Structure shows that a glycosaminoglycan and protein recognition site in factor H is perturbed by age-related macular degeneration-linked single nucleotide polymorphism. The Journal of biological chemistry 282, 18960-18968.

Holz, F.G., Jubb, C., Fitzke, F.W., Bird, A.C., Pope, F.M., 1994. Dark adaptation and scotopic perimetry over 'peau d'orange' in pseudoxanthoma elasticum. The British journal of ophthalmology 78, 79-80.

Jagell, S., Polland, W., Sandgren, O., 1980. Specific changes in the fundus typical for the Sjogren-Larsson syndrome. An ophthalmological study of 35 patients. Acta Ophthalmol (Copenh) 58, 321-330.

Jain, N., Farsiu, S., Khanifar, A.A., Bearelly, S., Smith, R.T., Izatt, J.A., Toth, C.A., 2010. Quantitative comparison of drusen segmented on SD-OCT versus drusen delineated on color fundus photographs. Invest Ophthalmol Vis Sci 51, 4875-4883.

Jansen, J., Delaere, L., Spielberg, L., Leys, A., 2013. Long-term fundus changes in acquired partial lipodystrophy. BMJ case reports 2013.

Jin, M., Li, S., Moghrabi, W.N., Sun, H., Travis, G.H., 2005. Rpe65 is the retinoid isomerase in bovine retinal pigment epithelium. Cell 122, 449-459.

Joachim, N., Mitchell, P., Younan, C., Burlutsky, G., Cheng, C.Y., Cheung, C.M., Zheng, Y., Moffitt, M., Wong, T.Y., Wang, J.J., 2014. Ethnic variation in early age-related macular degeneration lesions between white Australians and Singaporean Asians. Invest Ophthalmol Vis Sci 55, 4421-4429.

Kaemmerer, E., Schutt, F., Krohne, T.U., Holz, F.G., Kopitz, J., 2007. Effects of lipid peroxidation-related protein modifications on RPE lysosomal functions and POS phagocytosis. Investigative ophthalmology & visual science 48, 1342-1347.

Kanagasingam, Y., Bhuiyan, A., Abramoff, M.D., Smith, R.T., Goldschmidt, L., Wong, T.Y., 2014. Progress on retinal image analysis for age related macular degeneration. Prog Retin Eye Res 38, 20-42.

Kandori, F., 1959. Very rare cases of congenital non-progressive night blindness with fleck retina. . Jpn. J. Ophthal. 13, 384-386.

Kandori, F., Setogawa, T., Tamai, A., 1966. Electroretinographical studies on "fleck retina with congenital nonprogressive nightblindness". Yonago acta medica 10, 98-108.

Kandori, F., Tamai, A., Kurimoto, S., Fukunaga, K., 1972. Fleck retina. American journal of ophthalmology 73, 673-685.

Kenyon, K.R., Maumenee, A.E., Ryan, S.J., Whitmore, P.V., Green, W.R., 1985. Diffuse drusen and associated complications. American journal of ophthalmology 100, 119-128.

Khanifar, A.A., Koreishi, A.F., Izatt, J.A., Toth, C.A., 2008. Drusen ultrastructure imaging with spectral domain optical coherence tomography in age-related macular degeneration. Ophthalmology 115, 1883-1890.

Kjellin, K., 1959. Familial spastic paraplegia with amyotrophy, oligophrenia, and central retinal degeneration. Archives of neurology 1, 133-140.

Klein, R., Davis, M.D., Magli, Y.L., Segal, P., Klein, B.E., Hubbard, L., 1991. The Wisconsin age-related maculopathy grading system. Ophthalmology 98, 1128-1134.

Klein, R.J., Zeiss, C., Chew, E.Y., Tsai, J.Y., Sackler, R.S., Haynes, C., Henning, A.K., SanGiovanni, J.P., Mane, S.M., Mayne, S.T., Bracken, M.B., Ferris, F.L., Ott, J., Barnstable, C., Hoh, J., 2005. Complement factor H polymorphism in age-related macular degeneration. Science 308, 385-389.

Kruth, H.S., 1985. Subendothelial accumulation of unesterified cholesterol. An early event in atherosclerotic lesion development. Atherosclerosis 57, 337-341.

Kuehn, M.H., Hageman, G.S., 1999. Molecular characterization and genomic mapping of human IPM 200, a second member of a novel family of proteoglycans. Molecular cell biology research communications : MCBRC 2, 103-110.

Kumari, R., Black, G., Dore, J., Lloyd, I.C., 2009. Flecked retina associated with ring 17 chromosome. Eye 23, 2134-2135.

Kuntz, C.A., Jacobson, S.G., Cideciyan, A.V., Li, Z.Y., Stone, E.M., Possin, D., Milam, A.H., 1996. Sub-retinal pigment epithelial deposits in a dominant late-onset retinal degeneration. Investigative ophthalmology & visual science 37, 1772-1782.

Laine, M., Jarva, H., Seitsonen, S., Haapasalo, K., Lehtinen, M.J., Lindeman, N., Anderson, D.H., Johnson, P.T., Jarvela, I., Jokiranta, T.S., Hageman, G.S., Immonen, I., Meri, S., 2007. Y402H polymorphism of complement factor H affects binding affinity to C-reactive protein. Journal of immunology 178, 3831-3836.

Lam, F.W., Chan, W.K., Lam, S.T., Chu, W.P., Kwong, N.S., 2000. Proximal 10q trisomy: a new case with anal atresia. Journal of medical genetics 37, E24.

Lamb, T.D., 2013. Evolution of phototransduction, vertebrate photoreceptors and retina. Progress in retinal and eye research 36, 52-119.

Laurent C, B.-L.M., Dutrillaux B, 1973. Trisomie 10 partielle par translocation familiale t(1;10)(q44;q22). Human genetic 18, 321-327.

Le Saux, O., Urban, Z., Tschuch, C., Csiszar, K., Bacchelli, B., Quaglino, D., Pasquali-Ronchetti, I., Pope, F.M., Richards, A., Terry, S., Bercovitch, L., de Paepe, A., Boyd, C.D., 2000. Mutations in a gene encoding an ABC transporter cause pseudoxanthoma elasticum. Nature genetics 25, 223-227.

Lee, M.Y., Ham, D.I., 2014. Subretinal drusenoid deposits with increased autofluorescence in eyes with reticular pseudodrusen. Retina 34, 69-76.

Lengyel, I., Flinn, J.M., Peto, T., Linkous, D.H., Cano, K., Bird, A.C., Lanzirotti, A., Frederickson, C.J., van Kuijk, F.J., 2007. High concentration of zinc in sub-retinal pigment epithelial deposits. Exp Eye Res 84, 772-780.

Li, C.M., Clark, M.E., Chimento, M.F., Curcio, C.A., 2006. Apolipoprotein localization in isolated drusen and retinal apolipoprotein gene expression. Investigative ophthalmology & visual science 47, 3119-3128.

Loeffler, K.U., Lee, W.R., 1998. Terminology of sub-RPE deposits: do we all speak the same language? The British journal of ophthalmology 82, 1104-1105.

Loffler, K.U., Lee, W.R., 1986. Basal linear deposit in the human macula. Graefe's archive for clinical and experimental ophthalmology = Albrecht von Graefes Archiv fur klinische und experimentelle Ophthalmologie 224, 493-501.

Lois, N., Owens, S.L., Coco, R., Hopkins, J., Fitzke, F.W., Bird, A.C., 2002. Fundus autofluorescence in patients with age-related macular degeneration and high risk of visual loss. American journal of ophthalmology 133, 341-349.

Macauley, S.L., Roberts, M.S., Wong, A.M., McSloy, F., Reddy, A.S., Cooper, J.D., Sands, M.S., 2012. Synergistic effects of central nervous system-directed gene therapy and bone marrow transplantation in the murine model of infantile neuronal ceroid lipofuscinosis. Ann Neurol 71, 797-804.

Malek, G., Li, C.M., Guidry, C., Medeiros, N.E., Curcio, C.A., 2003. Apolipoprotein B in cholesterol-containing drusen and basal deposits of human eyes with age-related maculopathy. The American journal of pathology 162, 413-425.

Malorni, W., Iosi, F., Mirabelli, F., Bellomo, G., 1991. Cytoskeleton as a target in menadione-induced oxidative stress in cultured mammalian cells: alterations underlying surface bleb formation. Chemico-biological interactions 80, 217-236.

Manes, G., Meunier, I., Avila-Fernandez, A., Banfi, S., Le Meur, G., Zanlonghi, X., Corton, M., Simonelli, F., Brabet, P., Labesse, G., Audo, I., Mohand-Said, S., Zeitz, C., Sahel, J.A., Weber, M., Dollfus, H., Dhaenens, C.M., Allorge, D., De Baere, E., Koenekoop, R.K., Kohl, S., Cremers, F.P., Hollyfield, J.G., Senechal, A., Hebrard, M., Bocquet, B., Ayuso Garcia, C., Hamel, C.P., 2013. Mutations in IMPG1 cause vitelliform macular dystrophies. American journal of human genetics 93, 571-578.

Marin-Castano, M.E., Csaky, K.G., Cousins, S.W., 2005. Nonlethal oxidant injury to human retinal pigment epithelium cells causes cell membrane blebbing but decreased MMP-2 activity. Investigative ophthalmology & visual science 46, 3331-3340.

Mata, N.L., Moghrabi, W.N., Lee, J.S., Bui, T.V., Radu, R.A., Horwitz, J., Travis, G.H., 2004. Rpe65 is a retinyl ester binding protein that presents insoluble substrate to the isomerase in retinal pigment epithelial cells. The Journal of biological chemistry 279, 635-643.

Mata, N.L., Radu, R.A., Clemmons, R.C., Travis, G.H., 2002. Isomerization and oxidation of vitamin a in cone-dominant retinas: a novel pathway for visual-pigment regeneration in daylight. Neuron 36, 69-80.

Mathieson, P.W., Wurzner, R., Oliveria, D.B., Lachmann, P.J., Peters, D.K., 1993. Complement-mediated adipocyte lysis by nephritic factor sera. The Journal of experimental medicine 177, 1827-1831.

McAvoy, C.E., Silvestri, G., 2005. Retinal changes associated with type 2 glomerulonephritis. Eye 19, 985-989.

Meadway, A., Wang, X., Curcio, C.A., Zhang, Y., 2014. Microstructure of subretinal drusenoid deposits revealed by adaptive optics imaging. Biomedical optics express 5, 713-727.

Meyerle, C.B., Smith, R.T., Barbazetto, I.A., Yannuzzi, L.A., 2007. Autofluorescence of basal laminar drusen. Retina 27, 1101-1106.

Michaelides, M., Jeffery, G., Moore, A.T., 2012. Developmental macular disorders: phenotypes and underlying molecular genetic basis. The British journal of ophthalmology 96, 917-924.

Michaelides, M., Jenkins, S.A., Brantley, M.A., Jr., Andrews, R.M., Waseem, N., Luong, V., Gregory-Evans, K., Bhattacharya, S.S., Fitzke, F.W., Webster, A.R., 2006. Maculopathy due to the R345W substitution in fibulin-3: distinct clinical features, disease variability, and extent of retinal dysfunction. Investigative ophthalmology & visual science 47, 3085-3097.

Michaelides, M., Johnson, S., Tekriwal, A.K., Holder, G.E., Bellmann, C., Kinning, E., Woodruff, G., Trembath, R.C., Hunt, D.M., Moore, A.T., 2003. An early-onset autosomal dominant macular dystrophy (MCDR3) resembling North Carolina macular dystrophy maps to chromosome 5. Investigative ophthalmology & visual science 44, 2178-2183.

Milam, A.H., Curcio, C.A., Cideciyan, A.V., Saxena, S., John, S.K., Kruth, H.S., Malek, G., Heckenlively, J.R., Weleber, R.G., Jacobson, S.G., 2000. Dominant late-onset retinal degeneration with regional variation of sub-retinal pigment epithelium deposits, retinal function, and photoreceptor degeneration. Ophthalmology 107, 2256-2266.

Mimoun, G., Soubrane, G., Coscas, G., 1990. [Macular drusen]. Journal francais d'ophtalmologie 13, 511-530.

Mirshahi, A., Piri, N., 2009. Fundus autofluorescence changes in two cases of Sjogren-Larsson syndrome. International ophthalmology 29, 541-545.

Misra, A., Peethambaram, A., Garg, A., 2004. Clinical features and metabolic and autoimmune derangements in acquired partial lipodystrophy: report of 35 cases and review of the literature. Medicine 83, 18-34.

Moore, D.J., Hussain, A.A., Marshall, J., 1995. Age-related variation in the hydraulic conductivity of Bruch's membrane. Invest Ophthalmol Vis Sci 36, 1290-1297.

Muller, H., 1856. Anatomische Beitrage zur Ophthalmologie - Untersuchungen uber die Glashaute des Auges, insbesondere die Glaslamelle der Choroidea und ihre senilen Veranderungen. Graefe's archive for clinical and experimental ophthalmology = Albrecht von Graefes Archiv fur klinische und experimentelle Ophthalmologie 2, 1-69.

Mullins, R.F., 2007. Genetic insights into the pathobiology of age-related macular degeneration. International ophthalmology clinics 47, 1-14.

Mullins, R.F., Aptsiauri, N., Hageman, G.S., 2001. Structure and composition of drusen associated with glomerulonephritis: implications for the role of complement activation in drusen biogenesis. Eye 15, 390-395.

Nan, R., Tetchner, S., Rodriguez, E., Pao, P.J., Gor, J., Lengyel, I., Perkins, S.J., 2013. Zinc-induced self-association of complement C3b and Factor H: implications for inflammation and age-related macular degeneration. J Biol Chem 288, 19197-19210.

Neely, K., Mets, M.B., Wong, P., Szego, K., 1988. Ocular findings in partial trisomy 10q syndrome. American journal of ophthalmology 106, 82-87.

Nguyen, A.D., Itoh, S., Jeney, V., Yanagisawa, H., Fujimoto, M., Ushio-Fukai, M., Fukai, T., 2004. Fibulin-5 is a novel binding protein for extracellular superoxide dismutase. Circulation research 95, 1067-1074.

Nolis, T., 2014. Exploring the pathophysiology behind the more common genetic and acquired lipodystrophies. Journal of human genetics 59, 16-23.

O'Brien, C., Duvall-Young, J., Brown, M., Short, C., Bone, M., 1993. Electrophysiology of type II mesangiocapillary glomerulonephritis with associated fundus abnormalities. The British journal of ophthalmology 77, 778-780.

Okajima, T.I., Wiggert, B., Chader, G.J., Pepperberg, D.R., 1994. Retinoid processing in retinal pigment epithelium of toad (Bufo marinus). The Journal of biological chemistry 269, 21983-21989.

Ono, K., Suzuki, Y., Fujii, I., Takeshita, K., Arima, M., 1974. [A case of ring chromosome E 17: 46, XX, r(17) (p13 yields q25) (author's transl)]. Jinrui idengaku zasshi. The Japanese journal of human genetics 19, 235-242.

Ooto, S., Vongkulsiri, S., Sato, T., Suzuki, M., Curcio, C.A., Spaide, R.F., 2014. Outer retinal corrugations in age-related macular degeneration. JAMA ophthalmology 132, 806-813.

Orlen, H., Melberg, A., Raininko, R., Kumlien, E., Entesarian, M., Soderberg, P., Pahlman, M., Darin, N., Kyllerman, M., Holmberg, E., Engler, H., Eriksson, U., Dahl, N., 2009. SPG11 mutations cause Kjellin syndrome, a hereditary spastic paraplegia with thin corpus callosum and central retinal degeneration. American journal of medical genetics. Part B, Neuropsychiatric genetics : the official publication of the International Society of Psychiatric Genetics 150B, 984-992.

Osusky, R., Dorio, R.J., Arora, Y.K., Ryan, S.J., Walker, S.M., 1997. MHC class II positive retinal pigment epithelial (RPE) cells can function as antigen-presenting cells for microbial superantigen. Ocular immunology and inflammation 5, 43-50.

Ozaki, S., Johnson, L.V., Mullins, R.F., Hageman, G.S., Anderson, D.H., 1999. The human retina and retinal pigment epithelium are abundant sources of vitronectin mRNA. Biochemical and biophysical research communications 258, 524-529.

Patel, D., Page, B., 2006. Ocular complications in acquired partial lipodystrophy. Postgraduate medical journal 82, 774.

Pichi, F., Morara, M., Veronese, C., Nucci, P., Ciardella, A.P., 2013. Multimodal imaging in hereditary retinal diseases. Journal of ophthalmology 2013, 634351.

Pikuleva, I.A., Curcio, C.A., 2014. Cholesterol in the retina: the best is yet to come. Prog Retin Eye Res 41, 64-89.

Pilli, S., Zawadzki, R.J., Werner, J.S., Park, S.S., 2011. High-resolution Fourier-domain optical coherence tomography findings in vitelliform detachment associated with basal laminar drusen. Retina 31, 812-814.

Platano, D., Magli, M.C., Ferraretti, A.P., Gianaroli, L., Aicardi, G., 2005. L- and T-type voltage-gated Ca2+ channels in human granulosa cells: functional characterization and cholinergic regulation. The Journal of clinical endocrinology and metabolism 90, 2192-2197.

Prenner, J.L., Rosenblatt, B.J., Tolentino, M.J., Ying, G.S., Javornik, N.B., Maguire, M.G., Ho, A.C., Group, C.R., 2003. Risk factors for choroidal neovascularization and vision loss in the fellow eye study of CNVPT. Retina 23, 307-314.

Procter, K.L., Rudolf, M.C., Feltbower, R.G., Levine, R., Connor, A., Robinson, M., Clarke, G.P., 2008. Measuring the school impact on child obesity. Social science & medicine 67, 341-349.

Prosperi, L., Bernasconi, S., Forabosco, A., 1977. Ocular phenotype in partial trisomy 10 q. Ophthalmologica. Journal international d'ophtalmologie. International journal of ophthalmology. Zeitschrift fur Augenheilkunde 175, 269-274.

Puech, B., Lacour, A., Stevanin, G., Sautiere, B.G., Devos, D., Depienne, C., Denis, E., Mundwiller, E., Ferriby, D., Vermersch, P., Defoort-Dhellemmes, S., 2011. Kjellin syndrome: long-term neuro-ophthalmologic follow-up and novel mutations in the SPG11 gene. Ophthalmology 118, 564-573.

Querques, G., Canoui-Poitrine, F., Coscas, F., Massamba, N., Querques, L., Mimoun, G., Bandello, F., Souied, E.H., 2012a. Analysis of progression of reticular pseudodrusen by spectral domain-optical coherence tomography. Investigative ophthalmology & visual science 53, 1264-1270.

Querques, G., Guigui, B., Leveziel, N., Querques, L., Bandello, F., Souied, E.H., 2013. Multimodal morphological and functional characterization of Malattia Leventinese. Graefe's archive for clinical and experimental ophthalmology = Albrecht von Graefes Archiv fur klinische und experimentelle Ophthalmologie 251, 705-714.

Querques, G., Massamba, N., Guigui, B., Lea, Q., Lamory, B., Soubrane, G., Souied, E.H., 2012b. In vivo evaluation of photoreceptor mosaic in early onset large colloid drusen using adaptive optics. Acta ophthalmologica 90, e327-328.

Rattner, A., Smallwood, P.M., Williams, J., Cooke, C., Savchenko, A., Lyubarsky, A., Pugh, E.N., Nathans, J., 2001. A photoreceptor-specific cadherin is essential for the structural integrity of the outer segment and for photoreceptor survival. Neuron 32, 775-786.

Raychaudhuri, S., Iartchouk, O., Chin, K., Tan, P.L., Tai, A.K., Ripke, S., Gowrisankar, S., Vemuri, S., Montgomery, K., Yu, Y., Reynolds, R., Zack, D.J., Campochiaro, B., Campochiaro, P., Katsanis, N., Daly, M.J., Seddon, J.M., 2011. A rare penetrant mutation in CFH confers high risk of age-related macular degeneration. Nature genetics 43, 1232-1236.

Redmond, T.M., Poliakov, E., Yu, S., Tsai, J.Y., Lu, Z., Gentleman, S., 2005. Mutation of key residues of RPE65 abolishes its enzymatic role as isomerohydrolase in the visual cycle. Proceedings of the National Academy of Sciences of the United States of America 102, 13658-13663.

Redmond, T.M., Yu, S., Lee, E., Bok, D., Hamasaki, D., Chen, N., Goletz, P., Ma, J.X., Crouch, R.K., Pfeifer, K., 1998. Rpe65 is necessary for production of 11-cis-vitamin A in the retinal visual cycle. Nature genetics 20, 344-351.

Ringpfeil, F., Lebwohl, M.G., Christiano, A.M., Uitto, J., 2000. Pseudoxanthoma elasticum: mutations in the MRP6 gene encoding a transmembrane ATP-binding cassette (ABC) transporter. Proceedings of the National Academy of Sciences of the United States of America 97, 6001-6006.

Rogers, G.R., Markova, N.G., De Laurenzi, V., Rizzo, W.B., Compton, J.G., 1997. Genomic organization and expression of the human fatty aldehyde dehydrogenase gene (FALDH). Genomics 39, 127-135.

Rudolf, M., Clark, M.E., Chimento, M.F., Li, C.M., Medeiros, N.E., Curcio, C.A., 2008a. Prevalence and morphology of druse types in the macula and periphery of eyes with age-related maculopathy. Investigative ophthalmology & visual science 49, 1200-1209.

Rudolf, M., Malek, G., Messinger, J.D., Clark, M.E., Wang, L., Curcio, C.A., 2008b. Sub-retinal drusenoid deposits in human retina: organization and composition. Experimental eye research 87, 402-408.

Russell, S.R., Mullins, R.F., Schneider, B.L., Hageman, G.S., 2000. Location, substructure, and composition of basal laminar drusen compared with drusen associated

with aging and age-related macular degeneration. American journal of ophthalmology 129, 205-214.

Saari, J.C., 1982. Isolation of cellular retinoid-binding proteins from bovine retina with bound endogenous ligands. Methods in enzymology 81, 819-826.

Saari, J.C., Bredberg, D.L., 1989. Lecithin:retinol acyltransferase in retinal pigment epithelial microsomes. The Journal of biological chemistry 264, 8636-8640.

Saari, J.C., Nawrot, M., Kennedy, B.N., Garwin, G.G., Hurley, J.B., Huang, J., Possin, D.E., Crabb, J.W., 2001. Visual cycle impairment in cellular retinaldehyde binding protein (CRALBP) knockout mice results in delayed dark adaptation. Neuron 29, 739-748.

Saari, J.C., Teller, D.C., Crabb, J.W., Bredberg, L., 1985. Properties of an interphotoreceptor retinoid-binding protein from bovine retina. The Journal of biological chemistry 260, 195-201.

Saksens, N.T., Fleckenstein, M., Schmitz-Valckenberg, S., Holz, F.G., den Hollander, A.I., Keunen, J.E., Boon, C.J., Hoyng, C.B., 2014. Macular dystrophies mimicking age-related macular degeneration. Prog Retin Eye Res 39, 23-57.

Sarks, J., Arnold, J., Ho, I.V., Sarks, S., Killingsworth, M., 2011. Evolution of reticular pseudodrusen. The British journal of ophthalmology 95, 979-985.

Sarks, J.P., Sarks, S.H., Killingsworth, M.C., 1988. Evolution of geographic atrophy of the retinal pigment epithelium. Eye 2 (Pt 5), 552-577.

Sarks, S., Cherepanoff, S., Killingsworth, M., Sarks, J., 2007. Relationship of Basal laminar deposit and membranous debris to the clinical presentation of early age-related macular degeneration. Investigative ophthalmology & visual science 48, 968-977.

Sarks, S.H., 1973. New vessel formation beneath the retinal pigment epithelium in senile eyes. The British journal of ophthalmology 57, 951-965.

Sarks, S.H., Van Driel, D., Maxwell, L., Killingsworth, M., 1980. Softening of drusen and subretinal neovascularization. Transactions of the ophthalmological societies of the United Kingdom 100, 414-422.

Savage, D.B., Semple, R.K., Clatworthy, M.R., Lyons, P.A., Morgan, B.P., Cochran, E.K., Gorden, P., Raymond-Barker, P., Murgatroyd, P.R., Adams, C., Scobie, I., Mufti, G.J., Alexander, G.J., Thiru, S., Murano, I., Cinti, S., Chaudhry, A.N., Smith, K.G., O'Rahilly, S., 2009. Complement abnormalities in acquired lipodystrophy revisited. The Journal of clinical endocrinology and metabolism 94, 10-16.

Savige, J., Colville, D., 2009. Opinion: Ocular features aid the diagnosis of Alport syndrome. Nature reviews. Nephrology 5, 356-360.

Savige, J., Liu, J., DeBuc, D.C., Handa, J.T., Hageman, G.S., Wang, Y.Y., Parkin, J.D., Vote, B., Fassett, R., Sarks, S., Colville, D., 2010. Retinal basement membrane abnormalities and the retinopathy of Alport syndrome. Investigative ophthalmology & visual science 51, 1621-1627.

Schmitz-Valckenberg, S., Steinberg, J.S., Fleckenstein, M., Visvalingam, S., Brinkmann, C.K., Holz, F.G., 2010. Combined confocal scanning laser ophthalmoscopy and spectral-domain optical coherence tomography imaging of reticular drusen associated with age-related macular degeneration. Ophthalmology 117, 1169-1176.

Seddon, J.M., Reynolds, R., Rosner, B., 2009. Peripheral retinal drusen and reticular pigment: association with CFHY402H and CFHrs1410996 genotypes in family and twin studies. Investigative ophthalmology & visual science 50, 586-591.

Seddon, J.M., Yu, Y., Miller, E.C., Reynolds, R., Tan, P.L., Gowrisankar, S., Goldstein, J.I., Triebwasser, M., Anderson, H.E., Zerbib, J., Kavanagh, D., Souied, E., Katsanis, N., Daly, M.J., Atkinson, J.P., Raychaudhuri, S., 2013. Rare variants in CFI, C3 and C9 are associated with high risk of advanced age-related macular degeneration. Nature genetics 45, 1366-1370.

Sergouniotis, P.I., Davidson, A.E., Mackay, D.S., Lenassi, E., Li, Z., Robson, A.G., Yang, X., Kam, J.H., Isaacs, T.W., Holder, G.E., Jeffery, G., Beck, J.A., Moore, A.T., Plagnol, V., Webster, A.R., 2011a. Biallelic mutations in PLA2G5, encoding group V phospholipase A2, cause benign fleck retina. American journal of human genetics 89, 782-791.

Sergouniotis, P.I., Sohn, E.H., Li, Z., McBain, V.A., Wright, G.A., Moore, A.T., Robson, A.G., Holder, G.E., Webster, A.R., 2011b. Phenotypic variability in RDH5 retinopathy (Fundus Albipunctatus). Ophthalmology 118, 1661-1670.

Servais, A., Fremeaux-Bacchi, V., Lequintrec, M., Salomon, R., Blouin, J., Knebelmann, B., Grunfeld, J.P., Lesavre, P., Noel, L.H., Fakhouri, F., 2007. Primary glomerulonephritis with isolated C3 deposits: a new entity which shares common genetic risk factors with haemolytic uraemic syndrome. Journal of medical genetics 44, 193-199.

Shashi, V., White, J.R., Pettenati, M.J., Root, S.K., Bell, W.L., 2003. Ring chromosome 17: phenotype variation by deletion size. Clinical genetics 64, 361-365.

Shimuzu, K., 1961. Mottled fundus in association with pseudoxanthoma elasticum. Jap J Ophthalmol 5, 1-13.

Shu, X., Tulloch, B., Lennon, A., Vlachantoni, D., Zhou, X., Hayward, C., Wright, A.F., 2006. Disease mechanisms in late-onset retinal macular degeneration associated with mutation in C1QTNF5. Human molecular genetics 15, 1680-1689.

Simon, A., Hellman, U., Wernstedt, C., Eriksson, U., 1995. The retinal pigment epithelial-specific 11-cis retinol dehydrogenase belongs to the family of short chain alcohol dehydrogenases. The Journal of biological chemistry 270, 1107-1112.

Skarlatos, S.I., Rao, R., Dickens, B.F., Kruth, H.S., 1993. Phospholipid loss in dying platelets. Virchows Archiv. B, Cell pathology including molecular pathology 64, 241-245.

Small, K.W., DeLuca, A.P., Whitmore, S.S., Rosenberg, T., Silva-Garcia, R., Udar, N., Puech, B., Garcia, C.A., Rice, T.A., Fishman, G.A., Heon, E., Folk, J.C., Streb, L.M., Haas, C.M., Wiley, L.A., Scheetz, T.E., Fingert, J.H., Mullins, R.F., Tucker, B.A., Stone, E.M., 2015. North Carolina Macular Dystrophy Is Caused by Dysregulation of the Retinal Transcription Factor PRDM13. Ophthalmology.

Smith, J.G., Jr., Davidson, E.A., Taylor, R.W., 1964. Cutaneous Acid Mucopolysaccharides in Pseudoxanthoma Elasticum. The Journal of investigative dermatology 43, 429-430.

Smith, R.T., Chan, J.K., Busuoic, M., Sivagnanavel, V., Bird, A.C., Chong, N.V., 2006. Autofluorescence characteristics of early, atrophic, and high-risk fellow eyes in age-related macular degeneration. Investigative ophthalmology & visual science 47, 5495-5504.

Smith, R.T., Sohrab, M.A., Busuioc, M., Barile, G., 2009. Reticular macular disease. American journal of ophthalmology 148, 733-743 e732.

Sohn, E.H., Wang, K., Thompson, S., Riker, M.J., Hoffmann, J.M., Stone, E.M., Mullins, R.F., 2015. Comparison of drusen and modifying genes in autosomal dominant radial drusen and age-related macular degeneration. Retina 35, 48-57.

Sohrab, M.A., Smith, R.T., Salehi-Had, H., Sadda, S.R., Fawzi, A.A., 2011. Image registration and multimodal imaging of reticular pseudodrusen. Invest Ophthalmol Vis Sci 52, 5743-5748.

Sorsby, A., 1949. Genetically determined ocular lesions simulating inflammatory reactions. Acta neurologica et psychiatrica Belgica 49, 611.

Spaide, R.F., Curcio, C.A., 2010. Drusen characterization with multimodal imaging. Retina 30, 1441-1454.

Spraul, C.W., Grossniklaus, H.E., 1997. Characteristics of Drusen and Bruch's membrane in postmortem eyes with age-related macular degeneration. Archives of ophthalmology 115, 267-273.

Starita, C., Hussain, A.A., Pagliarini, S., Marshall, J., 1996. Hydrodynamics of ageing Bruch's membrane: implications for macular disease. Exp Eye Res 62, 565-572.

Starita, C., Hussain, A.A., Patmore, A., Marshall, J., 1997. Localization of the site of major resistance to fluid transport in Bruch's membrane. Invest Ophthalmol Vis Sci 38, 762-767.

Steinmetz, R.L., Polkinghorne, P.C., Fitzke, F.W., Kemp, C.M., Bird, A.C., 1992. Abnormal dark adaptation and rhodopsin kinetics in Sorsby's fundus dystrophy. Investigative ophthalmology & visual science 33, 1633-1636.

Stone, E.M., Braun, T.A., Russell, S.R., Kuehn, M.H., Lotery, A.J., Moore, P.A., Eastman, C.G., Casavant, T.L., Sheffield, V.C., 2004. Missense variations in the fibulin 5 gene and age-related macular degeneration. The New England journal of medicine 351, 346-353.

Stone, E.M., Lotery, A.J., Munier, F.L., Heon, E., Piguet, B., Guymer, R.H., Vandenburgh, K., Cousin, P., Nishimura, D., Swiderski, R.E., Silvestri, G., Mackey, D.A., Hageman, G.S., Bird, A.C., Sheffield, V.C., Schorderet, D.F., 1999. A single EFEMP1 mutation associated with both Malattia Leventinese and Doyne honeycomb retinal dystrophy. Nature genetics 22, 199-202.

Suzuki, M., Curcio, C.A., Mullins, R.F., Spaide, R.F., 2015. REFRACTILE DRUSEN: Clinical Imaging and Candidate Histology. Retina 35, 859-865.

Suzuki, M., Sato, T., Spaide, R.F., 2014. Pseudodrusen subtypes as delineated by multimodal imaging of the fundus. American journal of ophthalmology 157, 1005-1012.

Tabandeh, H., Carothers, T., Levine, L., Monshizadeh, R., 2000. Drusen-like macular deposits in partial trisomy 10q. Retina 20, 678-679.

Thompson, R.B., Reffatto, V., Bundy, J.G., Kortvely, E., Flinn, J.M., Lanzirotti, A., Jones, E.A., McPhail, D.S., Fearn, S., Boldt, K., Ueffing, M., Ratu, S.G., Pauleikhoff, L., Bird, A.C., Lengyel, I., 2015. Identification of hydroxyapatite spherules provides new insight into subretinal pigment epithelial deposit formation in the aging eye. Proceedings of the National Academy of Sciences of the United States of America 112, 1565-1570.

Trabucchi, G., Sannace, C., Introini, U., Brancato, R., 1998. Partial lipodystrophy with associated fundus abnormalities: an optical coherence tomography study. The British journal of ophthalmology 82, 326.

Tuten, W.S., Tiruveedhula, P., Roorda, A., 2012. Adaptive optics scanning laser ophthalmoscope-based microperimetry. Optom Vis Sci 89, 563-574.

Ueda-Arakawa, N., Ooto, S., Ellabban, A.A., Takahashi, A., Oishi, A., Tamura, H., Yamashiro, K., Tsujikawa, A., Yoshimura, N., 2014. Macular choroidal thickness and volume of eyes with reticular pseudodrusen using swept-source optical coherence tomography. American journal of ophthalmology 157, 994-1004.

Ueda-Arakawa, N., Ooto, S., Tsujikawa, A., Yamashiro, K., Oishi, A., Yoshimura, N., 2013. Sensitivity and specificity of detecting reticular pseudodrusen in multimodal imaging in Japanese patients. Retina 33, 490-497.

Uyemura, M., 1928. Uber eine merkwurdige augenhintergrundveranerung bei zwei fallen vo idiopathischer hemerlopie. Klin Monatsbl Augenheilkd 471-473.

van de Ven, J.P., Boon, C.J., Fauser, S., Hoefsloot, L.H., Smailhodzic, D., Schoenmaker-Koller, F., Klevering, J., Klaver, C.C., den Hollander, A.I., Hoyng, C.B., 2012. Clinical evaluation of 3 families with basal laminar drusen caused by novel mutations in the complement factor H gene. Arch Ophthalmol 130, 1038-1047.

van der Schaft, T.L., de Bruijn, W.C., Mooy, C.M., Ketelaars, D.A., de Jong, P.T., 1991. Is basal laminar deposit unique for age-related macular degeneration? Archives of ophthalmology 109, 420-425.

van der Schaft, T.L., Mooy, C.M., de Bruijn, W.C., de Jong, P.T., 1993. Early stages of age-related macular degeneration: an immunofluorescence and electron microscopy study. The British journal of ophthalmology 77, 657-661.

Vogt, A., 1925. Die Ophthalmoskopie im rotfreien Licht. . Graefe A, 1-118.

Voigt, M., Querques, G., Atmani, K., Leveziel, N., Massamba, N., Puche, N., Bouzitou-Mfoumou, R., Souied, E.H., 2010. Analysis of retinal flecks in fundus flavimaculatus using high-definition spectral-domain optical coherence tomography. American journal of ophthalmology 150, 330-337.

Weber, B.H., Vogt, G., Pruett, R.C., Stohr, H., Felbor, U., 1994. Mutations in the tissue inhibitor of metalloproteinases-3 (TIMP3) in patients with Sorsby's fundus dystrophy. Nature genetics 8, 352-356.

Weleber, R.G., Michaelides, M., Trzupek, K.M., Stover, N.B., Stone, E.M., 2011. The phenotype of Severe Early Childhood Onset Retinal Dystrophy (SECORD) from mutation of RPE65 and differentiation from Leber congenital amaurosis. Investigative ophthalmology & visual science 52, 292-302.

Wu, Q., Blakeley, L.R., Cornwall, M.C., Crouch, R.K., Wiggert, B.N., Koutalos, Y., 2007. Interphotoreceptor retinoid-binding protein is the physiologically relevant carrier that removes retinol from rod photoreceptor outer segments. Biochemistry 46, 8669-8679.

Xu, H., Chen, M., Forrester, J.V., 2009. Para-inflammation in the aging retina. Progress in retinal and eye research 28, 348-368.

Yang, Z., Tong, Z., Chorich, L.J., Pearson, E., Yang, X., Moore, A., Hunt, D.M., Zhang, K., 2008. Clinical characterization and genetic mapping of North Carolina macular dystrophy. Vision research 48, 470-477.

Yehoshua, Z., Wang, F., Rosenfeld, P.J., Penha, F.M., Feuer, W.J., Gregori, G., 2011. Natural history of drusen morphology in age-related macular degeneration using spectral domain optical coherence tomography. Ophthalmology 118, 2434-2441.

Yu, Y., Triebwasser, M.P., Wong, E.K., Schramm, E.C., Thomas, B., Reynolds, R., Mardis, E.R., Atkinson, J.P., Daly, M., Raychaudhuri, S., Kavanagh, D., Seddon, J.M., 2014. Whole-exome sequencing identifies rare, functional CFH variants in families with macular degeneration. Human molecular genetics 23, 5283-5293.

Yunis, J.J., Sanchez, O., 1974. A new syndrome resulting from partial trisomy for the distal third of the long arm of chromosome 10. The Journal of pediatrics 84, 567-570.

Zanzottera, E.C., Messinger, J.D., Ach, T., Smith, R.T., Freund, K.B., Curcio, C.A., 2015. The Project MACULA Retinal Pigment Epithelium Grading System for Histology and Optical Coherence Tomography in Age-Related Macular Degeneration. Investigative ophthalmology & visual science 56, 3253-3268.

Zhan, X., Larson, D.E., Wang, C., Koboldt, D.C., Sergeev, Y.V., Fulton, R.S., Fulton, L.L., Fronick, C.C., Branham, K.E., Bragg-Gresham, J., Jun, G., Hu, Y., Kang, H.M., Liu, D., Othman, M., Brooks, M., Ratnapriya, R., Boleda, A., Grassmann, F., von Strachwitz, C., Olson, L.M., Buitendijk, G.H., Hofman, A., van Duijn, C.M., Cipriani, V., Moore, A.T., Shahid, H., Jiang, Y., Conley, Y.P., Morgan, D.J., Kim, I.K., Johnson, M.P., Cantsilieris, S., Richardson, A.J., Guymer, R.H., Luo, H., Ouyang, H., Licht, C., Pluthero, F.G., Zhang, M.M., Zhang, K., Baird, P.N., Blangero, J., Klein, M.L., Farrer, L.A., DeAngelis, M.M., Weeks, D.E., Gorin, M.B., Yates, J.R., Klaver, C.C., Pericak-Vance, M.A., Haines, J.L., Weber, B.H., Wilson, R.K., Heckenlively, J.R., Chew, E.Y., Stambolian, D., Mardis, E.R., Swaroop, A., Abecasis, G.R., 2013. Identification of a rare coding variant in complement 3 associated with age-related macular degeneration. Nature genetics 45, 1375-1379.

Zhou, Q., Daniel, E., Maguire, M.G., Grunwald, J.E., Martin, E.R., Martin, D.F., Ying, G.S., Comparison of Age-Related Macular Degeneration Treatments Trials Research, G., 2016. Pseudodrusen and Incidence of Late Age-Related Macular Degeneration in Fellow Eyes in the Comparison of Age-Related Macular Degeneration Treatments Trials. Ophthalmology.

Zweifel, S.A., Maygar, I., Berger, W., Tschuor, P., Becker, M., Michels, S., 2012. Multimodal imaging of autosomal dominant drusen. Klinische Monatsblatter fur Augenheilkunde 229, 399-402.

Zweifel, S.A., Spaide, R.F., Curcio, C.A., Malek, G., Imamura, Y., 2010. Reticular pseudodrusen are subretinal drusenoid deposits. Ophthalmology 117, 303-312 e301.

Figure Legends

Figure 1. Development of subclinical deposits and soft drusen. In this cartoon the healthy configuration is shown on the left. With ageing (middle diagram), basal laminar deposits accumulate (internal to the RPE basement membrane) and vacuoles appear within RPE cells; early basal linear deposits (external to the RPE basement membrane) may also develop. The right-hand side shows more extensive BlinD coalescing to form soft drusen. (PR OS, photoreceptor outer segment; RPE, retinal pigment epithelium; BL, basal lamina; CL, collagenous layer; EL, elastic layer; CC, choriocapillaris; BlamD, basal laminar deposit; BlinD, basal linear deposit).

Figure 2. Retinal imaging from the left eye of an 84-year old man with AMD. *A*, colour photograph shows multiple drusen of varying size (small, medium and large) as well as pigmentary change. *B*, Short-wavelength AF image shows variable hyper- and hypo-autofluorescence. *C*, Horizontal OCT scan with corresponding infrared reflectance image showing OCT appearance of large and small drusen.

Figure 3. Images from the right eye of a 47 year-old man with cuticular drusen. *A,* Colour fundus photograph showing drusen and pigmentary change. *B,* Fundus fluorescein angiogram (at 27 seconds after dye injection) showing the characteristic "starry sky" appearance. *C,* Short-wavelength AF showing a mixture of hypo and hyper-autofluorescence. *D,* Horizontal enhanced depth OCT scan with corresponding infrared reflectance image.

Figure 4. Appearance of reticular pseudodrusen (RPD) on OCT and infrared reflectance. *A*, Infrared reflectance and horizontal OCT scan through the fovea of an 81 year-old subject with a healthy macula. *B*, Corresponding images from an 87 year-old patient with both conventional sub-RPE drusen and RPD (clearly visible on the infrared reflectance image). *C* and *D*, images from the superior macula in both subjects. "Light stripes" in the choroid are also evident in the patient with RPD.

Figure 5. Hyperreflective pyramidal structures ("ghost drusen"). *A*, Short wavelength AF image from the right eye of a 68 year-old male patient with genetically confirmed late-onset retinal degeneration (L-ORD), showing marked RPE loss at the posterior pole. *B*, Infrared reflectance (left) and corresponding horizontal OCT line scan (right) through an area of geographic atrophy. C and D, Corresponding images from a patient with Sorsby Fundus Dystrophy (SFD). Hyperreflective pyramidal structures are visible on the OCT images.

Figure 6. Schematic representation of the retinoid cycle. Asterisks indicate particular proteins in which mutations in the coding genes can give rise to white dots. ABCA4 is shown here facilitating removal of all-trans-retinal from the outer segment disc lumen.

Figure 7. Fundus appearance of a patient with genetically proven biallelic mutations in *ABCA4* (Stargardt macular dystrophy), aged 16 (left images), 21 (middle images) and 25 years (right images). *A-C*, colour fundus photographs, with the macular region magnified in

the middle panels (Amel et al.), and corresponding short wavelength autofluorescence images in the lower panels (*G-I*). The characteristic hyperautofluorescent flecks are evident in the later images, but white dots are also apparent, particularly in the earliest image.

Figure 8. Retinal imaging in a 6 year old patient (*A-F*) and a 75 year old patient (*G,H*) with Bothnia Dystrophy. *A-D*, colour fundus images from the younger patient (*A* and *B* show widefield images; *C* and *D* show the posterior pole). *E*, Infrared reflectance image of right macula with OCT scan through the fovea. *F*, OCT and infrared reflectance image for the left eye. The OCT shows what appear to be subretinal drusenoid deposits. *G,H,* Wide-field fundus images from the older patient showing widespread chorioretinal atrophy.

Figure 9. Images from a patient with fundus albipunctatus (*RDH5*-associated retinopathy). *A* and *B*, colour fundus images from right eye aged 7 (*A*) and 10 (*B*) years. The later image shows a few additional deposits. *C* and *D*, Infrared reflectance and OCT images from the right eye (aged 10): the deposits appear to be subretinal, but with some discontinuity in the ellipsoid layer seen also. *E*, Short wavelength autofluorescence image from the right eye (aged 11): a low overall autofluorescence is seen, but the deposits have higher levels of autofluorescence than the background and are visible when the gain is increased.

Figure 10. Retinal images of a 39 year-old female with bi-allelic mutation in *PLA2G5*. *A,B,C* Images from the right eye. *D,E,F,* Images from left eye. *A* and *D* are colour fundus photographs showing numerous white dots. *B* and *E* are short wavelength AF images showing that the lesions are hyperautofluorescent. *C* and *F* show infrared reflectance and OCT images.

Figure 11. Examples of phenotypes seen in *EFEMP1* disease ("dominant drusen"). The panels show (from left to right) colour fundus photographs, short wavelength autofluorescence, infrared reflectance and horizontal OCT scans, all from the right eye. Upper panels (*A-C*) are from a 21 year old patient with early disease. The middle and lower panels are from a sister and brother showing how expression can be variable in the same family. The middle panels (Amel et al.) are from a 62 year old female with severe disease. The lower panels (*G-I*) are from her brother (aged 59) who has mild disease. The commonly described appearance of radially distributed drusen is not evident in these cases, but drusen abutting the optic nerve head are visible (middle and lower panels).

Figure 12. Retinal imaging from two patients with early or mild SFD. *A*, Colour fundus photograph from the right eye of a 41 year-old female patient. *B*, Colour fundus photograph from the right eye of a 49 year-old female patient. *C* and *D*, "Multicolor" and short-wavelength AF imaging with CSLO of the patient in *A*. *E* and *F*, corresponding images from patient in *B*. *G* and *H*, Infrared reflectance and OCT imaging from both patients. The lesions are more possibly more easily defined on the CSLO images (Gauter-Fleckenstein et al.) than on the colour fundus photographs (*A,B*), and OCT imaging shows the majority to be SDD. An SFD patient with more advanced disease is shown in Figure 5.

Figure 13. Images from a 60 year-old female with late-onset retinal degeneration. *A,*

colour fundus photograph from the right eye. *B,* Infrared reflectance and horizontal foveal OCT scan. *C,* Short wavelength autofluorescence imaging. *D,* Slit lamp photograph of anterior segment showing anteriorly placed zonular insertions, which are seen in this condition. Images from a patient with more advanced disease are shown in Fig. 5.

Figure 14. Fundus images from patients with *IMPG2* mutations. *A*, Wide-field colour fundus photograph of the right eye of a 19 year-old male with retinitis pigmentosa found to have bi-allelic mutations in IMPG2. *B-D*, images from the right eye of the patient's mother (aged 39). *B*, Colour fundus photograph showing subtle drusen-like lesions around the fovea and superotemporally. *C*, Short-wavelength autofluorescence image showing hyper-autofluorescence of the lesions. *D*, Infrared reflectance image with horizontal foveal OCT scan.

Figure 15. Images from the right eye of a patient with bi-allelic mutations in *CDHR1*. *A*, Colour fundus photograph shows a bulls-eye maculopathy appearance, with fine yellow dots at the periphery of the lesion. *B,* Short wavelength autofluorescence shows speckled hyperautofluorescent foci throughout the lesion. *C*, Infrared reflectance with a horizontal OCT scan showing, in addition to outer retinal/RPE atrophy, fine hyperreflective foci at the level of the photoreceptor outer segments.

Figure 16. Images from a mother and son affected by North Carolina Macular Dystrophy. Upper panels show colour fundus photographs; lower panels show short wavelength AF images. *A,C,* Images from 16 year-old male with grade 1 NCMD. *B,D,* Images from 42 year-old female with grade 3 disease.

Figure 17. Images from patients with albinotic spots. *A-C*, 9 year-old girl; *D-F*, 25 year-old female; *G,H*, 11 year-old male). Images are colour fundus photographs (*A,D,E*), short wavelength autofluorescence (*B,D,G*) and infrared reflectance with horizontal OCT scans (*C,F*).

Figure 18. Retinal imaging of a 19 year-old female with large colloid drusen. *A* and *B*, Colour fundus photographs from right and left eye respectively. *C* and *D*, Short wavelength AF images. *E* and *F*, Infrared reflectance and horizontal OCT scans from right and left eye respectively.

Fig 19. Retinal images from a 41 year-old female with bilateral drusen. This patient underwent testing for mutations in the known genes underlying retinal or macular dystrophies with a negative result. The symmetry suggests a genetic aetiology. *A*, Colour fundus photographs (from a wide-field imaging system). *B*, Horizontal enhanced depth OCT image through the fovea of the right eye with corresponding infrared reflectance image. *C*, Short wavelength AF images. *D*, OCT and infrared images from the left eye.

Figure 20. Retinal images from a 21 year-old female with histologically confirmed MPGN type 2. *A*, Colour fundus photographs. *B*, Horizontal OCT image through the fovea of the right eye with corresponding infrared reflectance image. *C*, Short wavelength AF images. *D*, OCT and infrared images from the left eye. The drusen-like lesions are visible on colour,

AF and infrared imaging, but not easily discernible on OCT.

Figure 21. Retinal imaging from patients with X-linked Alport syndrome (*A*-*C*) and autosomal recessive Alport syndrome (Amel et al.). *A*, Horizontal OCT line scan through the fovea of a male patient with X-linked Alport syndrome, showing inner retinal thinning largely temporal to the foveola and hyper-reflectivity of the ILM. *B*, Colour fundus photograph from the left eye showing the dot/fleck maculopathy and the macular "lozenge" appearance. *C*, OCT from the left eye (corresponding to the green arrow in *B*) showing that the white yellow lesions appear to correspond to the hyper-reflective ILM rather than any drusenoid deposits. *D*, Montage of colour fundus photographs from a male patient with autosomal recessive Alport syndrome showing minimal macular dots, but mid-peripheral changes that could be drusenoid. *E*, *F*, infrared reflectance and OCT images from the right and left eye of the patient depicted in *D*. Temporal macular thinning is again seen together with a hyper-reflective ILM.

Figure 22. Retinal imaging from a patient with vitamin A deficiency due to liver disease. *A*, Colour fundus photograph showing white dots. *B*, "Multicolour" CSLO imaging showing small discrete deposits. *C*, Short-wavelength AF imaging showing hypo-autofluorescent spots. *D*, Infrared reflectance imaging and OCT scan showing that the lesions are consistent with subretinal drusenoid deposits. *E*-*F*, Corresponding images from the left eye of the same patient.

Figure 23. Retinal images from a girl with PXE. *A*, Colour fundus photograph of the right eye aged 11 showing optic disc drusen as well as multiple white-yellow lesions. *B*, Short wavelength AF imaging taken aged 12, showing autofluorescence of disc drusen, but no obvious change in AF over the lesions. *C*, Infrared reflectance image and OCT: there is some mottling seen on the infrared reflectance image, but the OCT does not show discrete lesions, although BM may be thickened or hyper-reflective. *D*-*F*, corresponding images from the left eye.

Figure 24. Findings from a patient with ring choromosome 17. A, Karyotyping showing the abnormal chromosome. B, Colour fundus photograph from the left eye showing small yellow lesions at the macula.

Figure 25. Adaptive optics scanning laser ophthalmoscope imaging of the human RPE mosaic *in vivo*.

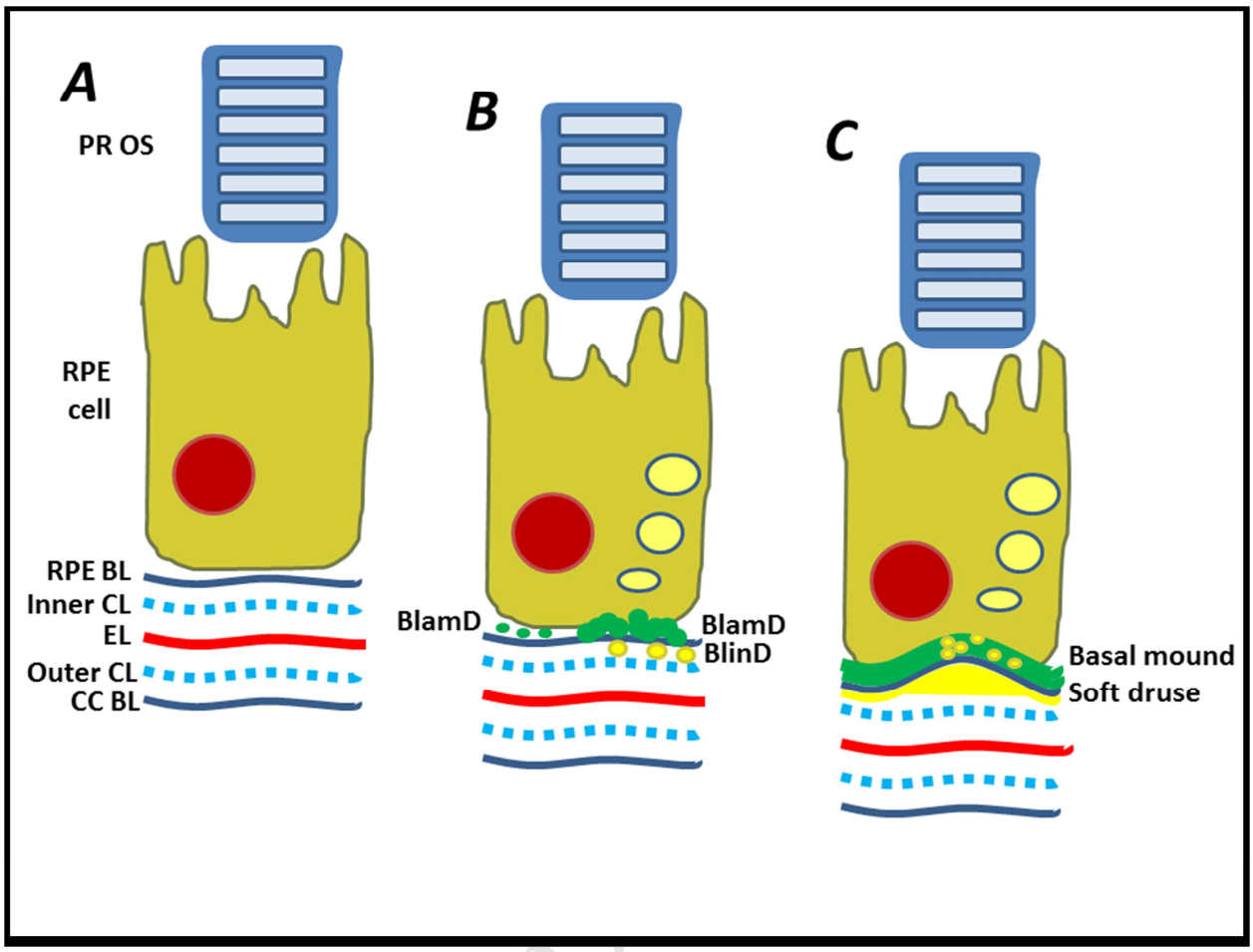
A
PR OS
RPE
cell
RPE BL
Inner CL
EL
Outer CL
CC BL
B
BlamD
BlamD
BlinD
C
Basal mound
Soft druse

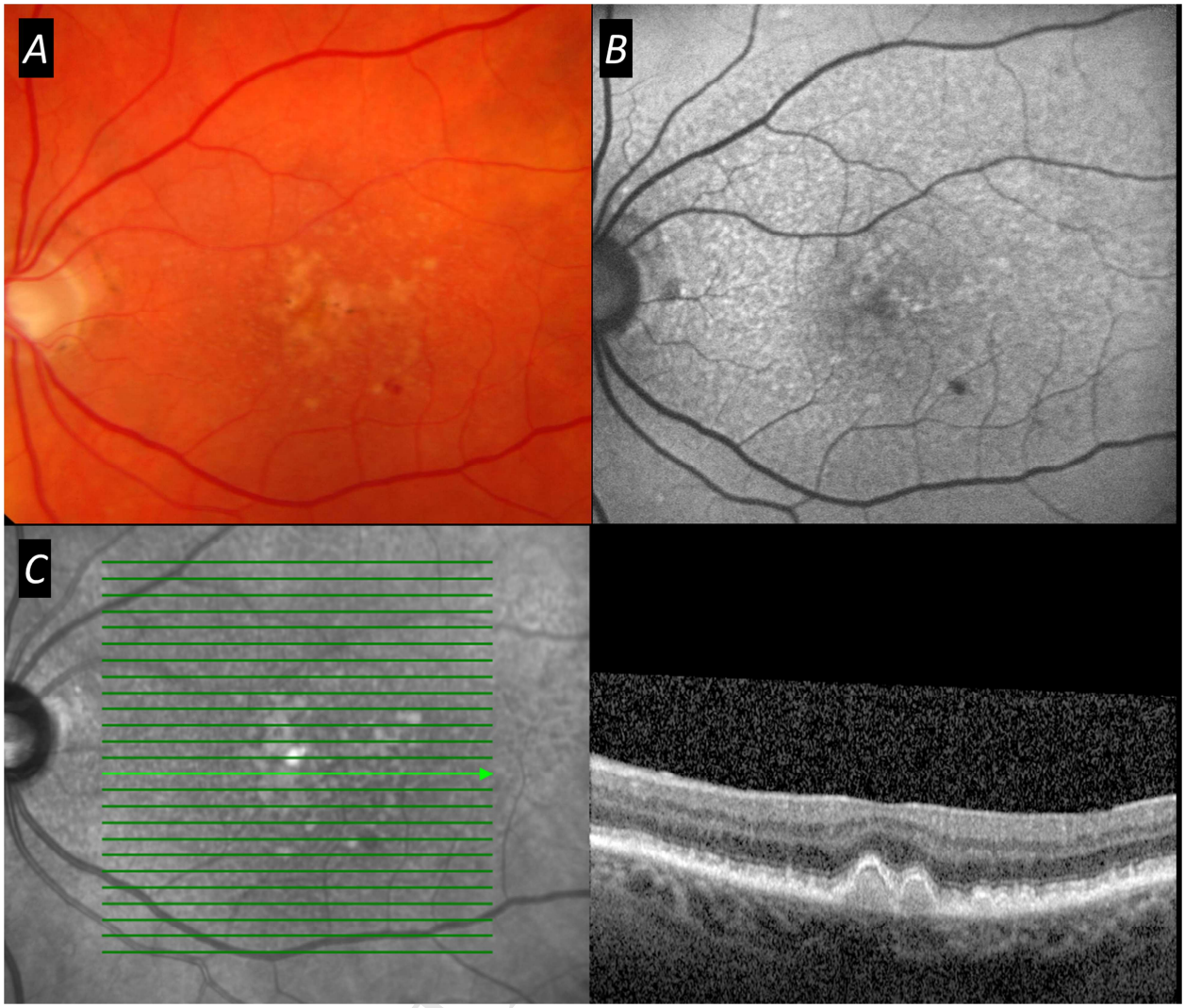

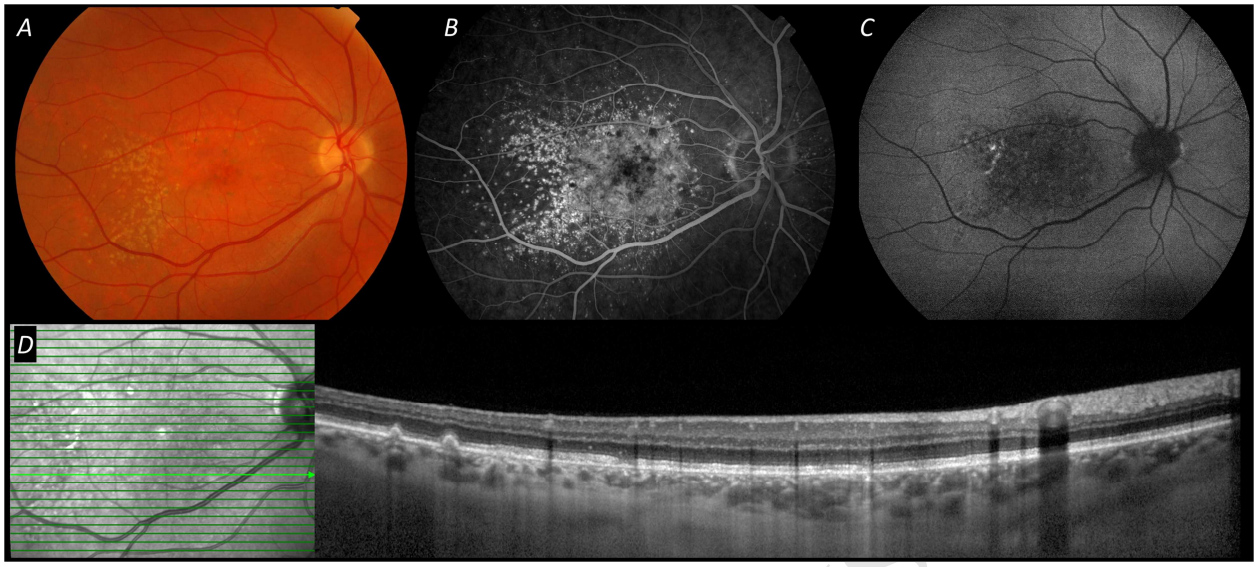

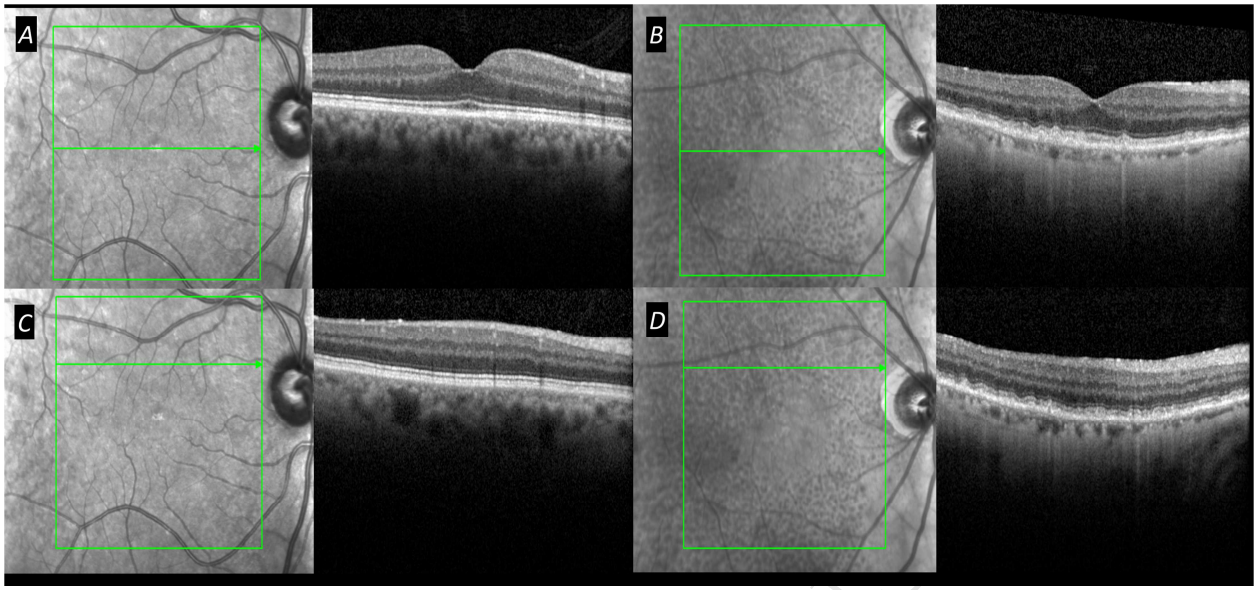

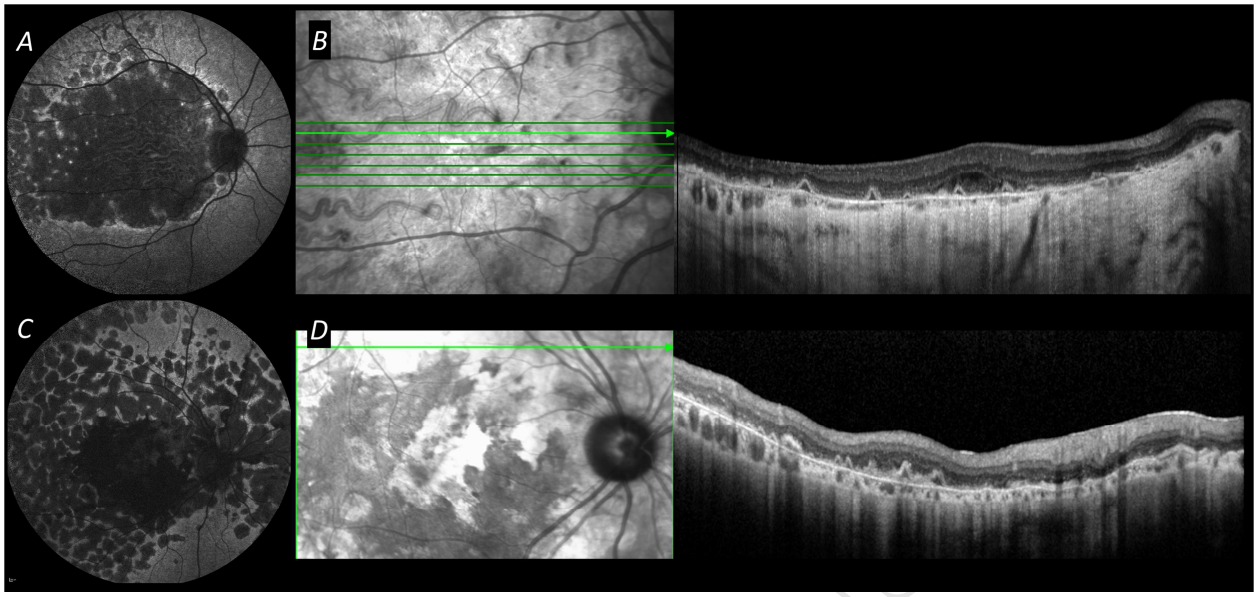

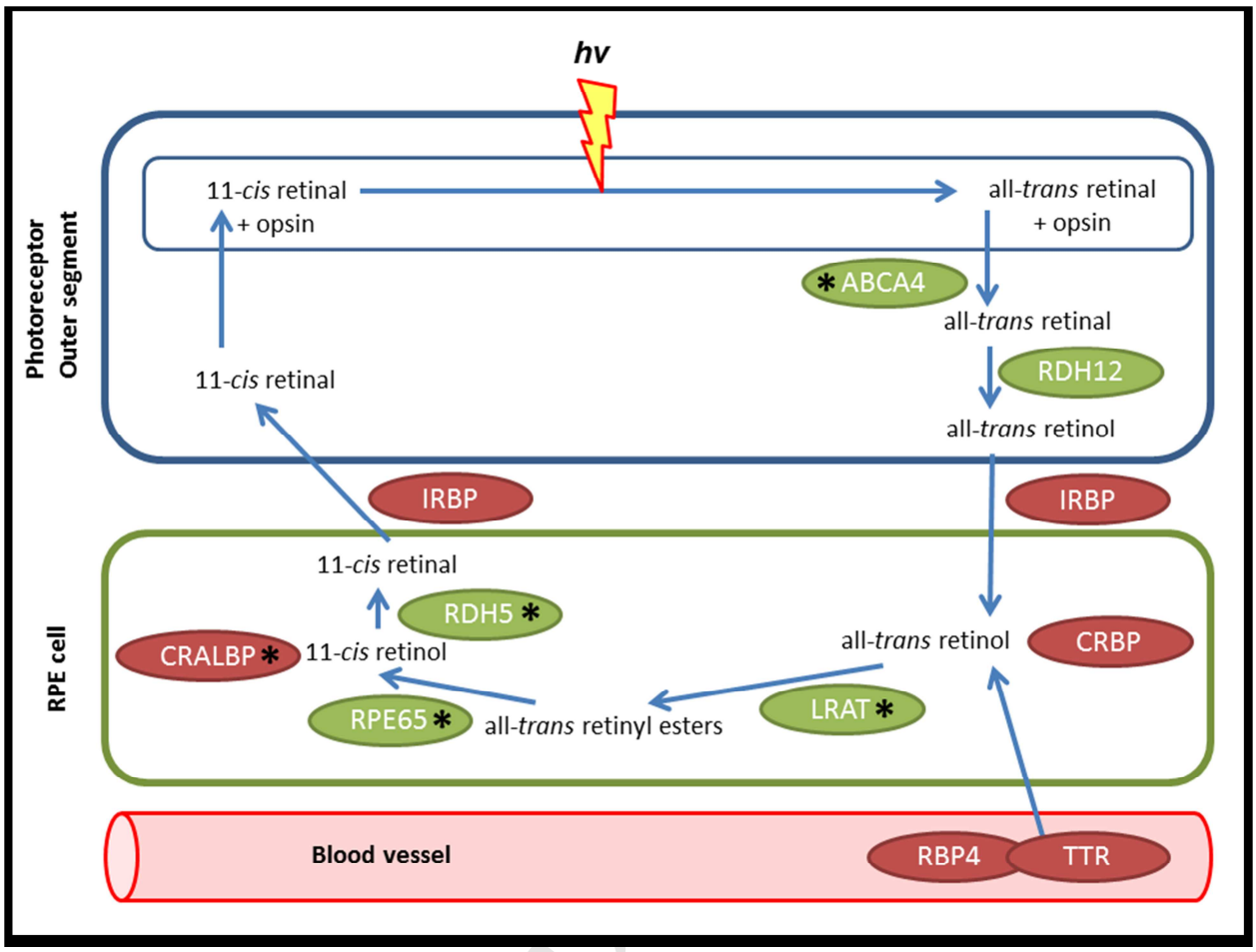
hv
Photoreceptor Outer segment
11-cis retinal + opsin
all-trans retinal + opsin
*ABCA4
all-trans retinal
RDH12
all-trans retinol
11-cis retinal
IRBP
IRBP
11-cis retinal
RDH5 *
RPE cell
CRALBP *
11-cis retinol
all-trans retinol
CRBP
RPE65 *
all-trans retinyl esters
LRAT *
Blood vessel
RBP4
TTR

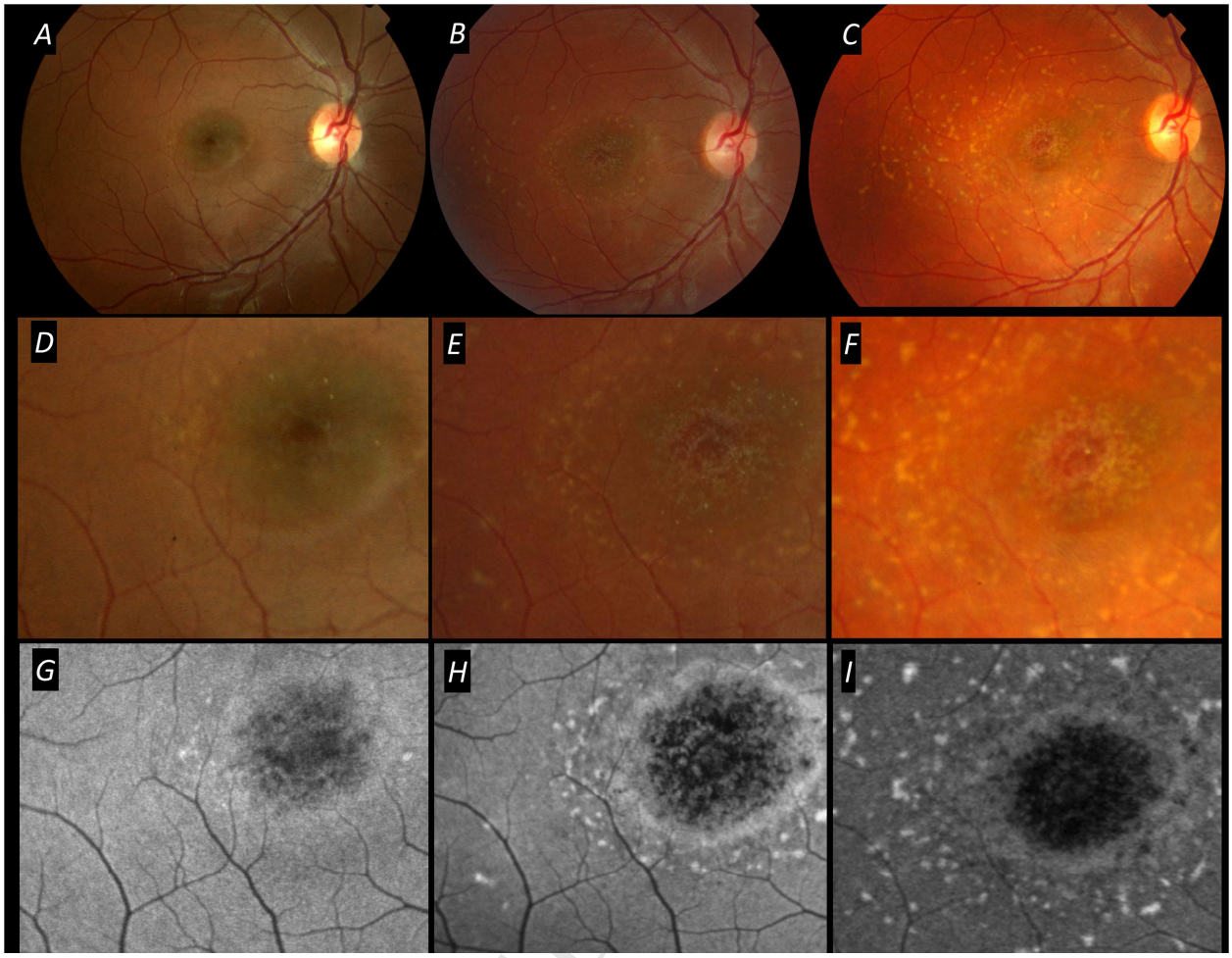

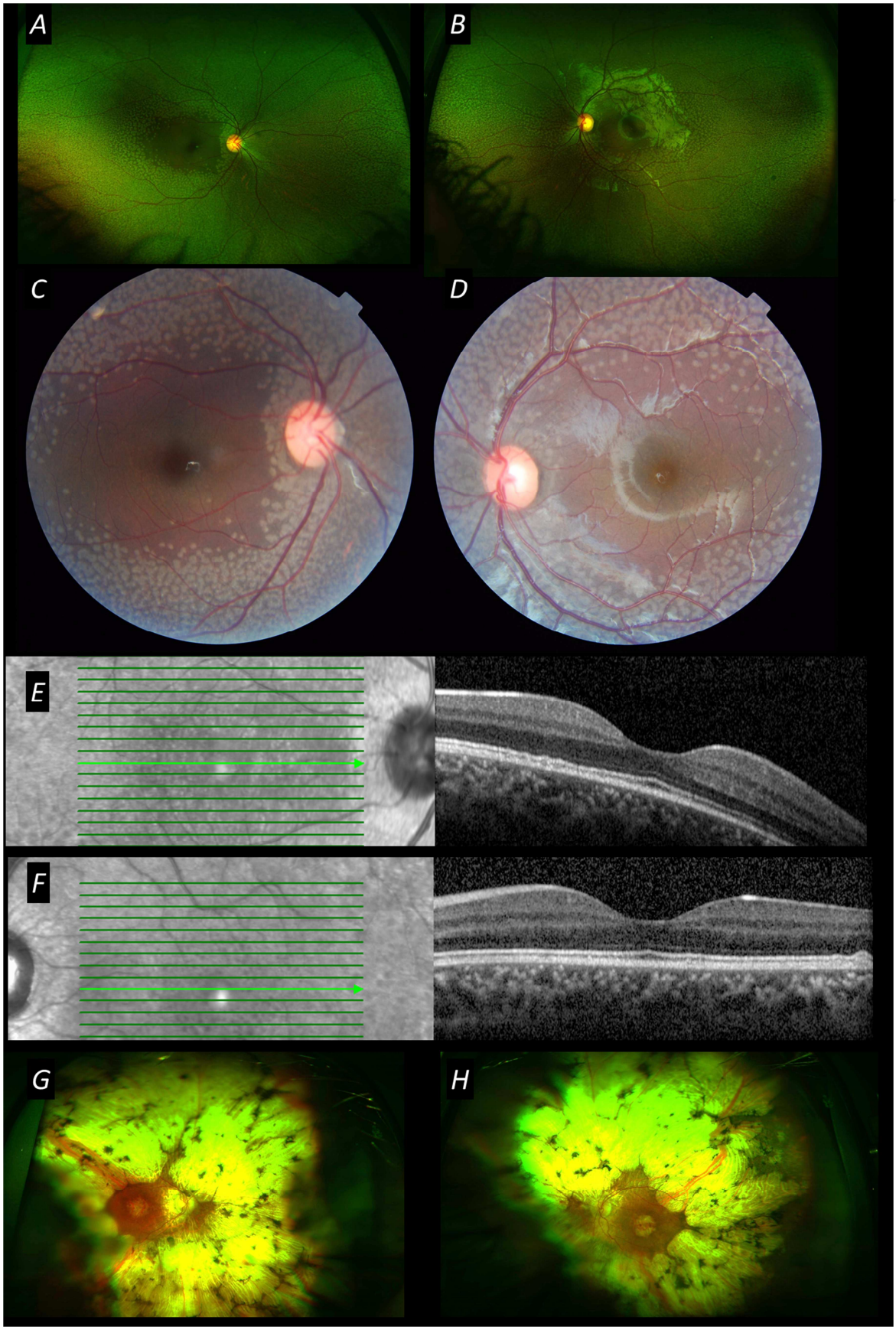
A
B
C
D
E
F
G
H

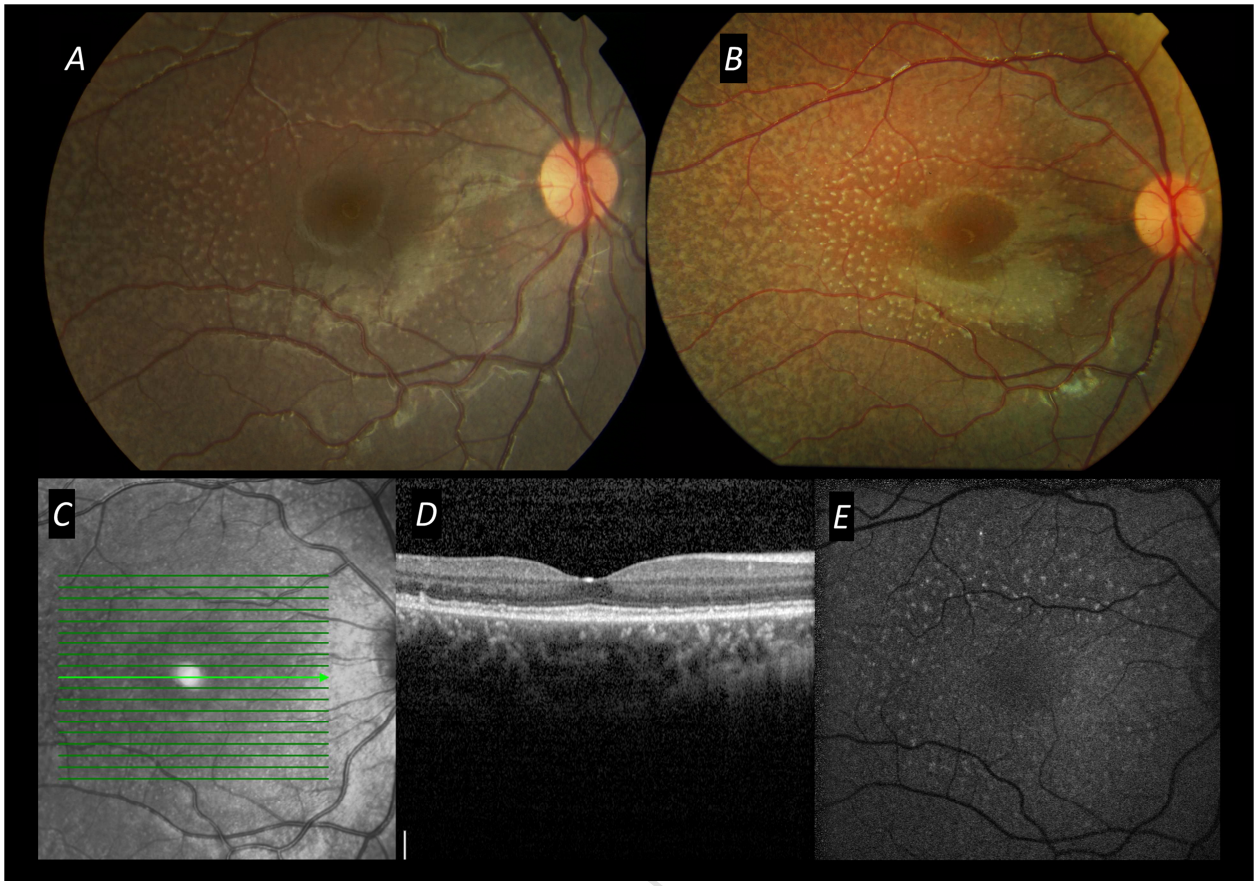

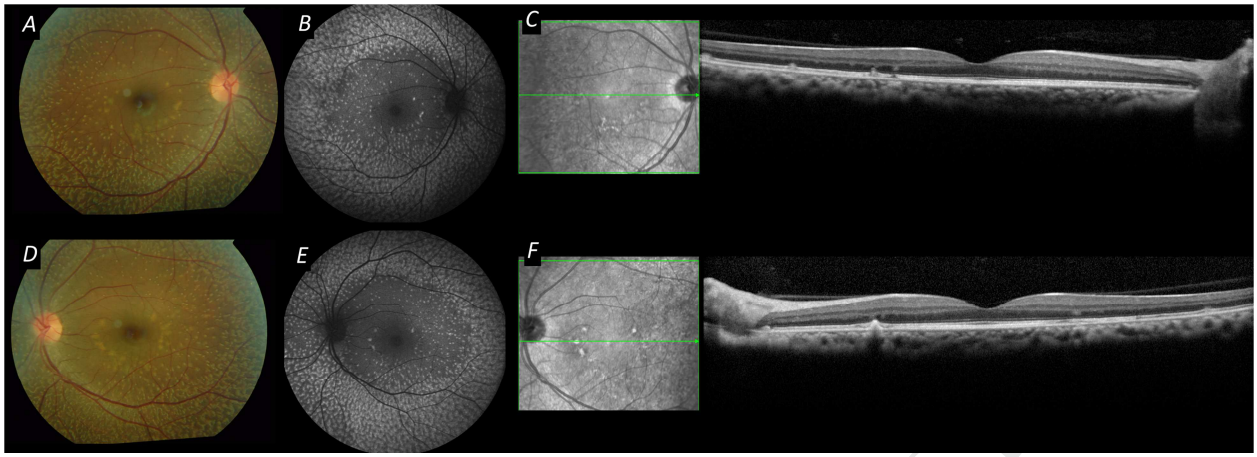

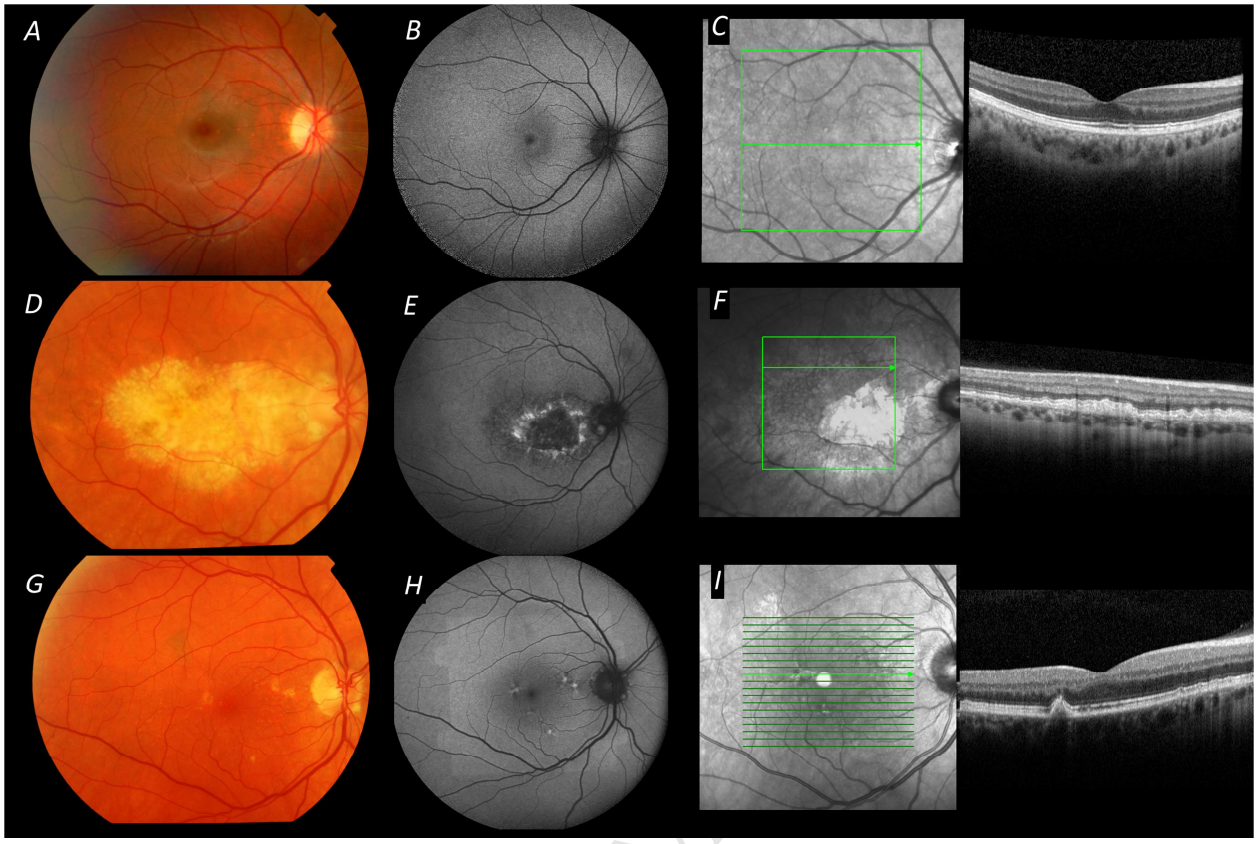

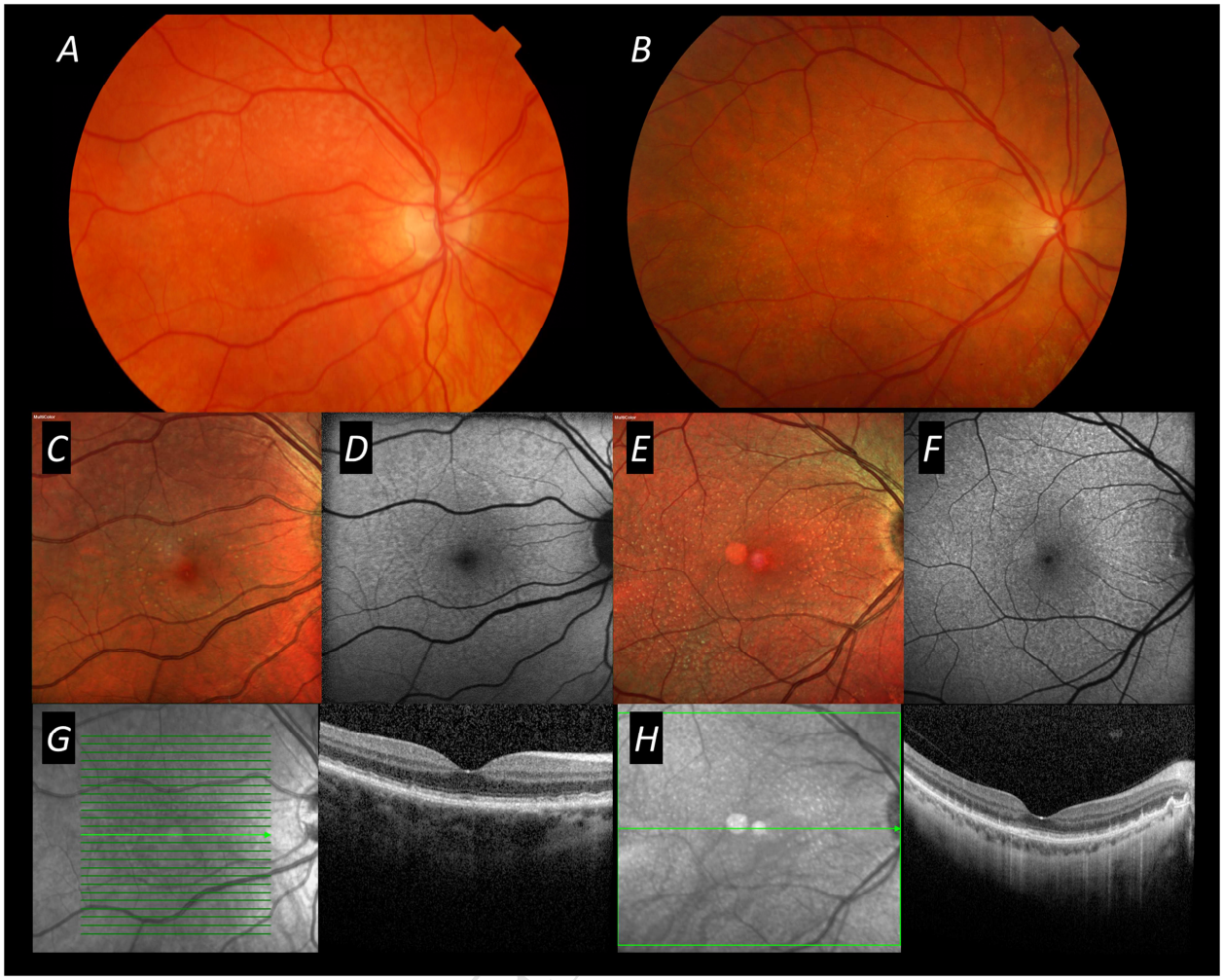

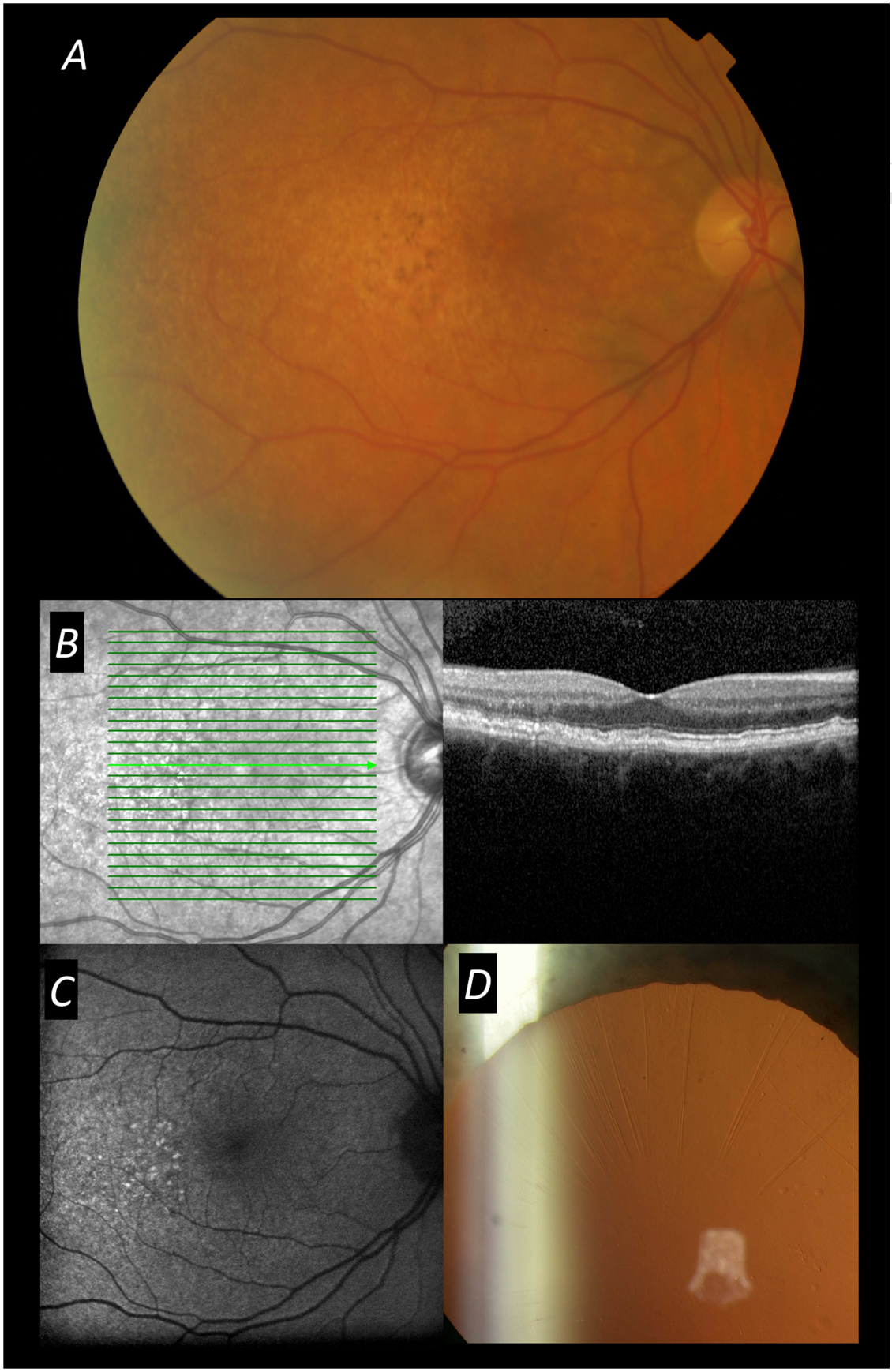
A
B
C
D

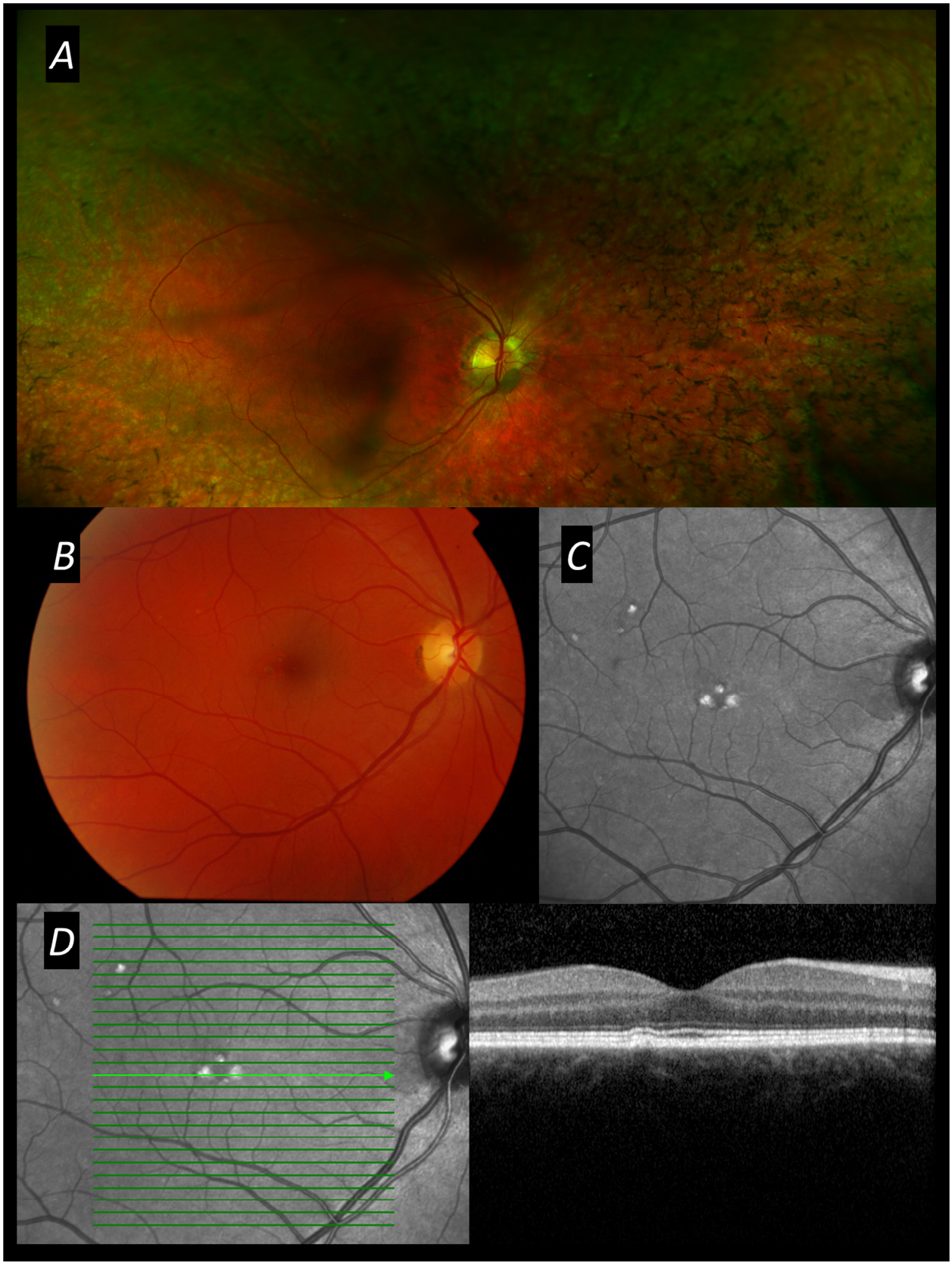
A
B
C
D

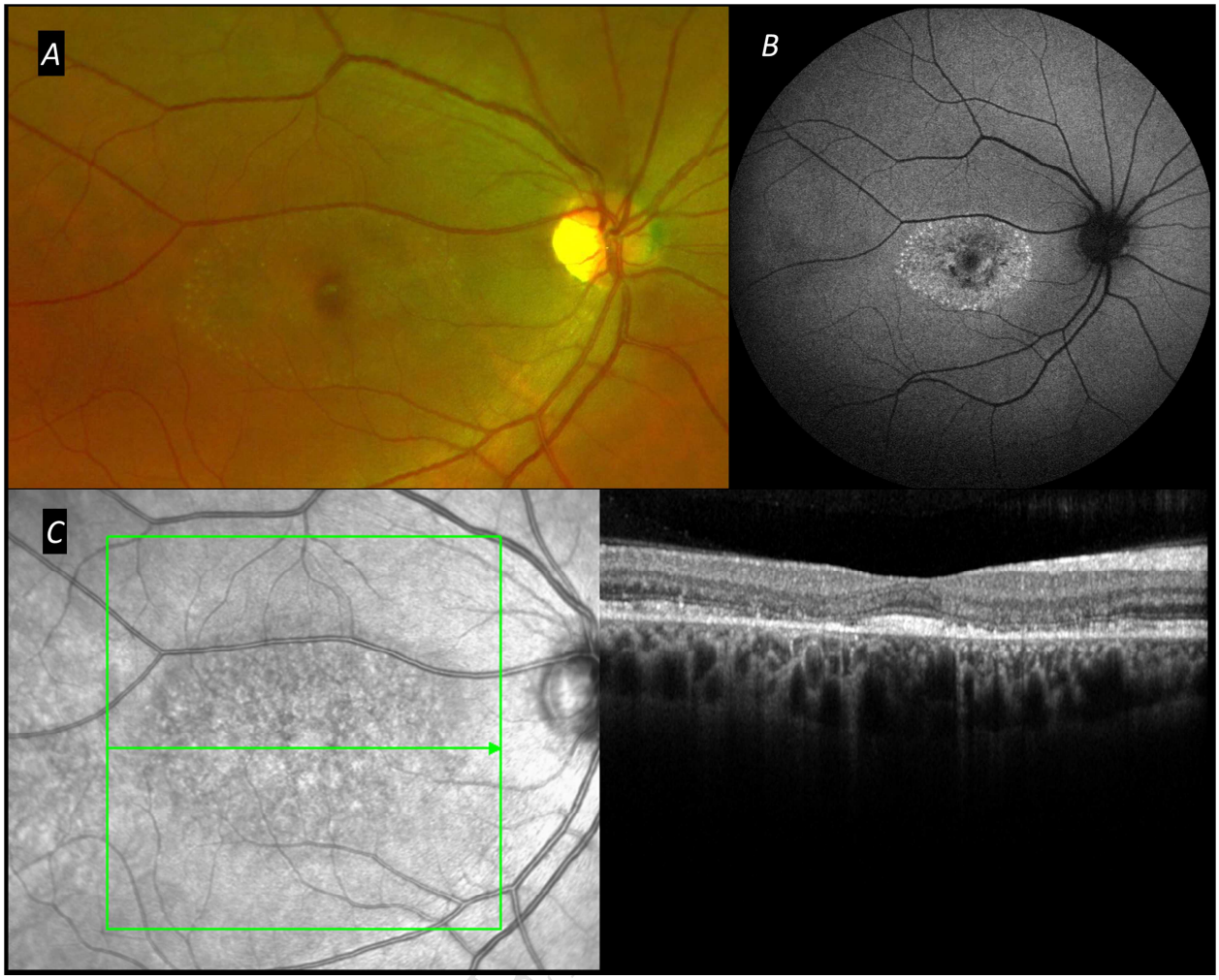

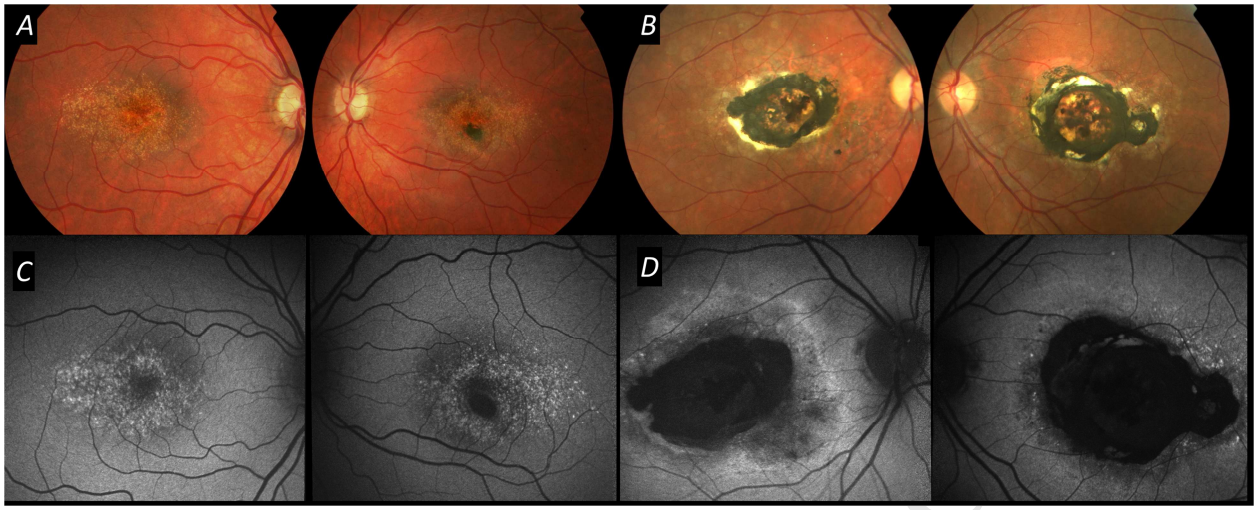

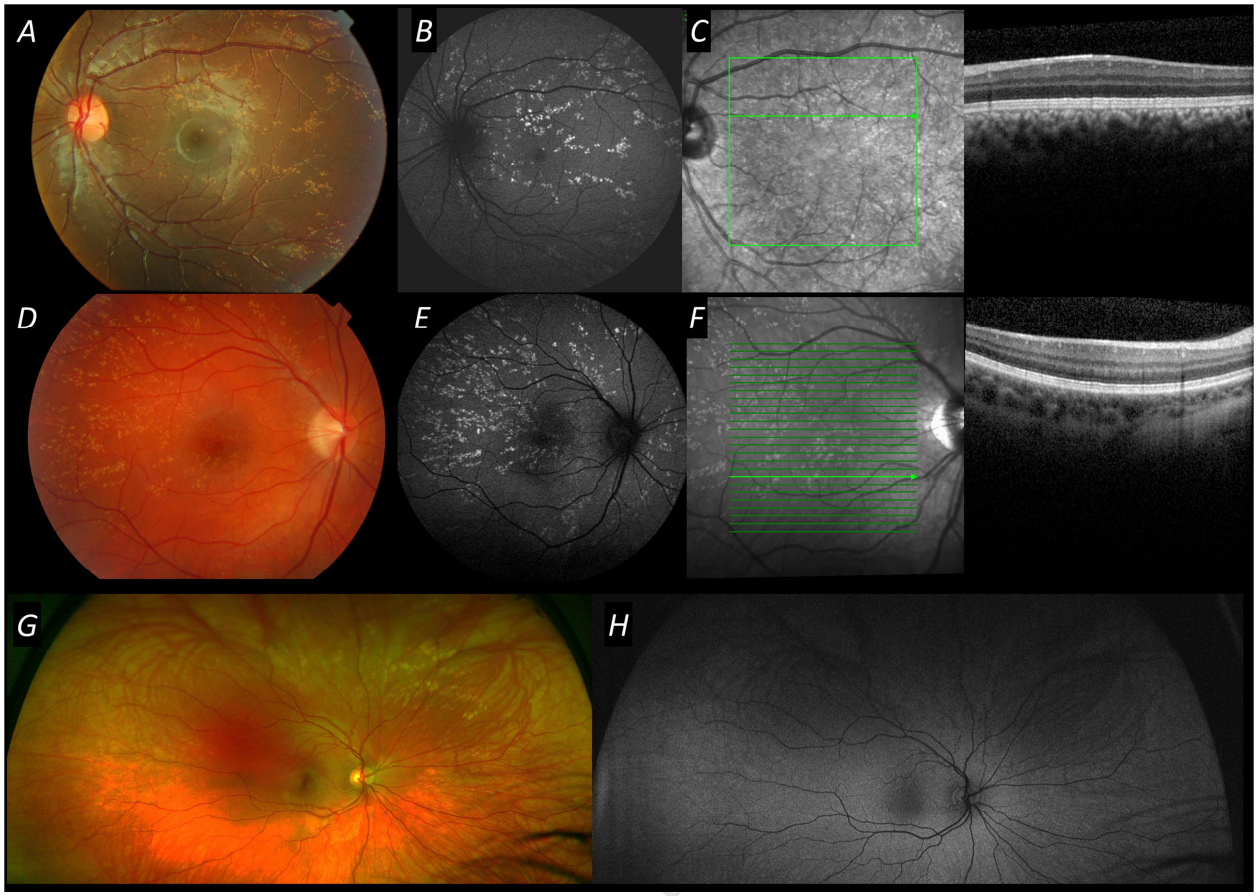

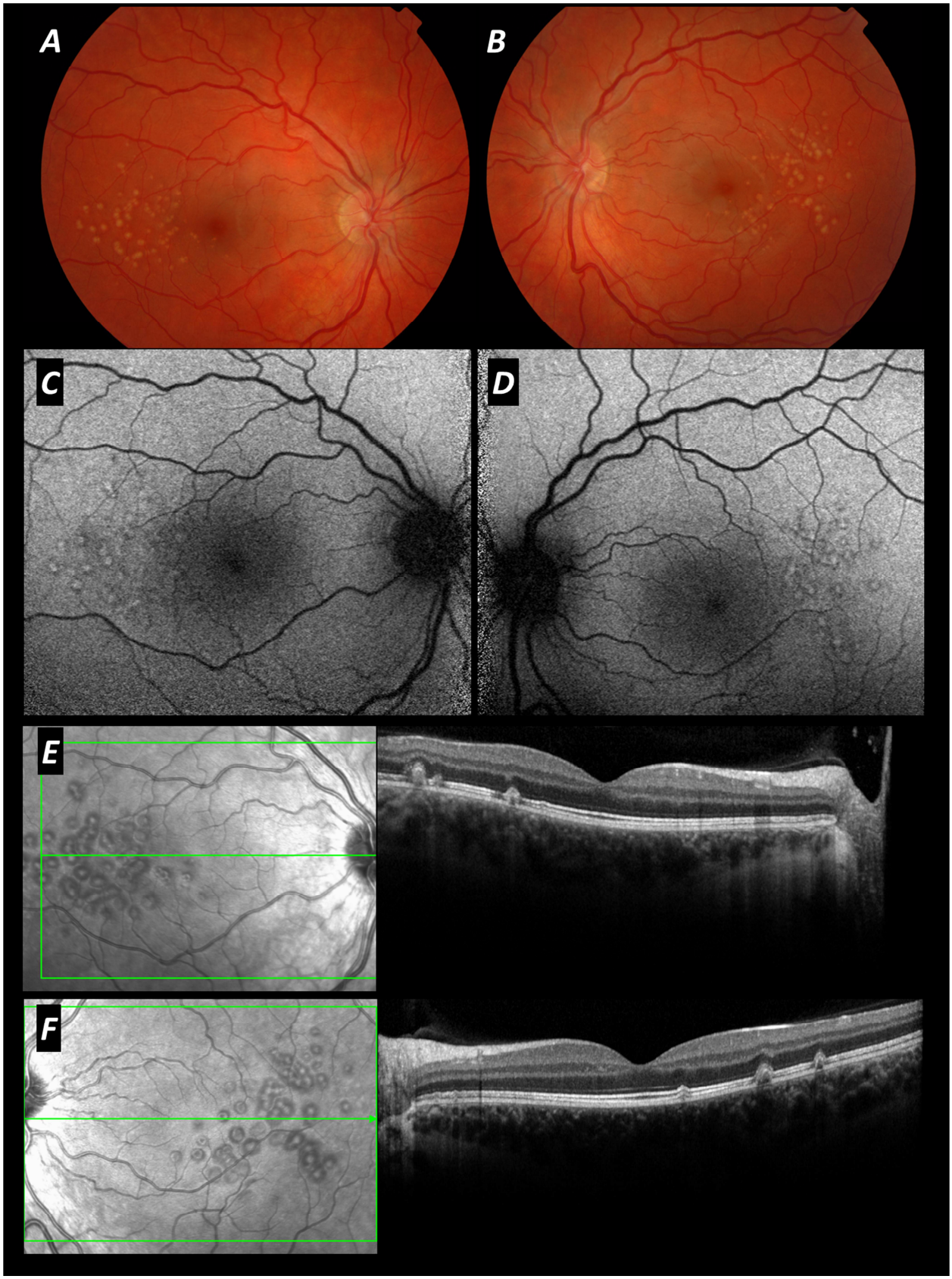
A
B
C
D
E
F

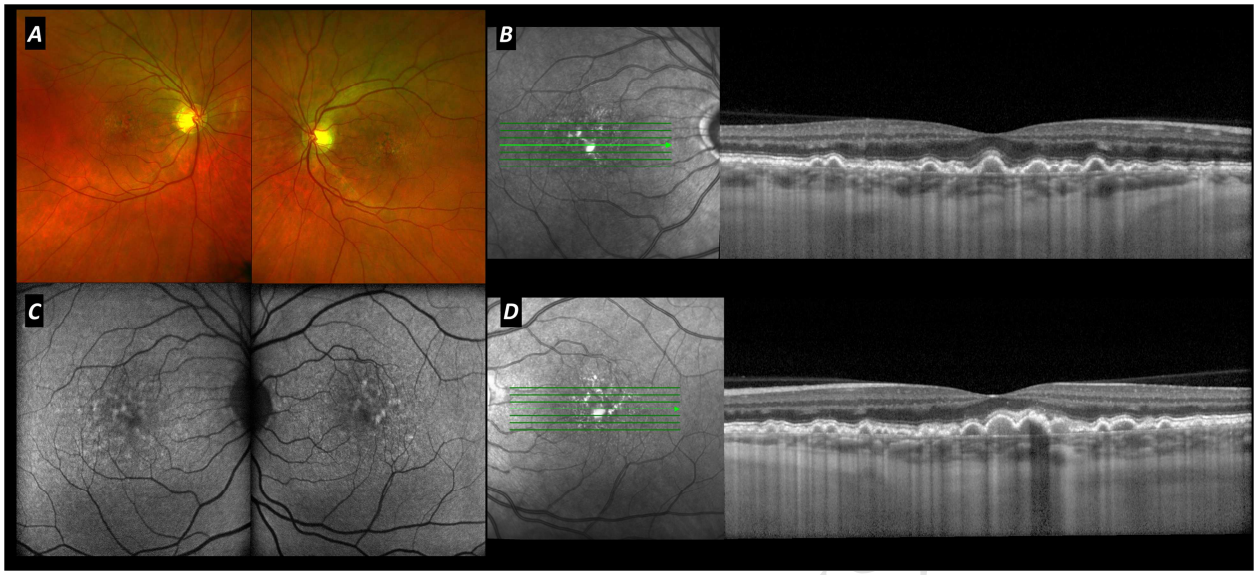

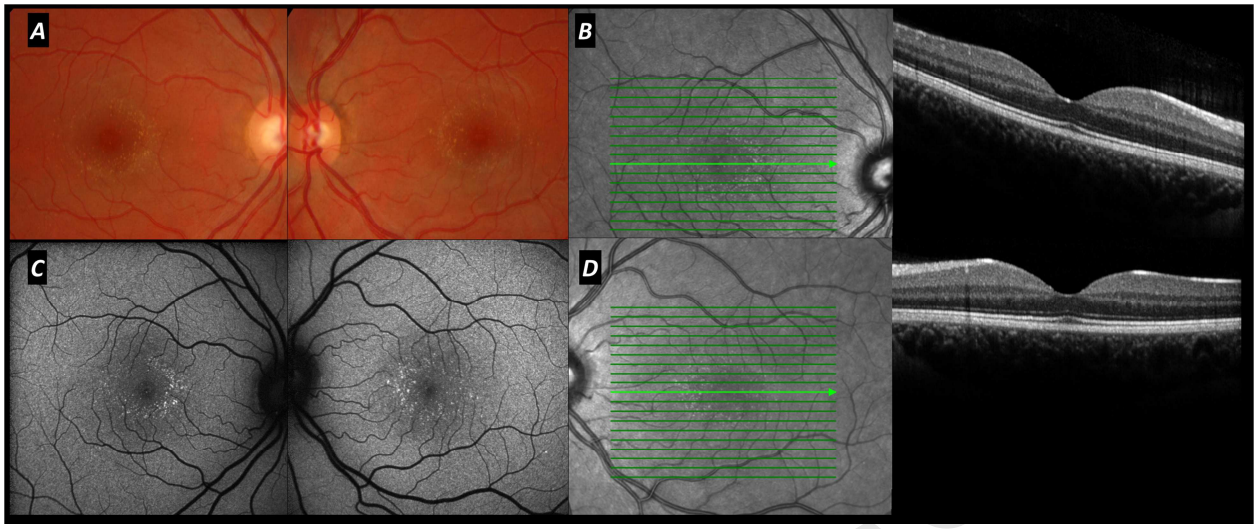

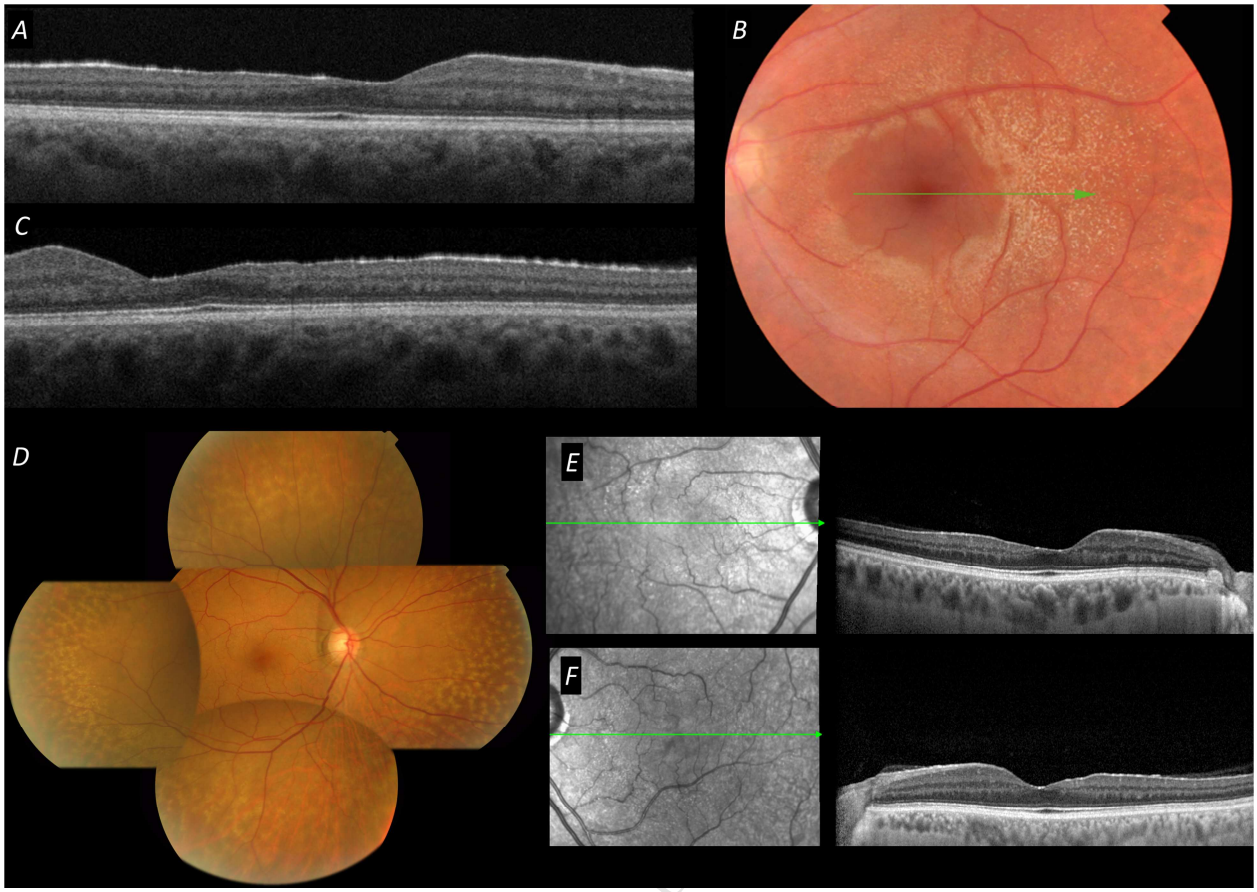

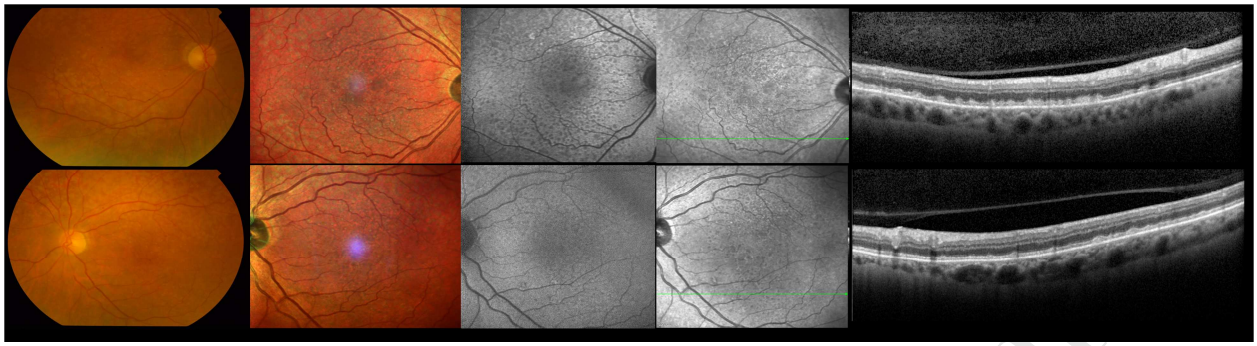

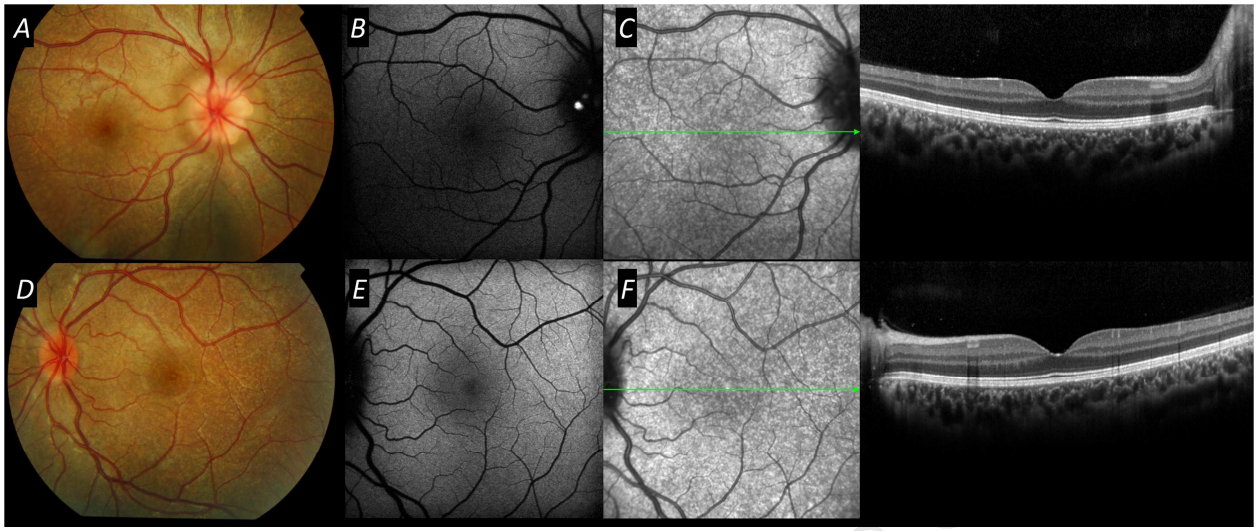

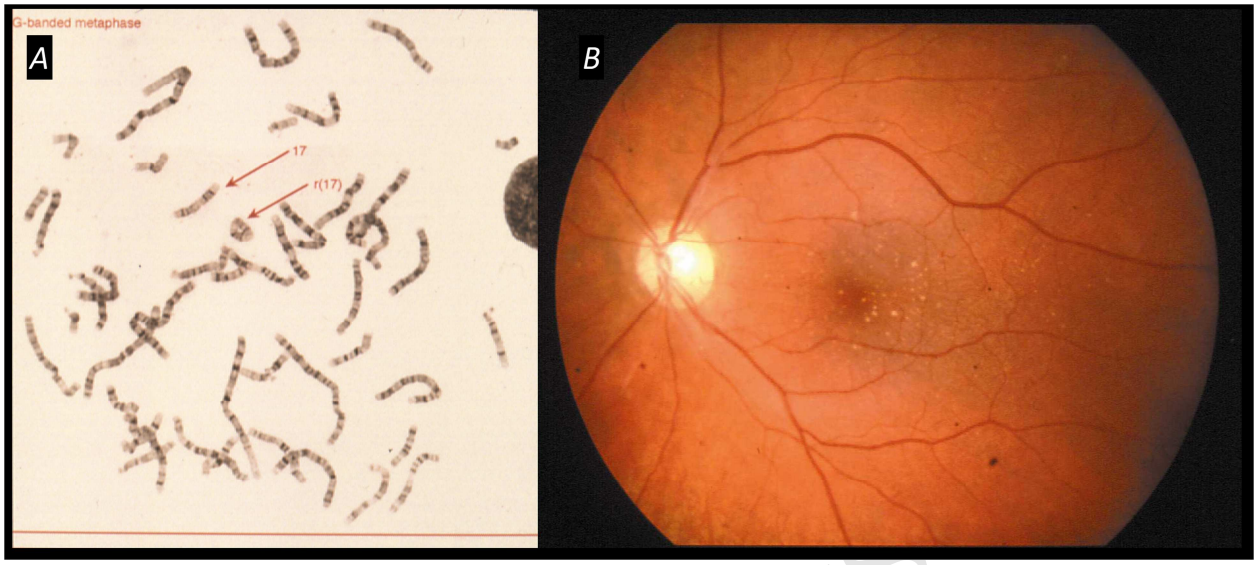

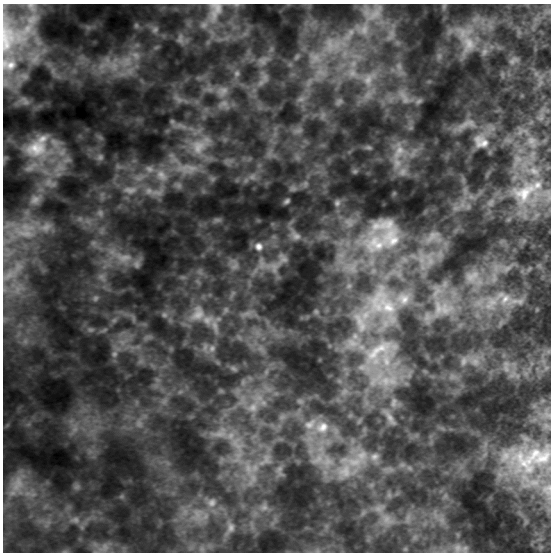

Highlights

- Besides age-related macular degeneration, drusen and drusen-like deposits can occur in normal ageing, and in young age groups; they can also be associated with inherited conditions and with systemic disorders. Multimodal imaging can afford a degree of differentiation.
- White dots, drusen or subretinal drusenoid deposits may be seen in a number of inherited eye disorders, including visual cycle disorders as well as mutations in the following genes: EFEMP1, PLA2G5, TIMP3, C1QTNF5, IMPG1, IMPG2, PRPH2, CDHR1.
- Common themes emerging include complement dysregulation and alterations in the transport of retinoid (either by visual cycle disruption or Bruch membrane thickening), yielding insight into pathogenetic mechanisms as well as potential therapeutic targets.